Investigating the Effect of Simulated Ischemia on Phosphatases: Comparing a cardiomyocyte (H9c2) cell line with a breast cancer (MDA-MB 231) cell line

Author: Maumela Lutendo

Thesis presented in fulfilment of the requirements for the degree of Master of Science in the Faculty of Medicine and Health Sciences at Stellenbosch University.

Supervision: Dr Derick Van Vuuren

Co- Supervision: Dr John Lopes

March 2020

DECLARATION

By submitting this thesis/dissertation electronically, I declare that the entirety of the work contained therein is my own original work, that I am the sole author thereof (save to the extent explicitly otherwise stated), that reproduction and publication thereof by Stellenbosch University will not infringe any third party rights and that I have not previously in its entirety or in part submitted it for obtaining any qualification.

Date: March 2020

Acknowledgement

Gratitude to all individuals who contributed towards the completion of the studies.

Abstract

Background: Reversible phosphorylation is responsible for an estimated 30% of protein regulation. Protein phosphorylation is catalysed by protein kinases and dephosphorylation by protein phosphatases. Ischemia, which is characterised by reduced blood flow to tissue and hypoxia has been implicated in causing pathology in the regulation of proteins involved in signalling both in the heart and in cancer cells.

Methods: 10000 cells/100µl/well of H9c2 and 25000 cells/100µl/well of MDA-MB 231 were cultured in Dulbecco's Modified Eagle Medium (DMEM) with 10 % Fetal Bovine Serum (FBS) and 1 % Penicilin Streptomycin (PenStrep). Incubation was done in a sterile environment in 95 % atmospheric air in 5 % CO_2 at 37 ºC in a humidified atmosphere. At 70 % - 80 % confluence, ischemia was simulated by Modified Esumi Buffer in conjugation with exposure to a hypoxic gas mixture [0% O_2/5 % CO_2/95 % N_2 (H9c2) or 0.5 % O_2/5 % CO_2/balance N_2 (MDA-MB 231)]. Incubation for simulated ischemia (SI) was done for 2 hours and acidic reperfusion for 30 minutes. Phosphatase activity was measured using both a p-nitrophenol phosphate (pNPP), as well as a 6,8-difluro-4methylumbelliferyl phosphate (DiFMUP) assay. Phosphatase expression was measured by Western blotting. Cell viability was measured using an ATP assay, as well as both propidium iodide (PI) and JC-1 staining. Cells were pharmacologically manipulated by administering cantharidin (2 µM and 5 µM), an inhibitor of both PP2A and PP1 and FTY 720 (1 µM and 5 µM), an activator of PP2A. All experiments were repeated three or four times on three or four different days. All data was analysed using Graphpad Prism version 5. All the data was expressed as mean ± standard error of the mean (SEM). For comparison between two groups, the student T-test was used. For multiple comparisons, one-way ANOVA with Bonferroni post hoc test was used. Differences were considered statistically significant at $p < 0.05$.

Results: Energy status was measured as ATP levels revealing that SI reduced ATP levels in both H9c2 cells (control: 1.000 ± 0.000 Arbitrary Unit (AU) vs SI: 0.597 ± 0.042 AU; n = 3; $p < 0.001$) and MDA-MB 231 cells (control: 1.000 ± 0.000 AU vs SI: 0.458 ± 0.025 AU; n = 4; $p < 0.01$). JC-1 stain showed no mitochondrial impairment and PI staining detected no significant cell membrane breakage in both H9c2 and MDA-MB 231 cell lines treated with SI. pNPP and DiFMUP assays showed no noticeable change in the activity of protein phosphatases in both the MDA-MB 231 and H9c2 under SI conditions. The total expression of Akt/PKB in MDA-MB 231 cell line showed a statistically significant reduction following 2 hours SI (control: 1.000 ± 0.000 AU vs SI: 0.556 ± 0.027 AU; n = 3; $p < 0.01$). In addition, the expression of PP2Ac was also inclined in MDA-MB 231 cell line due to SI (control: $1.482 \times 10^7 \pm 8.715 \times 10^5$ AU vs SI: $1.964 \times 10^7 \pm 1.406 \times 10^6$ AU; n = 3; $p < 0.05$). Protein phosphatase 2A was elected for pharmacological manipulation in both H9c2 and MDA-MB 231 cell lines under SI conditions. Normoxic MDA-MB 231 cell line was treated with 1 µM FTY 720 to show an increase in PI fluorescence (normoxia: 199.5 ± 8.381 relative fluorescence units (RFU) vs normoxia + 1 µM FTY 720: 228.1 ± 2.902 RFU; n= 4; $p < 0.05$). Data assessed by JC-1 staining showed that 5 µM cantharidin treatment under SI conditions reduced the mitochondrial function and integrity of the MDA-MB 231 cell line (SI: 1.000 ± 0.000 RFU vs SI + 5 µM cantharidin: 0.625 ± 0.112 RFU; n= 4; $p < 0.01$). JC-1 image analysis showed that SI + 5 µM cantharidin also reduced mitochondrial function and integrity in H9c2 cells (SI: 1.000 ± 0.000 RFU vs SI + 5 µM cantharidin: 0.285 ± 0.059 RFU; n= 3; $p < 0.01$).

Discussion and conclusion: Two hours SI did not significantly influence phosphatase activity in both H9c2 and MDA-MB 231 cell lines. In MDA-MB 231 cell line SI was associated with an increase

in the expression of PP2Ac. SI caused a significant reduction in ATP levels in both H9c2 and MDA-MB 231 cell lines as expected. However, 2 hours SI did not induce cell death as measured by PI and JC-1 staining.

Pharmacological inhibition of PP2A with 5 µM cantharidin in combination with SI protected the cells by reducing the consumption of ATP in H9c2 cells. Other studies showed that the inhibition of PP2A indeed protects heart cells from ischemia whereas, studies done in cancer report that the inhibition of PP2A induces cell death. Surprisingly, even though the inhibition of PP2A by 5 µM cantharidin under SI conditions reduced the consumption of ATP in H9c2 cells, JC-1 image analysis reported that it also reduced mitochondrial function and integrity. SI + 5 µM cantharidin also reduced mitochondrial function and integrity in MDA-MB 231 cell line. As stated, in the heart the inhibition of PP2A has been shown by other researchers to be protective. The activation of PP2A by 1 µM FTY 720 in MDA-MB 231 cell line under normoxic conditions induced cell death as measured by PI. Other studies have showed that it is indeed the activation of PP2A that induces cell death in cancer cells, making it a tumour suppressor. Interestingly, an increasing body of evidence shows that the inhibition of PP2A can also lead to cell death, making it a tumour promotor in other types of cancer. It is therefore concluded that PP2A may play a dual role in cell death depending on the targeted holoenzyme and maybe also cell type. More studies must be done to investigate the role of PP2A in cell death in different cell types, as well as to identify which holoenzymes should be targeted for a desired outcome. PP2A remains of great interest in the field of research for cancer therapy as well as cardioprotection.

Opsomming

Agtergrond: Dit word beraam dat omkeerbare fosforilasie betrokke is by nagenoeg 30% van proteïen-regulering. Proteïen fosforilering word gekataliseer deur proteïen kinases, terwyl defosforilering gemedieer word deur proteïen fosfatasases. Daar is al gevind dat iskemie, wat gekenmerk word deur ‘n afname in bloedvoorsiening asook hipoksie, kan lei na patologie in terme van die regulering van proteïene betrokke in seintransduksie in beide die hart-, asook kankerselle.

Metodes: 10000 selle/100µL/put van H9c2 en 25000 selle/100µL/put van MDA-MB-231 is gekweek in Dulbecco’s Modified Eagle Medium (DMEM) aangevul met 10% fetale bovienserum (FBS) en 1% Penisillien Streptomisien (PenStrep). Selle is gehandhaaf in ‘n steriele omgewing in 95% atmosferiese lug en 5% CO2 teen 37°C in ‘n gehumidifiseerde atmosfeer. Wanneer selle 70%-80% konfluensie bereik het is hulle blootgestel aan simuleerde iskemie (SI) wat bestaan het uit inkubasie met ‘n gemodifiseerde Esumi buffer, tesame met blootstelling aan ‘n hipoksie-gasmengsel [0% O2/5 % CO2/95 % N2 (H9c2) of 0.5 % O2/5 % CO2/balans N2 (MDA-MB 231)]. Selle is vir 2 ure aan hierdie SI ingreep blootgestel, gevolg deur 30 minutes van suur-herperfusie. Fosfatase aktiwiteit is gemeet deur gebruik te maak van twee verskillende analises: die p-nitrofenolfosfaat (pNPP) toets, asook die 6,8-difluro-4metielumbelliferielfosfaat (DiFMUP) toets. Die uitdrukking van fosfatases is bepaal met behulp van Westerse klad. Sellewensvatbaarheid is gemeet deur gebruik te maak van ‘n ATP toets, asook propidium jodied (PI) en JC-1 kleuring. Selle is farmakologies gemanipuleer deur óf ‘n inhibeerder (cantharidin, teen twee dosisse: 2 µM en 5 µM) óf ‘n aktiveerder (FTY 720, teen twee dosisse: 1 µM en 5 µM) van PP2A toe te dien. Alle eksperimente is drie of vier maal herhaal en gedoen op drie of vier verskillende dae. Alle data is statisties geanaliseer deur gebruik te maak van Graphpad Prism weergawe 5. Alle data is uitgedruk as gemiddeld±standaard fout van die gemiddeld (SEM). Waar twee groepe met mekaar vergelyk is, is die studente T-toets gebruik. In die geval van meervoudige vergelykings is eenrigting ANOVA met die Bonferroni toets gebruik. Verskille is as statisties beduidend geag indien die p-waarde laer as 0.05 is.

Resultate: Die ATP toets het getoon dat SI wel ATP vlakke verlaag het in H9c2 selle (kontrole: 1.000 ± 0.000 Arbitrêre Eenhede (AE) vs SI: 0.597 ± 0.042 AE; n = 3; $p < 0.001$). SI het ook ‘n afname in ATP vlakke in MDA-MB-231 selle geïnduseer (kontrole: 1.000 ± 0.000 AE vs SI: 0.458 ± 0.025 AE; n = 4; $p < 0.01$). SI was egter nie geassosieer met ‘n toename in seldood in H9c2 en MDA-MB-231 selle nie, soos bepaal deur PI en JC-1 kleuring. SI het ook geen invloed op fosfatase aktiwiteit gehad in beide H9c2 en MDA-MB-231 selle nie, soos bepaal deur beide die pNPP en die DiFMUP toets. Die uitdrukking van PKB/Akt in MDA-MB-231 selle was wel beduidend laer na 2 ure van iskemie (kontrole: 1.000 ± 0.000 AE vs SI: 0.556 ± 0.027 AE; n = 3; $p < 0.01$). Tesame hiermee was daar ‘n beduidende toename in die uitdrukking van PP2Ac in die MDA-MB 231 selle in assosiasie met iskemie (kontrole: $1.482 \times 10^7 \pm 8.715 \times 10^2$ AE vs SI: $1.964 \times 10^7 \pm 1.406 \times 10^6$ AE; n = 3; $p < 0.05$) soos bepaal met ‘n studente T-toets. Behandeling met ‘n kombinasie van SI en middels (cantharidin en FTY 720) was geassosieer met ‘n afname in ATP vlakke in beide H9c2 en MDA-MB 231 selle. Daar was egter wel ‘n afname in die verbruik van ATP in H9c2 selle behandel met 5µM cantharidin onder SI kondisies, in vergelyking met die standaard SI-alleen behandeling. Behandeling met 1 µM FTY 720 het gelei na ‘n toename in PI fluorosensie, kenmerkend van nekrose, in normoksiese MDA-MB 231 selle (normoksie: 199.5 ± 8.381 relatiewe fluorosensie eenhede (RFE) vs normoksie + 1 µM FTY 720: 228.1 ± 2.902 RFE; n= 4; $p < 0.05$). 5 µM FTY 720 het egter verbasend geen effek ontlok nie. Data gegenereer deur die plaatleser het getoon dat 5µM cantharidin behandeling tesame met SI blootstelling mitochondriale funksie en integriteit verlaag het, soos bepaal deur JC-1 kleuring (SI: 1.000 ± 0.000 RFU vs 5µM cantharidin: 0.625 ± 0.112 RFU; n= 4; $p < 0.01$). Beeld analiese van die JC-1 kleuring in

H9c2 selle het getoon dat SI + 5 µM cantharidin ook in hierdie seltipe mitochondriale funksie en integriteit verlaag het (SI: 1.000 ± 0.000 RFU vs SI + 5 µM cantharidin: 0.285 ± 0.059 RFU; n= 3; $p < 0.01$).

Bespreking en gevolgtrekking: Twee ure van simuleerde iskemie het geen effek op fosfatase aktiwiteit in beide H9c2 en MDA-MB-231 selle gehad nie. SI was wel geassosieer met ‘n toename in die uitdrukking van PP2Ac in MDA-MB-231 selle, terwyl Akt/PKB afgeneem het. SI het soos verwag ‘n afname in ATP vlakke in beide H9c2 en MDA-MB-231 selle teweeg gebring. Ten spyte hiervan, het 2 ure van SI nie seldood veroorsaak nie, soos bepaal deur PI en JC-1 kleuring. Ander navorsers het getoon dat iskemie seldood kan induseer binne 6 tot 48 uur van inkubasie. Vorige studies in ons laboratorium het egter getoon dat 2 ure genoegsaam was om seldood te induseer in H9c2 selle, soos gemeet deur ‘n Anneksin/PI toets.

Farmakologiese inhibisie van PP2A met 5µM cantharidin in kombinasie met SI het selle beskerm deur die verbruik van ATP in die H9c2 selle te beperk. Ander studies het getoon dat PP2A inhibisie inderdaad hartselle beskerm teen iskemie, terwyl studies in kanker gerapporteer het dat PP2A inhibisie seldood induseer. Dit was wel onverwags dat, ondanks die feit dat PP2A inhibisie ten tye van iskemie, deur die toediening van 5µM cantharidin, ATP verbruik beperk het in H9c2 selle, dit ook mitochondriale integriteit en funksie benadeel het, soos getoon deur JC-1 kleuring. SI + 5 µM cantharidin was ook geassosieer met ‘n afname in mitokondriale funksie en integriteit in MDA-MB-231 selle. Nieteenstaande, PP2A inhibisie in die hart is deur ander navorsers as beskermend getoon. Die aktivering van PP2A deur 1 µM FTY 720 in normoksiese MDA-MB-231 selle het nekrose veroorsaak soos getoon deur PI kleuring. Ander studies het ook getoon dat PP2A aktivering lei na seldood in kankerselle. Dit is dus ‘n tumor-onderdukker. Daar is egter ook toenemend bewyse dat PP2A inhibisie ook na seldood kan lei, wat dit dus impliseer as ‘n tumor-promotor in sekere tipes kanker. Die gevolgtrekking is dus dat PP2A moontlik ‘n tweevoudige rol in seldood speel, afhangend van die betrokke holo-ensiem, asook moontlik die seltipe. Meer studies moet gedoen word om die rol van PP2A in seldood in verskillende seltipes te ondersoek, asook om te bepaal watter holo-ensieme geteiken moet word om die gewenste uitkoms te bewerkstellig. PP2A bly relevant in die veld van navorsing aangaande kankerterapie, asook kardiobeskerming.

Table of Contents

List of Figures

Chapter 1: Introduction

Chapter 3: Optimization for Hypoxia

Chapter 4: The effect of simulated ischemia on cell viability

Chapter 5: The effect of simulated ischemia on the activity and expression of protein phosphatases

Chapter 6: Pharmacological modulation of PP2A

List of Tables

Chapter 2: Methodology

Chapter 6: Pharmacological modulation of PP2A

Glossary

- **2-DG** - Deoxy-glucose- to inhibit glycolysis
- **AB** - Assay buffer
- **Akt/PKB** - Protein kinase B
- **ANOVA** - Analysis of variance
- **ATP Assay** - Adenosine triphosphate levels in viable cells
- **AU** - Arbitrary Units
- **cAMP** - Cyclic adenosine monophosphate
- **cGMP** -Cyclic guanosine monophosphate
- **DMEM** - Dulbecco's Modified Eagle Medium
- **DuSP** - Dual Specificity Phosphatase
- **EDTA** - Ethylenediamineretraacetic acid
- **EGTA** – Ethylene glycol-bis (b-aminoethyl ether)-N, N, N`, N`-tetratacetic acid
- **ERK** - Extracellular signal–regulated kinases
- **ETC** - Electron transport chain
- **FBS** - Fetal Bovine Serum
- **Graph prism v5** – Statistical software used for analysis
- **GSK 3β** - Glycogen synthase kinase 3β
- **H9c2** – Cardiomyocyte cell line from rat origin
- **HEPES** - (4-(2-hydroyethyl)-1-piperazineethanesulfonic acid
- **JAK-STAT-3** - Janus kinases- Signal Transducer and Activator of Transcription proteins (STATs)
- **JC-1 stain** - Fluorescence dye that stains the mitochondria
- **JNK- c** -Jun N-terminal kinases
- **MAPK** - Mitogen-activated protein kinase
- **MEK** - MAPK/ERK kinase
- **Modified Esumi buffer** - Buffer used to induce ischemia
- **MDA -MB 231** - Triple negative breast cancer cell line
- **MPTP** - Mitochondrial permeability transition pore
- **mtDNA** - Mitochondrial DNA
- **Na_3VO_4** – Sodium orthovanadate
- **NaF** – Sodium Fluoride
- **NO** - Nitric oxide
- **OXPHOS** - Oxidative phosphorylation

- **P70 S6K** - Ribosomal protein S6 kinase beta-1
- **P38 MAPK** - P38 mitogen-activated protein kinases
- **Pan serine phosphor** - Antibody probe for phosphorylated serine residues
- **PI3K** - Phosphatidylinositol 3-kinase
- **PKA** - Protein kinase A
- **PKG** -Protein kinase G
- **PLC** - Phosphoinositide phospholipase C
- **PLD** - Phospholipase D
- **pNPP** - Para-Nitrophenylphosphate- synthetic protein phosphatase
- **PP** (1, 2A, 2B, 2C, 4, 5, 6, and 7) -Protein Phosphatase (1, 2A, 2B, 2C, 4, 5,6, and 7)
- **PP2B** - Protein phosphatase 2B
- **PPMs** - Mg2+ - dependent protein phosphatases
- **PPPs** - Phosphoprotein Phosphatase
- **PSP** - Protein Serine/threonine Phosphatase
- **PTEN** - Phosphatase and Tensin homolog
- **PTP** - Protein Tyrosine Phosphatase
- **PI** – Propidium Iodide
- **RGB** – Red green blue composition
- **RFU** - Relative fluorescence unit
- **RISK** - Reperfusion Injury Salvaging Kinase pathway
- **ROS** – Reactive oxygen species
- **SAFE** - Survivor Activating Factor Enhancement pathway
- **SDT** - Sodium dithionate
- **SI** - Simulated ischemia
- **Shc** - SHC-transforming protein 1
- **T-test** – A test used to test the hypothesis between 2 groups
- **VEGF** - Vascular endothelial growth factor

Introduction

The heart and cancer are two very different entities and therefore comparing them could seem odd. Comparing them based of their similarities and differences could however highlight interesting and noteworthy biological phenomena. Ischemia is a common stressor that can induce metabolic stress in both the systems at some point. Ischemic metabolic stress has been notoriously reported to induce sudden heart muscle death while in cancer it may cause tumour progression. The key factor marking a margin in metabolic adaptation is the substrates preferred per cell type. Heart cells are one of the earliest differentiated cells, whereas cancer is notorious for being highly proliferated. Proliferating cells have been observed and reported to be well adapted to low saturated O_2 cellular environment. Therefore, Warburg effect explains how even in the presence of O_2, tumour cells would favour anaerobic glycolysis (Warburg, 1931). In contradiction, differentiated cells such as the cardiomyocytes highly prefers lipid oxidation and oxidative phosphorylation which are highly O_2 dependent and maladaptive in ischemic conditions.

The phenomenon of pre-conditioning has been used to study signalling pathways involved during ischemia/reperfusion injury in the heart (Murry, et al., 1986). These studies have shown that the heart has an innate ability to adapt to ischemic injury, although this adaptation is transient. Cellular signalling is regulated by reversible phosphorylation. Our interest in protein phosphatases attracted us to investigate phosphatase interactions in both cell lines to assess their relevance in ischemic adaptation. Moreover, most loss of function mutations observed in cancer studies involves phosphatases. Which led us to posit that we could use our understanding of the mutative evolution of cancer to better understand the maladaptive heart. Below is a thorough literature review discussing the metabolic adaptation of both cell types as well as in terms of cellular signalling and reversible phosphorylation.

Chapter 1: Literature review

Ischemia is characterised by reduced blood flow to tissue. Most proliferative cells such as embryonic cells, liver cells and cancer cells have been shown to be able to adapt to a degree to long-term exposure to ischemia or hypoxia (characterised by low oxygen levels) (Ma, et al., 2009). However, terminally differentiated cells, such as cardiomyocytes (heart muscle cells) and brain cells, show a limited capacity to adapt to the same ischemic or hypoxic conditions (Burke & Virmani, 2007). Proliferative cells are more adapted to anaerobic glycolysis (oxygen independent) than terminally differentiated cells which rely relatively more on aerobic metabolism (oxygen-dependent) (Lunt & Vander Heiden, 2011). Thus, proliferative cells tend to be well adapted to fluctuating levels of O_2 compared to terminally differentiated cells (Vander Heiden, et al., 2009). It therefore follows that metabolic flexibility accompanies the ability to adapt to ischemic conditions (Smith, et al., 2018).

In cancer cells, studies have reported that extended exposure to hypoxia facilitates neo-vascularization to increase the likelihood of survival through reperfusion (Gilkes, et al., 2014).

For the purpose of our study, we will focus on the regulation of phosphatases in both a breast cancer cell line, as well as a heart cell line. Comparison of cancer and heart cell lines in terms of their response to ischemia could share some light on ways in which cells can navigate the stress of ischemia.

Cellular Energy metabolism

A normal cell is typically comprised of catabolic and anabolic metabolism. In catabolic metabolism, macromolecules are broken down for energy (de Bolster, 1997). For an example: a glucose molecule enters the glycolytic cycle for ATP production (2ATPs). In the presence of oxygen, the molecules are further broken down in the Krebs cycle and ultimately enters oxidative phosphorylation (OXPHOS) for more ATP production (36 ATPs). Lipids can also be broken down and directly enters the Krebs cycle for further processing (Alberts, et al., 2002). Substrates from the glycolytic cycle and Krebs cycle can enter the pentose phosphate pathway for anabolic metabolism where macromolecules such as nucleotides, lipids and amino acids are built to create a new cell (Kruger & von Schaewen, 2003). Differentiated cells tend to favour the catabolic metabolism more by utilising aerobic glycolysis, the Krebs cycle and OXPHOS for high ATP yield, mostly using lipids and glucose as their main substrates. Whereas, proliferative cells favour the anaerobic glycolysis for fast ATP production and the anabolic metabolism to build new cells (Lunt & Vander Heiden, 2011)(Figure 1.1).

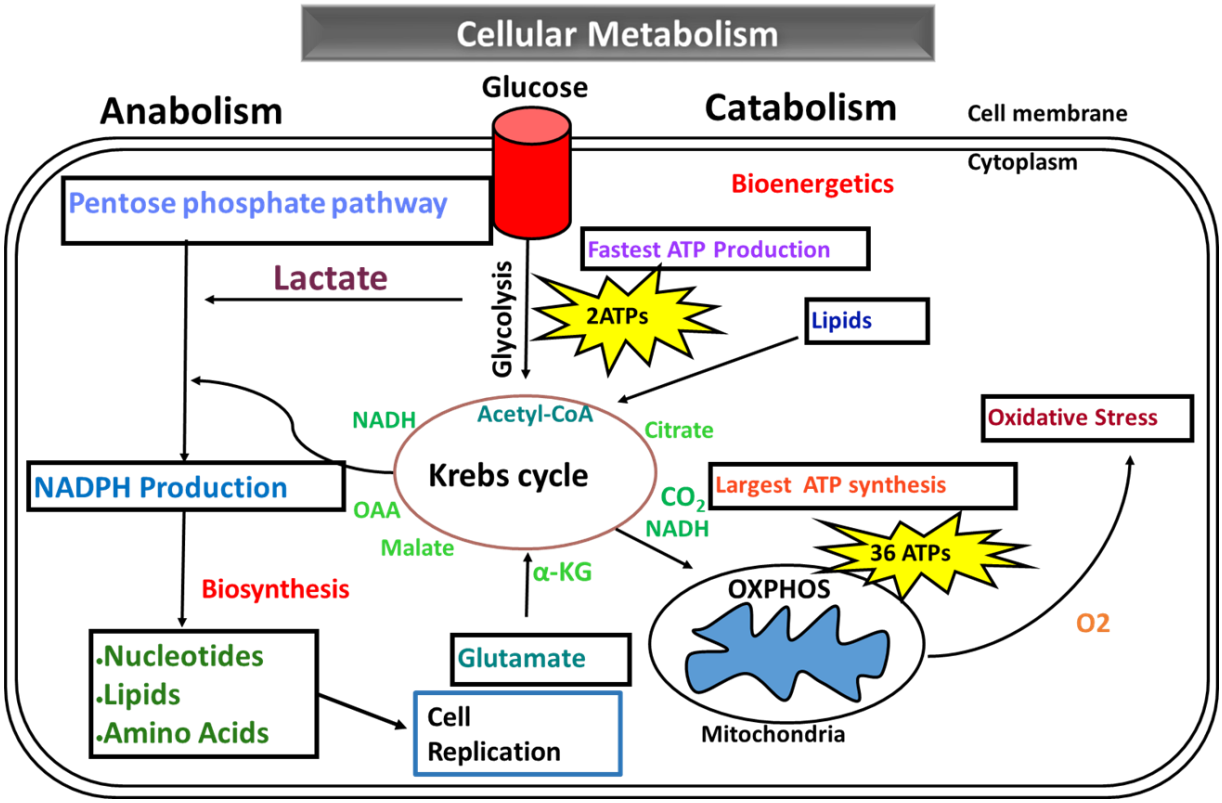

Figure 1.1. A schematic diagram depicting differences in energy metabolism in the presence and absence of oxygen. A normal eukaryotic cell contains both catabolic and anabolic metabolic processes. Differentiated cells tend to favour catabolism whereas, proliferative cells favours anabolism and glycolysis.

Cardiomyocyte metabolism

In early embryonic development, as the embryo grows, it becomes progressively harder for cells to obtain nutrients or evacuate nitrogenous waste. After about 18 days, the heart begins to develop and function to assume the circulatory function (Moorman, et al., 2003). Beside the fact that heart cells are terminally differentiated, they are also muscle cells that contract to facilitate the heart's function as a blood pump (Paradis, et al., 2014). The mammalian heart must contract continuously and as such has an immense requirement for energy to fuel this level of mechanical work. The vasculature supplying nutrients to the heart for ATP synthesis and cellular maintenance is called the coronary circulation (Deussen, et al., 2012). Together with the liver that has about 2000 mitochondria per cell; the heart contains the highest density of mitochondria. Cardiomyocytes have an extremely high ATP demand which can be efficiently met by OXPHOS in the mitochondria. More than 95% of the ATP utilized by cardiomyocytes are produced through mitochondrial OXPHOS (Campbell, et al., 2006). Cardiomyocytes can utilize all types of energy substrates, including carbohydrates, lipids, amino acids and ketone bodies, for ATP production in both the mitochondrion and cytosol (glycolysis) depending on both substrate availability and cell energy demands. It is however known that fatty acids followed

by carbohydrates are the most preferred substrates for OXPHOS in the heart (D'Souza, et al., 2016). As mentioned above, the heart is however adaptive in the energy substrates it uses, for an example, during intense exercise, when levels of oxygen are significantly reduced, cardiomyocyte metabolism readily shifts from OXPHOS to anaerobic glycolysis, where NADH reduces pyruvate to lactic acid forming NAD^+ (Greenberg, et al., 2006). During starvation, or exposure to a ketogenic diet, when ketone bodies levels are elevated in the blood, ketones utilization as an energy substrate is enhanced (Aubert, et al., 2016). This remarkable metabolic flexibility and its ability to rapidly adapt to fluctuating circulatory substrate concentrations allows for optimal energy homeostasis (Smith, et al., 2018).

Cancer cell metabolism

In vivo studies have demonstrated that prior to implantation, the environment within the uterine lumen containing embryonic cells is hypoxic (Fischer & Bavister, 1993). Moreover, studies have also shown that embryonic stem cells have few mitochondria and that these lack cristae development and show limited mitochondrial DNA (mtDNA) replication. These properties are not favourable for OXPHOS; rendering embryonic cells solely reliant on anaerobic glycolytic metabolism to meet their energy demands (Brown GC, 1992). However, during implantation, the mitochondrial genome undergoes significant replication of mtDNA and the levels of oxygen increases to match the OXPHOS demands of differentiating cells (Thundathil, et al., 2005). It has therefore been postulated that an increase in ATP content in a cell may be indicative of a loss of stemness and the subsequent onset of differentiation (St John, et al., 2005).

Non-proliferative cells, including quiescent or differentiated cells, use the mitochondria as their main source of energy production via the Krebs cycle and OXPHOS. In contrast to this, proliferative cells, including both those under normal physiological conditions (e.g. embryonic cells) and cancer, prefer a more rapid form of ATP synthesis via glycolysis (Vander Heiden, et al., 2009). When Warburg observed that cancer cells harbour plenty of mitochondrial mutations, he suggested that these mutations abolish the functioning of the mitochondria and its metabolism (Warburg, 1931). However, accumulating evidence suggests that the function of the mitochondria is not necessarily impaired, but rather altered. Desjardins et al. (1985) conducted an experiment, where they eliminated the mtDNA of different cancer types to confirm that functional mitochondria are pertinent for tumour growth. In their experiments, they created a model of ethidium bromide-induced loss of mitochondrial DNA. The mtDNA deficient cancer cells showed reduced growth rates, decreased colony formation in soft agar and markedly reduced tumour formation in nude mice (Desjardins, et al., 1985). Brandon et al. (2006), suggested the possibility of two classes of mtDNA mutations in cancer cells: mutations that stimulate neo-plastic transformation by impairing OXPHOS, and those that facilitate bioenergetic adaptation to changing

environments. A meta-analysis of many cancer-associated mtDNA mutations revealed that many cancer cell mtDNA mutations inhibit OXPHOS (Brandon, et al., 2006).

Under normal physiological conditions, glycolysis is 100 times faster than mitochondrial OXPHOS. Whereas, under pathological conditions, rapidly growing tumour cells typically have glycolytic rates up to 200 times higher than those of the normal tissues of origin (Kemp & Daly, 2016). However, the metabolism of glucose to lactate generates only 2 ATPs per molecule of glucose, whereas OXPHOS generates up to 36 ATPs per glucose molecule, which is 18 times more. Otto Warburg (1931) was first to observe that most cancer cells are predominantly dependent on a high rate of cytosol dependent energy production by glycolysis which is accompanied by lactic acid production. Moreover, it has also been demonstrated that glycolytic dominance in the cancer cell is maintained even when oxygen is plentiful. This was named the Warburg effect (Warburg, 1931). Proliferative cells prefer glycolysis, therefore why would proliferative cells favour a less efficient approach to producing ATP in terms of amount compared to differentiated cells? Vander Heiden et al. (2009) reasoned that although comparatively, glycolytic energy metabolism seems “insufficient”, it is evident that this type of metabolism can provide enough energy for cell proliferation. Furthermore, it could be that perhaps more energy is required to sustain the differentiated cellular state than to produce new cells. Vander Heiden et al. (2009) further reasoned that “inefficient” ATP production is a problem only when resources are limited. Moreover, other metabolic studies on proliferative cells show that there is evidence that ATP is never a limiting factor in these types of cells. Therefore, since there is a continuous supply of nutrients to proliferative cells, the “inefficient” glycolytic supply of ATP is not a limiting factor, thus there is no selective pressure to optimize metabolism for ATP yield. Another suggestion for glycolytic preference in proliferative cells is that, perhaps proliferating cells have more important metabolic needs that supersede ATP production from anabolic metabolism for building a new cell. For an example, immune response and wound repair require cell proliferation, and in such cases selective pressure for a rate of metabolism rather than the amount of ATP produced is more pertinent (Vander Heiden, et al., 2009).

Therefore, cancer cells are characterised by high proliferation and thus need to adapt their cellular metabolism to provide constant support for the increased division rate which includes: rapid ATP generation to maintain energy status, increased biosynthesis of macromolecules and tight regulation of the cellular redox status (Vander Heiden, et al., 2009). Metabolic reprogramming in cancer is largely due to oncogenic activation of signal transduction pathways and transcription factors. It is suspected that these metabolic alterations are initiated by epigenetic mechanisms that contribute to the regulation of metabolic gene expression in cancer (Miranda-Gonçalves, et al., 2018).

Introduction to cellular signalling

Cells are required to interpret information they receive from their environment. These include alterations in the concentrations of nutrients, growth factors, cytokines, cell damaging agents, physical stimulation etc. Accordingly, cells have defined mechanisms to enable them to receive signals, transmit the information and orchestrate appropriate biological responses (Bradshaw & Dennis, 2010). These signal transductions involve numerous signalling molecules that are alternately switched "On" or "Off" per requirement. One of the important phenomena involved in this "On" and "Off" molecular cycling is reversible post-translational modification of proteins. Post-translational modifications are the covalent and enzymatic modification of proteins during or after protein biosynthesis. Proteins can be modified by different post-translational modification mechanisms such as phosphorylation, acetylation, ubiquitynation, sumoylation, glycosylation, lipidation, disulfide bonding and carbonylation (Bürkle, 2001). Of these, reversible phosphorylation plays a major role. *In vitro* studies have shown that the regulation of proteins by phosphorylation accounts for about 30% of post-translational modifications (Burnett, 1954). Protein phosphorylation can modulate a cascade of signalling by altering many cellular functions such as cell division, growth and development, survival, proliferation, and apoptosis.

Reversible phosphorylation involves a phosphorylation reaction, which is the addition of an energetic phosphate group to a molecule; and a dephosphorylation reaction, which is the removal of a phosphate group from the molecule. The phosphorylation reaction is catalysed by protein kinases, whereas the dephosphorylation reaction is catalysed by protein phosphatases (Smoly, et al., 2017). When major protein kinases or receptors are activated, they phosphorylate a wide range of downstream substrates, which if they are kinases as well, will also phosphorylate other proteins thereby initiating a phosphorylation cascade (Kresge, et al., 2005). Protein phosphatases are important to ensure rapid and regulated dephosphorylation of proteins and per implication signalling pathways. The major protein kinases include, PKA (Protein Kinase A), Akt/PKB (Protein Kinase B), PKC (Protein Kinase C), PKG (Protein Kinase G), MAPK (Mitogen Activated Protein Kinase) and Tyrosine protein kinases (Forrest, et al., 2003). We will briefly look at signalling pathways in different cellular phenomenon, and how these major kinases regulate it.

Cellular signalling in Cardiomyocytes during ischemia/reperfusion

Interest in signalling in the heart has been stimulated by the phenomenon referred to as pre-conditioning. Ischemic pre-conditioning (IPC) in the heart is characterised by the exposure of the heart to brief episodes of ischemia followed by subsequent reperfusion (Murry, et al., 1986). By investigating this phenomenon, researchers have managed to study the signalling pathways involved in cell survival and death. In the absence of conditioning, when the heart cells are exposed to prolonged hypoxia/ ischemia, they die. However, when exposed to prolonged hypoxic/ischemic stress after conditioning; the heart

retains the memory of signalling pathways induced for adaptation during conditioning and survives better. Post-conditioning (PostC), characterised by short intervals of reperfusion after prolonged ischemia is considered to have more clinical potential and also make use of the same signalling pathways as IPC (Zhao, et al., 2003). Another type of conditioning is remote-conditioning, where a brief episode of ischemia and reperfusion is induced on a different region of the heart or at a distant organ or limb (Morita, 2011). These cardioprotective mechanisms elicit two phases of protection: early protection, which lasts for a few hours, and the second window of protection which appears after 24 hours and lasts for a few days. Early protection is rapid and transient and is mediated by post-translational modifications whereas the second window of protection is mediated by gene transcription and is thus slow and more sustained (Jennings, et al., 1991).

Studies suggest that the observed protection is mediated by the release of upstream signalling molecules that act as ligands that trigger cascades of signalling events that mediate increased survival and reduced apoptosis. These signalling molecules include adenosine, noradrenaline, acetylcholine, bradykinin, opioids, ROS (Reactive Oxygen Species) and nitric oxide (Hausenloy, et al., 2005). These ligands trigger signal transduction that modulates a wide range of mediator protein kinases which are broadly classified into two pathways: The Reperfusion Injury Salvaging Kinase (RISK) pathway and the Survivor Activating Factor Enhancement (SAFE) pathway. RISK pathway involves protein kinase signalling pathways such as: Phosphoinositide 3-Kinase (PI3K)/Akt/PKB pathway, the MEK/ERK pathway, PKC and MAPK. The SAFE pathway induces the JAK-STAT-3 pathway via TNFα mediated receptor activation. The mediator protein kinases are regulated by secondary messenger molecules such as cAMP, cGMP, DAG/IP3 and Ca^{2+} (Hausenloy & Yellon, 2004). These pathways target antiapoptotic pathways such as the phosphorylation and inhibition of Bax and Bad as well as the inhibition of the release of cytochrome c from the mitochondria. One of the main endpoints of cardioprotection, which inhibits the release of cytochrome c, is keeping the mitochondrial permeability transition pore (MPTP) closed (Juhaszova, et al., 2004).

Figure 1.2 shows a generic representation of signal transduction in cardioprotection, also illustrating interactions between protein kinases and protein phosphatase to regulate survival or cell death. The abbreviations of proteins included in this figure can be found in the glossary.

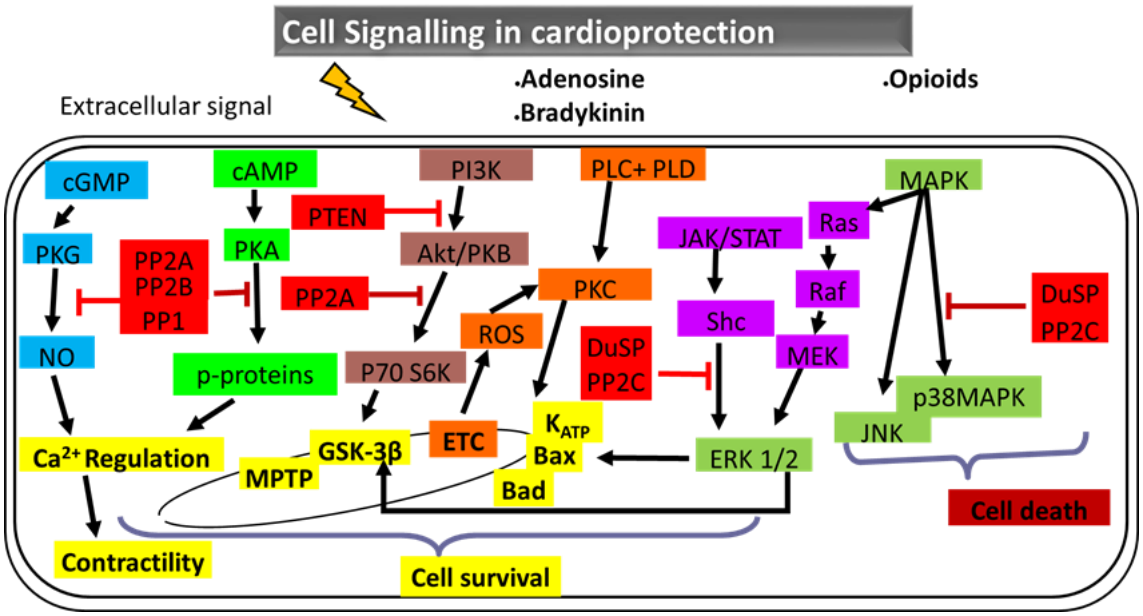

Figure 1.2: A schematic diagram annotated with different colour coding depicting signalling pathways involved in muscle contraction, cell death and cell survival. Protein phosphatases are coloured red and tend to be involved in an inhibitory role in the signalling pathways. The abbreviations of these molecules are listed in the glossary.

Metabolic Signalling in Cancer

Signalling is often dysregulated in cancer. The PI3-K/Akt/PKB pathway is pertinent in facilitating glucose uptake by cells (Świderska, et al., 2018). It has been observed that in cancer cells the PI3-K/Akt/PKB pathway is often overactivated through the loss of its negative regulator PTEN (Chalhoub & Baker, 2009). This leads to an increase in glucose uptake and utilization. 18F-deoxyglucose positron emission tomography (FDG-PET) shows that the disruption of PI3-K/Akt/PKB signalling leads to decreased glucose uptake by tumours, which corresponded with tumour regression (Ma, et al., 2009). Glucose withdrawal induces cell death in a manner indistinguishable from that seen upon withdrawal of growth factor signalling (Vander Heiden, et al., 2001). Glycolysis can be overactivated via the induction of glycolytic enzymes and glucose transporters by oncogenes, such as Ras or Myc (Marbaniang & Kma, 2018). In many human tumours, the MAPK pathway via the extracellular signal-regulated kinases (ERK) 1 and 2, is constitutively active. This is often associated with somatic mutations in genes that encode components that activate the pathway, such as Ras or Raf (Burotto, et al., 2014). Oncogenic mutations can be selected for in cancer populations during metabolic stress. Findings by Yun et al. (2009) showed that glucose deprivation in colon carcinoma cells increased the rate of Ras mutation activation leading to the upregulation of the transporter GLUT1. Surviving clones could cope with limited glucose due to their upregulation of the GLUT1 transporter. Some clones demonstrated KRAS mutations (it is called KRAS because it was first identified as an oncogene in Kirsten RAt Sarcoma virus), and mutant KRAS was shown to upregulate GLUT1 expression (Yun, et al., 2009). In

contrast to oncogenes, the activation of the tumour suppressor p53 leads to the downregulation of glycolysis and increased rate of mitochondrial OXPHOS by inducing the expression and synthesis of cytochrome oxidase assembly 2 (SCO2) (Matoba, et al., 2006). However, p53 is often deactivated in cancer cells, thereby reducing mitochondrial respiration, enhancing glycolysis and anabolic synthesis from glycolytic intermediates (Bensaad & Vousden, 2007). Therefore, the overall activation of oncogenes, loss of the tumour suppressor p53, and activation of PI3-K/Akt/PKB pathway enhance glycolytic flux in cancer cells. Additionally, the loss of p53 promotes the mammalian target of rapamycin complex 1 (mTORC1) activation (Puzio-Kuter, et al., 2009). Taken together: in many cancers, the PI3-K/Akt/PKB /mTOR pathway is overactive, thus reducing apoptosis and allowing proliferation (Agarwal, et al., 2016).

Findings by Duvel et al.(2010) shows that the activation of one of the major targets of mTORC1 activation, namely hypoxia inducible factor 1 alpha (HIF-1α) (a subunit of a heterodimeric transcription factor hypoxia-inducible factor 1 (HIF-1) that is encoded by the HIF-1A gene) can enhance the expression of pyruvate dehydrogenase kinase 1 (PDK1) to inhibit pyruvate dehydrogenase (PDH) activity. The latter enzyme is responsible for converting pyruvate into acetyl-CoA, and concomitantly inhibit mitochondrial metabolism by reducing the delivery of acetyl-CoA to the Krebs cycle, as well as the levels of NADH + H^+ and FADH2 carrying electrons to the electron transport chain. HIF-1 is composed of two subunits: an oxygen-sensitive HIF-1α subunit and a constitutively expressed HIF-1β subunit. Under normal oxygen conditions HIF-1α is polyubiquitinated and targeted for degradation by an E3 ubiquitin ligase complex. HIF-1α is stabilized and functional at low oxygen levels. Moreover, HIF-1α can enhance glycolysis by increasing the expression of genes that encode glycolytic enzymes and glucose transporters (Duvel, et al., 2010).

Hypoxia and cellular pathology

Hypoxia is characterised by critically low oxygen levels and is often the result of ischemia. Cells require a continuous supply of blood. The disruption of the blood supply is a stressor which induces a wide range of pathological responses in the cell. The severity of hypoxia determines whether cells become apoptotic, necrotic or adapt and survive (Jacob & Cory, 2008). We will explore how hypoxia is a stressor that affects both proliferative cancer cells and differentiated cardiomyocytes.

Cardiomyocytes and hypoxia

Mammals are born with a definite number of cardiomyocytes, which increase in size as the organism grows during post-natal development. It is believed that when the organism matures, the cardiomyocytes regenerative capacity reduces to minimal, although a small degree of regenerative capacity is retained (Ali, et al., 2014). If cardiac tissue is damaged, as in the case of hypoxia, there is

reduced chance that it will self-renew (Uygur & Lee, 2016). Hypoxia in the heart is mostly induced by ischemia characterised by reduced blood flow in the coronary circulation, leading to oxygen supply/demand mismatch. As discussed earlier in the text, terminally differentiated cardiomyocytes are aerobic with high oxygen and ATP demands necessary for continuous contraction. Heart cells are therefore dependent on a constant supply of nutrients (Paradis, et al., 2014). When this supply is compromised, as is the case during hypoxia, it leads to metabolic shifts, from mitochondrial OXPHOS to anaerobic glycolysis. Sustained ischemia is associated with reduced ATP levels, cell death and reduced or dysregulated contractility activity (Jennings, 2013).

Cardiomyocytes and hypoxia signalling

Ischemic pre-conditioning and post-conditioning uncovered some of the mechanisms involved during ischemia and reperfusion. A study by Cai et al. (2008) showed that heterozygous HIF-1α - deficient mice exposed to ischemic preconditioning lost the protective effect, suggesting the importance of HIF-1α in survival signalling. Hypoxic gene regulation involves transcription factors HIF-1α, activating protein -1 (AP-1), nuclear factor kappa-light-chain-enhancer of activated B cells (NF-κB), signal transducer and activator of transcription 1/3 (STAT 1/3) and survival protein 1 (SP1). The hypoxia induced transcription factors are reported to be regulated via the MAPK pathway (Cai, et al., 2008). It has also been reported that certain isoforms of PKC (Protein Kinase C) can activate the Ras/Raf/MEK/ERK signalling pathway on the level of the Ras GTPase and Raf kinase. A study on hypoxia in rat cardiomyocytes found that hypoxia induced the redistribution of specific PKC isoforms from the soluble to the particulate compartment, which lead the authors to suggest that the PKC pathway was activated during hypoxia. For further investigation, when they inhibited phospholipase C, the previously noted PKC redistribution was not observed. They therefore concluded that, hypoxic signalling might involve cross talk between protein kinase C and MAPK signalling pathways (Goldberg, et al., 1997).

Cardiomyocytes metabolic adaptation and hypoxia

Cardiomyocytes harbour the ability to utilise diverse substrates depending on their availability and the cell's energy demands. This metabolic flexibility is regulated by complex regulatory mechanisms at multiple levels, including transcription, post-translational modification and allosteric regulation by substrates and their metabolites (Ritchie & Delbridge, 2006). Examples include:

- The metabolic shifts of the glycolysis-dependent foetal heart to oxidative metabolism in the adult heart, via the regulation of transcription of the proteins involved in fatty acid oxidation (FAO).
- The HIF-1α transcriptional regulation in metabolic adaptation to hypoxic and ischemic conditions.
- The shift of substrate oxidation between glucose and fatty acid regulated by the phosphorylation and inactivation of PDH by pyruvate dehydrogenase kinase 4 (PDK4).

Moderate ischemia induces an increase in glucose uptake and glycolysis, thereby offering protection. However, when the severity of ischemia escalates, H^+, lactate and NADH increases and glucose uptake decreases, leading to reduced ATP levels, reduced pH, electrolyte imbalance and increased intracellular osmolarity and cellular swelling (Jennings, et al., 1964). Reduced ATP levels lead to the opening of K^+ channels with subsequent extracellular K^+ increase and depolarization of the cell membrane potential. This depolarization may lead to the inactivation of fast Na^+ channels and T-type Ca^{2+} channels (Klabunde, 2017). Initially, in response to increased H^+, the cell recruits necessary buffering mechanisms, which include an increase in Na^+/H^+ exchange that pumps Na^+ into the cell in exchange for H^+. However, this buffering mechanism leads to an increased Na^+ concentration, triggering another mechanism that exchanges Ca^{2+} for Na^+ which leads to increased intracellular Ca^{2+} levels via the Ca^{2+}/Na^+ exchanger. In addition, the increase in Ca^{2+} induces more Ca^{2+} efflux from the Sarcoplasmic Reticulum, leading to Ca^{2+} overload (Jennings, 2013). Refer to Figure 1.3. for an illustration of the metabolic response of the heart to ischemia.

Furthermore, ischemia inhibits membrane functions such as Na^+ pumps, mitochondrial ATP/ADP translocase and the phospholipid cycle. The breakdown of phospholipids by phospholipases also leads to increased intracellular Ca^{2+} levels. Ca^{2+} overload has diverse detrimental effects such as hypercontraction and induced cell death (Kalogeris, et al., 2012). Taken together, when the heart is exposed to ischemia, glycolysis is triggered and both OXPHOS and anabolic metabolism are inhibited (negative feedback loop due to product accumulation). This results in lactic acid accumulation, reduced pH, reduced ATP, electrolyte imbalance, calcium overload, and finally accelerated cell death through necrosis (Jennings, et al., 1964).

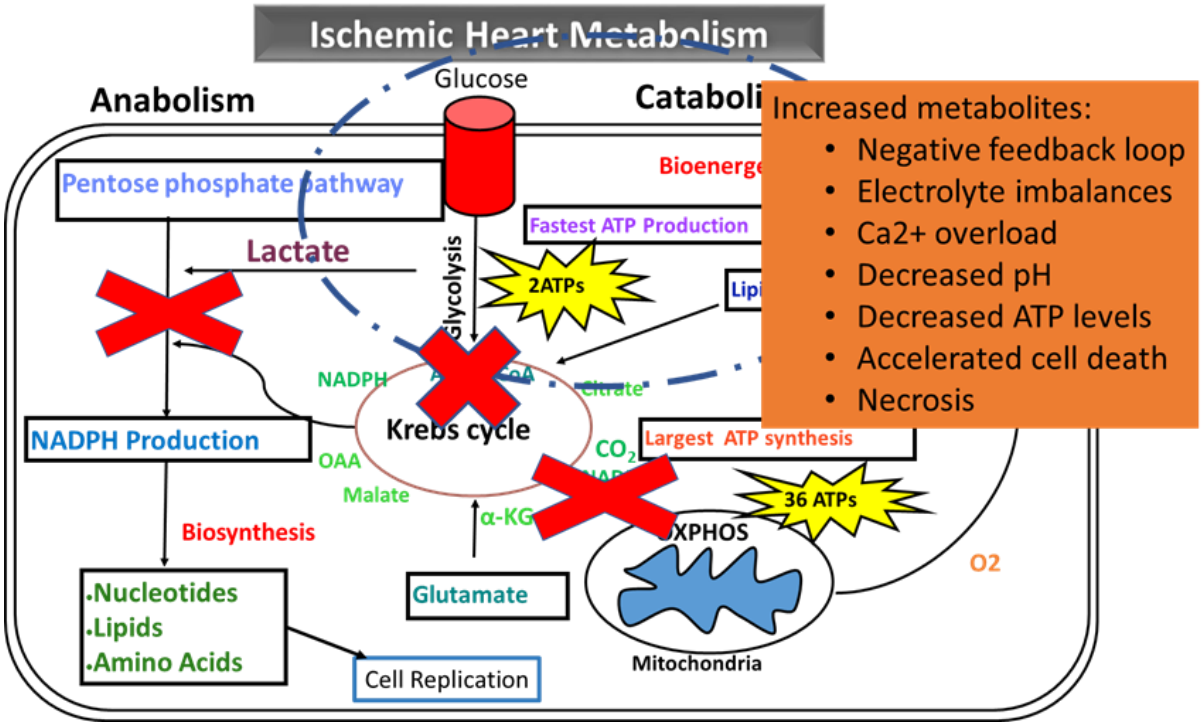

Figure 1.3. A schematic overview of the metabolic response of the heart during ischemia. This diagram shows that under ischemic conditions the heart favours glycolysis; while OXPHOS and anabolic metabolism is inhibited due to product accumulation. It also shows the consequences of this metabolic shift, including electrolyte imbalance, Ca^{2+} overload, low pH, low ATP levels, and accelerated cell death through necrosis.

Survival signalling pathways in the ischemic heart

Studies of cardioprotective interventions such as pre-conditioning, post-conditioning and remote conditioning have revealed the signalling pathways which orchestrate survival and mediate cell death. The protective RISK and SAFE pathways mediate survival by inhibiting apoptotic pathways. These include the phosphorylation of Glycogen synthase kinase-3B (GSK-3B), which inhibits the opening of the mitochondrial permeability transition pore (MPTP) and the endothelial Nitric oxide synthase (eNOS)/NO/PKG/PKC-α pathway (Tamareille, et al., 2011). This pathway mediates the opening of the ATP sensitive mitochondrial potassium ($mitoK_{ATP}$) channels and ROS production, concomitantly inhibiting the MPTP and modulating intracellular Ca^{2+} by increasing Ca^{2+} uptake by the sarcoplasmic reticulum Ca^{2+}-ATPase (SERCA) (Hausenloy & Yellon, 2006). The second window of protection is mediated by inducing the HIF-1α induced transcription of inducible nitric oxide synthase (iNOS), NFkB, MAP-1, phospholipase-1, cyclooxygenase-2 (COX-2), hemeoxygenase (HO)-1 and erythropoietin (EPO) (Cai, et al., 2003).

Cancer cells and hypoxia

As tumours grow, rapidly proliferating tumour cells outgrow their blood supply, thereby rendering portions of the tumour with regions exposed to hypoxia. In response to these changes, the tumour cells activate certain signal transduction pathways and gene regulatory mechanisms to adapt. In healthy eukaryotic cells, the response to hypoxia includes the expression of genes that are involved in cellular metabolism (e.g. anaerobic glycolysis), erythropoiesis, cellular proliferation and survival, as well as vascularization (Semenza, 2001). Moreover, transcription factors such as HIF-1α, AP-1, SP1 and NF-κB are also activated upon cellular hypoxia. HIF-1α is targeted for ubiquitination and degradation by von Hippel Lindau tumour suppressor protein under normoxic conditions (Haase, 2009). Ravi et al. (2000) showed that p53 can regulate HIF-1α. The expression of p53 has been shown to negatively regulate HIF-1α protein levels via induction of Murine double minute 2 (MDM2) mediated ubiquitination. Proteasomal degradation of HIF-1α and MDM2 negatively regulate p53 by acting as a specific E3 ligase for p53, and thus promotes p53 ubiquitination and degradation (Ravi, et al., 2000). Phosphorylated p53 causes cell growth arrest and/or apoptosis through p53 target gene transcription. Among many phosphorylation sites of p53, phosphorylation at serine 15 has been best characterized and has been shown to lead to p53 stabilization and an increase in protein levels and transcriptional activity (Brooks & Gu, 2003). An animal study using p53-deficient colon cancer enhanced tumour growth and neovascularization of tumour in nude mice. This loss of p53 enhanced HIF-1α activity and vascular endothelial growth factor (VEGF) expression under hypoxic conditions (Ravi, et al., 2000). Furthermore, in another study, HIF-1α activity was inhibited by an anti-sense technique in mouse tumour cells; this led to reduced aggressive tumour growth (Kung, et al., 2000).

Activated HIF-1α stimulates a variety of genes such as: erythropoietin, lactate dehydrogenase A (LDH-A) and vascular endothelial growth factor (VEGF). HIF-1α is also known to modulate glycolytic genes to adapt to the reduced oxygen availability and consumption (Semenza, et al., 1994). These genes include: glucose transport 2 (GLUT2), hexokinase (HK), phosphoglucose isomerase (PGI), phosphofructokinase (PFKL), fructose-bisphosphate aldolase (ALDO), glyceraldehyde-3-phosphate dehydrogenase (GAPDH), phosphoglycerate kinase (PGK), phosphoglycerate mutase (PGM), enolase 1 (ENOA), pyruvate kinase (PK), pyruvate dehydrogenase kinase, isozyme 1 (PDK1) and LDH-A (Denko, 2008).

Glycolysis in cancer has been shown to occur even in the presence of oxygen (Pauwels, et al., 1998). It can also be expected that tumour hypoxia will select for cells dependent on anaerobic metabolism (Vander Heiden, et al., 2009). Tumour hypoxia was once thought to be a determining factor in the cancer metabolic shift to glycolysis. However, evidence suggests tumour hypoxia to be a late-occurring event that might not have significant contribution in the switch to anaerobic glycolysis by cancer cells. In response to ischemia, the tumour reduces the production of biomass, and adapts metabolism

accordingly to favour anaerobic glycolysis (Romero-Garcia, et al., 2011). For a diagrammatic illustration of the metabolic response of cancer and other proliferative cells during ischemia refer to Figure 1.4.

Under normal physiological conditions, environmental stressor such as prolonged hypoxia induces apoptosis (Kerr, et al., 1972). However, in tumours, hypoxia serves as a positive selection pressure that selects for mutations that can survive hypoxia better. It has been shown that repeated exposure to low oxygen tension selected for p53 mutations and rendered tumour cells resistant to hypoxia-induced apoptosis (Graeber, et al., 1996). Moreover, many studies have shown that low oxygen tension confers resistance to irradiation therapy, possibly contributing to tumour aggressiveness, meaning that tumour hypoxia is not a limitation for tumour growth (Harris, 2002).

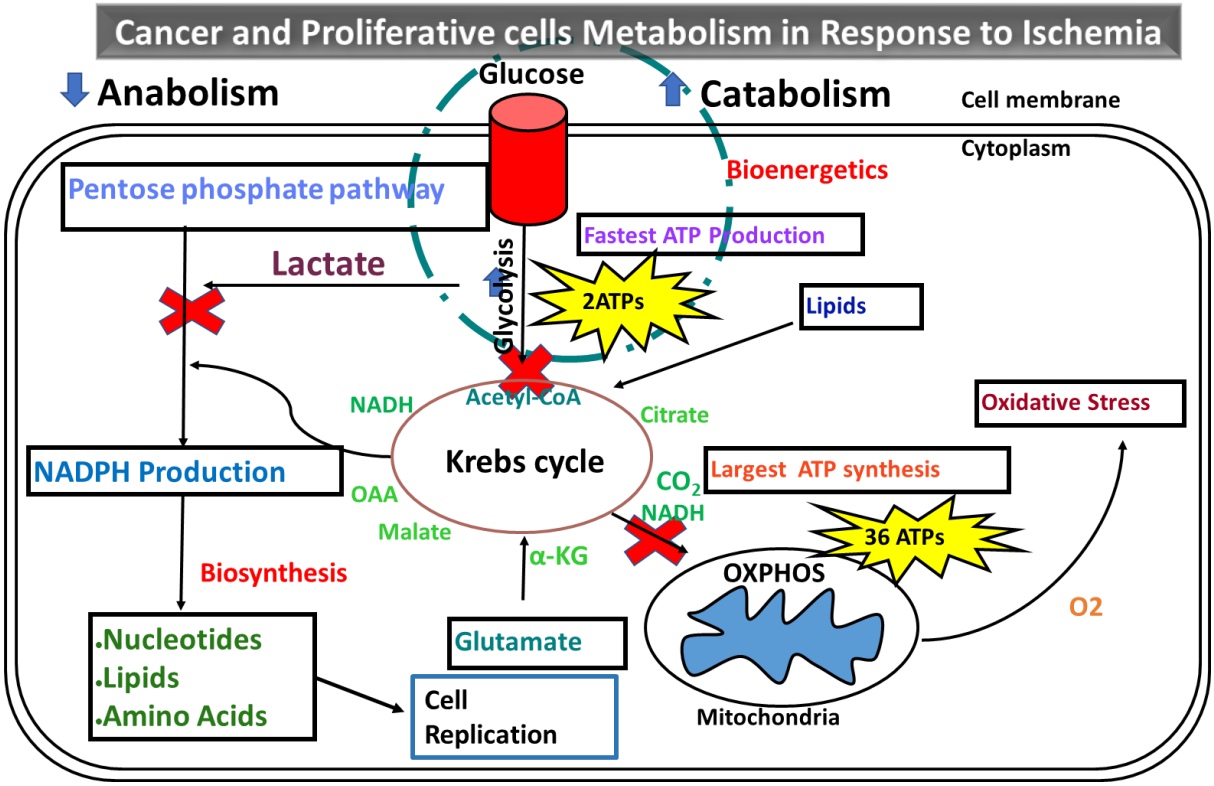

Figure 1. 4. A schematic overview of metabolic adaptation by cancer and proliferative cells during ischemia. During tumour hypoxia the cancer cells favour glycolysis, inhibiting OXPHOS. When hypoxia/ ischemia occurs, the cell goes into a starvation state; reducing all energy consuming processes such as anabolic metabolism, while increasing catabolic metabolism to promote glycolysis and maintain the cellular energy state. This metabolic shift in turn minimises cell death, especially necrotic death.

One of the well-studied signalling pathways implicated in the survival response to tumour hypoxia is the MAPK pathway. A study by Berra et al. (2000) on hamster fibroblasts suggested that the ERK superfamily directly phosphorylates and activates HIF-1α under conditions of low oxygen tension. Under hypoxic conditions, the phosphorylation status of HIF-1α is a critical factor which determines whether HIF-1α will promote apoptosis or not. Phosphorylated HIF-1α is anti-apoptotic, whereas

dephosphorylated HIF-1α exerts pro-apoptotic effects (Suzuki, et al., 2001). This phosphorylation enhances the HIF-1α dependent transcriptional activation of the VEGF gene (Berra, et al., 2000). *In vitro* studies in human squamous carcinoma cells have shown that hypoxia and hypoxia/reoxygenation signalling activates the JNK and p38 stress kinases. After 4 hours, they found that hypoxia induced the mRNA expression and activity of the JNK antagonist, mitogen-activated protein kinase phosphatase (MKP)-1. They suspected that MKP-1 enhanced expression and activity under hypoxia could account for the rapid decline of JNK activity that occurs after 4 hours (Laderoute, et al., 1999). In addition, a study in melanoma showed that JNK is indeed activated during the tumour hypoxia stage, leading to apoptosis. However, this JNK activity is eventually lost. Hypoxic activation of JNK has been shown to be able to induce cJun dependent transcription, a main downstream target of JNK kinase signalling (Kunz, et al., 2002). cJun is a defined member of the Jun/Fos family of transcription factors. The heterodimerization of cJun and cFos form the transcriptional active complex, activator protein-1 (AP-1) which acts as a tumour promotor (Chang & Karin, 2001; Karin, et al., 1997). A study by Rupec and Baeuerle (1995) provided evidence that AP-1 regulates gene transcription under hypoxic conditions (Rupec & Baeuerle, 1995). In this study, they also showed that the transcription factor NF-κB plays an integral role in the regulation of genes under hypoxia/reoxygenation conditions. The p38 pathway has also been suggested to activate NF-κB. Kunz et al., (2002) showed that the p38 pathway is activated by hypoxia/reoxygenation in melanoma cells. From previous observations that p38 mediated apoptosis is induced under conditions of oxidative stress; researchers suggest that p38 is possibly involved in the regulation of apoptosis under hypoxic conditions as well (Tobiume, et al., 2001).

Hypoxia mediated apoptosis utilizes different intracellular pathways involving molecules such as cytochrome c, members of the Bcl-2 family, Akt/PKB and PTEN. Apoptosis in tumour hypoxia is poorly understood. However, studies have reported that tumour regions that are poorly vascularized are characterised by apoptosis (Holmgren, et al., 1995). One of the proposed mechanisms is MPTP induced cytochrome c release and subsequent apoptosis (Srinivasan, 2012). In addition to the MPTP induced apoptosis theory, evidence suggests that hypoxia can induce apoptosis via Bax, a pro-apoptotic Bcl-2 family member, which induces mitochondrial outer membrane pore formation that facilitate cytochrome c release (Saikumar, et al., 1998). They propose that members of the Bcl-2 family of anti-apoptotic molecules Bcl-2 and Bcl-xL can inhibit the observed hypoxia induced apoptosis.

Another proposed mechanism of apoptosis by tumour hypoxia in Jurkat cells is the activation of the extrinsic apoptotic pathway mediated by caspase 8 (Malhotra, et al., 2001). From these observations it was hypothesized that cellular expression levels of caspase 8 influences the sensitivity to apoptosis inducing agents. To confirm their speculation, they knocked down caspase 8 in neuroectodermal brain tumour cells, where they observed that caspases 8-deficient tumour cells were resistant to TNF-related apoptosis-inducing ligand (TRAIL) induced apoptosis (Grotzer, et al., 2000).

Studies on PC12 cells showed that PI-3K/Akt/PKB activation by hypoxia prevented cells from hypoxia-induced apoptosis, possibly by phosphorylating HIF-1α. Empirical data showed that activation of the PI-3K/Akt/PKB pathway conferred resistance to hypoxia-induced apoptosis, which was reversed by treatment with PI-3K/Akt/PKB pathway inhibitors LY294002 and wortmannin. Linked to this, the activation of the PI-3K/Akt pathway is implicated in tumour aggressiveness by enhancing cell survival (Bacus, et al., 2002).

Introduction to phosphatases

As discussed, post-translational modification includes protein modulation by reversible phosphorylation with protein kinases catalysing the phosphorylation reaction and protein phosphatases catalysing the dephosphorylation reaction (Voet, et al., 2006). In eukaryotes, reversible phosphorylation occurs on the hydroxyl-group containing amino acid residues, serine (Ser), threonine (Thr) and tyrosine (Tyr). Consequently, proteins that catalyse the phosphorylation and dephosphorylation reactions are categorised per type of amino residues they target. Three fundamental groupings can be distinguished: those which target serine or threonine residues (serine/threonine kinase and phosphatase), those which target tyrosine residues (tyrosine kinase or phosphatase) and those that are able to target all of them (dual specificity kinase and phosphatase) (Vlastaridis, et al., 2017). A proteomic analysis study by Olsen et al. (2004) reported that of the 2244 total human proteins which they detected, there were 6600 phosphorylation sites with 86.4% on serine residues, 11.8% on threonine and 1.8% on tyrosine residues. The sequencing of the entire human genome revealed that there are about 518 genes encoding for protein kinases with 438 encoding for serine/threonine kinases and 90 encoding for tyrosine kinases (Olsen, et al., 2006). On the other hand, sequencing by Alonso (2004) reported that there are only about 30 genes encoding for serine/threonine phosphatase and 107 genes encoding tyrosine phosphatases (Alonso, et al., 2004).

As previously mentioned, protein phosphatases nucleophilically attack the phosphate group in the presence of a water molecule, thereby dephosphorylating the relevant phosphorylated amino acid (Barford, 1996). Phosphatases are classically categorised into three types: Protein Serine/threonine Phosphatase (PSP), Protein Tyrosine Phosphatase (PTP) and Dual Specificity Phosphatase (DuSP). PSPs are further categorised into two major families: Phosphoprotein phosphatases (PPPs) and Mg^{2+}-dependent phosphatases (PPMs). The members of PPPs include: type1 Protein Phosphatase (PP1), type 2A Protein Phosphatase (PP2A), type 2B Protein Phosphatase (PP2B- calcineurin), type 4 Protein Phosphatase (PP4), type 5 Protein Phosphatase (PP5), type 6 Protein Phosphatase (PP6) and type 7 Protein Phosphatase (PP7). The PPM family includes type 2C Protein Phosphatase (PP2C) (Tonks, 2006). As mentioned earlier, there are 438 genes encoding for serine/threonine kinases with only 30 encoding for PSPs. PSPs ensure specificity for numerous substrates via a modulatory approach in which

different combinations of regulatory and scaffolding subunits give rise to several holoenzymes with varied properties, including substrate specificity and subcellular distribution. In this regard it is useful to note that PSPs have many regulatory subunits (Shi, 2009).

On the other hand, genes encoding for PTPs match those encoding for tyrosine kinases (Bhaduri & Sowdhamini, 2003). PTPs are classically composed of a single chain with one or more domain that allows them to facilitate a more tightly regulated substrate specificity contrasted to PSPs, which generally have multiple subunits that generate a broader substrate specificity and flexibility (Shi, 2009). PTPs are classified into two groups: cytosolic non-receptor and transmembrane receptor-like PTPs. PTPs have a highly conserved catalytic subunit motif C(X)5R called the PTP signature motif (Barford, et al., 1998). DuSPs are generally categorized as a subfamily of PTP due to structural similarities. Indeed, the only structural difference is that DuSPs have a broader and shallower catalytic motif which allows for the pocketing of both serine/threonine and tyrosine phosphorylated substrates. However, they both have retained an evolutionary conserved consensus that contains a cysteine at the catalytic site, which forms a thiol-phosphate intermediate during catalysis. Thiol- reducing agents activate these enzymes, whereas oxidizing agents inactivate them (Eswaran, et al., 2006; Cho, et al., 1992).

Serine/ Threonine Protein Phosphatase

In this review, we will take a closer look at the three major proteins serine/threonine phosphatases, PP1, PP2A, and PP2B (calcineurin) in eukaryotes and how they are regulated in cardiomyocytes, cancer and by hypoxia. Of note, the mechanisms discussed in cardiomyocytes will be from pre-and post-conditioning applications, as well as pharmacological and laboratory genetic modulation of these phosphatases under hypoxic conditions.

Type-1 protein phosphatase (PP1)

Type-1 Protein phosphatase (PP1) is a multifunctional serine/threonine phosphatase, which is ubiquitously expressed in eukaryotes and influences diverse aspects of cellular biology (Ceulemans & Bollen, 2004; Cohen, 2002). PP1 is comprised of a 30-kDa single domain catalytic subunit and multiple regulatory subunits which form complexes with the catalytic domain (Goldberg, et al., 1995). The PP1 catalytic subunit exists as four different isoforms; namely; PP1α, PP1 γ1, PP1γ2, and PP1δ (Andreassen, et al., 1998). PP1 has about 100 regulatory subunits which modulate subcellular compartments, enzyme activity, localization, and substrate specificity. PP1 can also associate with other proteins thereby regulating their activity. The catalytic subunit of PP1 forms an α/β fold with a central β-sandwich

arranged between two α-helical domains. The interaction of the three β-sheets of the β-sandwich creates a channel for catalytic activity, as it is the site of coordination of metal ions (Egloff, et al., 1997). The catalytic site is made up of three histamines, two aspartic acids and one asparagine which allows for association with metal ions. The binding of two metals in the presence of water leads to the nucleophilic attack of the phosphorus atom of the target substrate (Andreassen, et al., 1998).

Type-2A protein phosphatase (PP2A)

Type-2A Protein Phosphatase (PP2A) is a highly complex molecule which exists in both a dimeric and a trimeric form. The heterodimeric form is known as the core enzyme and is composed of the catalytic and scaffold subunit, while the heterotrimeric form is comprised of catalytic, scaffold and regulatory subunits forming a holoenzyme. Up to 70 different combinations of the holoenzyme complex can be formed to perform diverse biological functions (Seshacharyulu, et al., 2013). The PP2A catalytic subunit is a 37kDa globular structure which is ubiquitously expressed in almost every tissue with high abundance in the heart and brain. PP2A catalytic subunits share 50% amino acid sequence similarity with PP1 and 40% identical sequences with PP2B (calcineurin) (Seshacharyulu, et al., 2013). The catalytic and scaffold subunits have two isoforms each (α and β); whereas, there are four different regulatory subunit families [B (commonly known as B55/PR55), B′ (B56/PR61), B″ (PR48/PR72/PR130), and B‴ (PR93/PR110)] containing different isoforms. Both PP2A catalytic subunit isoforms are comprised of 309 amino acids and share 97% sequence similarity. PP2ACα knockout mice die after 6 days of embryonic development suggesting its importance in embryonic development and gastrulation, as well as a lack of redundancy in terms of the β isoform (Khew-Goodall & Hemmings, 1988). The scaffolding subunit of the heterodimeric form of PP2A acts as a regulator by changing the catalytic specificity; whereas in the heterotrimeric form it acts as a structural assembly base to escort the catalytic subunit and to facilitate interaction with the regulatory subunit and other substrates (Cho & Xu, 2007).

The activity of PP2A can be regulated via post-translational modifications such as methylation and phosphorylation (DeGrande, et al., 2012). PP2A is localized both in the nucleus and cytoplasm where it plays a central role in many cellular functions such as metabolism, cell cycle, DNA replication, transcription and translation, signal transduction, cell proliferation, cytoskeletal dynamics, cell mobility and apoptosis. PP2A is a well-known tumour suppressor although some researchers have shown it to be a tumour promoter (Janssens, et al., 2005). It has therefore also been implicated in cell transformation and cancer development (Ciccone, et al., 2015).

Type-2B protein phosphatase (PP2B- Calcineurin)

Type-2B Protein Phosphatase (PP2B-calcineurin), is a calcium and calmodulin dependent serine/threonine phosphatase. PP2B is comprised of two subunits: a 61kDa calmodulin-binding catalytic subunit [calcineurin A (CNA)] and a 19kDa Ca^{2+} -binding regulatory subunit [calcineurin B (CNB)] (Rusnak & Mertz, 2000). The catalytic subunit has three isoforms encoded by three separate genes: PPP3CA, PPP3CB and PPP3CC. The regulatory subunit has two isoforms encoded by two genes, PPP3R1 and PPP3R2. In response to an increase in Ca^{2+} levels, calmodulin binds to PP2B, where it displaces the autoinhibitory domain from the active site, leading to the activation of PP2B and subsequent dephosphorylation of target proteins (Klee & Yang, 2010). PP2B substrates include transcription factors, proteins involved in the cell cycle and apoptosis, cytoskeletal proteins, scaffold proteins, membrane channels and receptors. The best studied substrate of PP2B is the nuclear factor of activated T cells (NFAT) transcription factor, which is translocated upon dephosphorylation to the nucleus where it regulates gene expression, including genes encoding cytokines in immune cells (Liu, et al., 2005; Yamashita, et al., 2000).

Protein Tyrosine phosphatases (PTP)

As mentioned earlier, Protein Tyrosine Phosphatases (PTPs) are categorised into cytosolic non-receptor and transmembrane receptor-like tyrosine phosphatases (Paul & Lombroso, 2003). Almost all PTPs are monomeric with various targeting domains that flank the catalytic domain, regulating the activity and subcellular localization of the enzyme. The receptor-like phosphatases are transmembrane receptors that contain a phosphatase domain. These types of PTPs are characterised by an extracellular domain, transmembrane region and C- terminal catalytic cytoplasmic domain. The extracellular domain may have MAM (meprin, A-5 protein, and receptor protein tyrosine phosphatase mu) domains, carbonic anhydrase-like domains, fibronectin type III repeats or immunoglobulin-like domains, while the C-terminal domain is comprised of both a catalytically active domain (D1), as well as an inactive domain (D2) (Neel & Tonks, 1997). The structural integrity of the D2 domain is essential in the stability of the receptor PTPs (RPTP) (Blanchetot, et al., 2002). It has also been speculated that D2 might be a regulator of D1 or involved in mediating substrate recognition. PTPs are classified into 4 classes: 1) class I which is the largest group with 99 members. They are subdivided into 38 classical PTPs and 61 VH-like or dual specificity phosphatases; 2) class II includes the low molecular weight (LMW) phosphatase or acid phosphatases; 3) class III includes Cdc25 phosphatases; and 4) class IV includes four classes of Eya pTy-specific phosphatases. All classes beside class IV, share a highly conserved active site motif and similar core structure comprised of a parallel β-sheet with flanking α-helices which contains a β loop-α

loop (Dixon & Denu, 1998; Sun, et al., 2003). The PTPs have multiple biological functions such as: regulation of signalling pathways, control of the cell cycle, cell growth, cell proliferation, differentiation, transformation and synaptic plasticity (Paul & Lombroso, 2003).

Dual specificity phosphatases

The Dual-Specificity Phosphatases (DuSP) are classified as a subtype of PTPs. Genome analysis reported that there are at least 61 different DuSPs identified in humans. All DuSPs families share a similar catalytic mechanism with a conserved cysteine residue that forms a covalent intermediate with the targeted phosphate group (Denu & Dixon, 1995). The amino acid residues around the core catalytic enzyme have a conserved consensus site: His-Cys-X-X-X-X-X-Arg-Ser. The serine and aspartate residue play a major role in the catalytic activity of the DuSPs. DuSPs are classified into 5 types based on the closeness of their evolutionary relation: Slingshot phosphatase, phosphatase of regenerating liver (PRLs), cdc14 phosphatases, PTEN and myotubularin phosphatases and the mitogen-activated protein kinase phosphatases (MKPs) (Denu & Dixon, 1995; Patterson, et al., 2009).

Phosphatase regulation in Cardiomyocytes and Cancer

Very little research has been done on phosphatases in the heart. However, phosphatase mutations have been reported in cancer cells (Cristofano & Pandolfi, 2000; Stemke-Hale, et al., 2008; Schönthal, 2001). Discussing and comparing the regulation of different phosphatases in these two systems might illuminate phosphatases mediated control of cell survival and cell death. It has been established that the activation of survival kinases protects the heart against ischemic injury (Hausenloy & Yellon, 2004). Many survival kinases are substrates for protein phosphatases and can therefore be regulated by protein phosphatases. In the ischemic rat heart, the inhibition of PP1 and PP2A by okadaic acid have been proven to promote cell survival characterized by reduced infarct size (Armstrong & Ganote, 1992). These findings were further confirmed by Weinbrenner et al. (1998) using fostriecin, an inhibitor of PP2A (Weinbrenner, 1998). Okadaic acid has been identified as a tumour promotor which inhibits the enzymatic activity of PP2A promoting carcinogenesis; confirming PP2A as a tumour suppressor (Suganuma, et al., 1988). With regards to PTPs, their inhibition in the heart by orthovanadate upregulated the phosphorylation and activation of the death pathway p38MAPK, which lead to high levels of lactate dehydrogenase, indicative of cell injury (Swarup, et al., 1982). Another group showed that treatment with sodium orthovanadate after 30 minutes of reperfusion reduced infarct size in a dosage dependent manner. Orthovanadate treatment also ameliorated contractile dysfunction of the left ventricle 72 h after reperfusion (Takada, et al., 2004). Most identified PTPs in cancer cells are mutated

and inhibited to promote cell survival, proliferation and migration. In the following section, we will discuss how different phosphatases are regulated in cardiomyocytes and cancer cells during hypoxic conditions, focussing on three-major serine/threonine phosphatases: PP1, PP2A and PP2B (calcineurin).

PP2A regulation in myocardial infarction (cardiomyocytes and hypoxia)

Weinbrenner et al. (1998) investigated the effect of PP2A inhibition by fostriecin on myocardial infarction in isolated rabbit hearts. They induced 30 minutes of cardiac regional ischemia, followed by a two hours reperfusion period. Fostriecin, was administered 10 to 15 minutes after the onset of ischemia. They quantified the infarct size (IFS) using triphenyltetrazolium chloride staining. Their results showed that isolated hearts pre-treated with fostriecin showed 25% less infarct compared to un-treated control. They observed that 8% infarct size following fostriecin pre-treatment was comparable with the 9% observed following pre-conditioning. Moreover, to investigate whether the protective effect in pre-conditioning was mediated by PP2A or PP1, they measured their activity. Their results suggested that there wasn't any measurable change in PP2A or PP1 activity during pre-conditioning. These findings suggest that the mechanism of protection by PP2A inhibition was not the same as with pre-conditioning, because PP2A activity was not identified during pre-conditioning (Weinbrenner, 1998). Earlier, similar effects of PP2A inhibition in myocardial infarction were observed by Armstrong & Ganote (1992) using okadaic acid and calyculin A.

Findings from Van Vuuren (2014) (PhD thesis) in our research group evaluated the effect of PP2A inhibition by okadaic acid and PP2A activation by FTY 720 in isolated working rat hearts. In this study, regional ischemia was induced for 35 minutes, where after infarct size was measured. Global ischemia was induced for 20 minutes where after functional recovery was assessed, and tissue was harvested for biochemical analysis. They found that okadaic acid pre-treatment reduced infarct size; whereas, pre-treatment with FTY 720 exacerbated infarct size. To investigate the effect of PP2A on intracellular signalling; the phosphorylation status of Akt/PKB, ERK1/2, GSK-3β and p38MAPK was quantified using Western blotting. The results showed that, okadaic acid pre-treatment lead to increased phosphorylation of survival proteins Akt/PKB, ERK1/2 and GSK-3β at the onset of reperfusion. While FTY 720 pre-treatment lead to reduced phosphorylation of Akt/PKB, GSK-3β and p38MAPK, both at the end of ischemia and onset of reperfusion (Van Vuuren, 2014). A study by Hoehn et al. (2015) investigated the effect of PP2A overexpression in mice suffering from chronic myocardial infarction. Myocardial infarction was induced by ligation, where after they assessed cardiac function using echocardiography. The cardiac function was measured before and 28 days after myocardial infarction. These procedures were followed in CD-1 mice overexpressing the α catalytic subunit of PP2A and CD-

1 mice with normal PP2A function. They observed that, the mice overexpressing PP2A had more adverse effects, characterized by a large infarct size compared to wild type. Moreover, mice overexpressing PP2A were observed to have adverse remodelling characterised by myocyte hypertrophy and interstitial collagen infiltration. Their results also showed that cell death in mice overexpressing PP2A was significantly higher than wild type 48 hours after myocardial infarction (Hoehn, et al., 2015). It therefore seems that PP2A increased activity is detrimental whereas the inhibition promotes cell survival in the heart in the context of ischemia/reperfusion.

PP2A regulation by hypoxia

Studies have shown that hypoxia induces the expression and activation of PP2A. An *in vitro* study using glioblastoma multiform- derived tumour stem cell-like cells (GBM-TSCs), reported that PP2A activity increased with increased HIF-1α during hypoxia (Hofstetter, et al., 2012). The activated PP2A mediated the inhibition of G1/S phase growth and reduced cellular ATP consumption in hypoxia, thereby promoting tumour cell survival. Conversely, the inhibition of PP2A lead to reduced intracellular ATP levels and increased p53-independent cell death under hypoxic conditions (Hofstetter, et al., 2012).

PP2A regulation in cancer

PP2A is reported to be functionally inactivated in most cancers. Among the targets of PP2A are proteins associated with oncogenic signalling cascades such as Raf, MEK and Akt/PKB, where PP2A acts as a tumour suppressor (Mumby, 2007). Okadaic acid, a known catalytic inhibitor of PP2A induces tumour development when injected into mice (Nagao, et al., 1995). Tumour antigen-SV40 small T antigen, which alters the activity of PP2A via interference with the regulatory subunit also induces tumour development (Campbell, et al., 1995). The scaffold and regulatory subunits of PP2A have been shown to be mutated or aberrantly expressed in many different types of cancer. Mutations in the scaffolding subunit have been reported in breast, skin, cervix, ovary and lung cancer as well as melanoma (Calin, et al., 2000). The regulatory subunit α isoform (PR65β/Aβ) has also been found to be mutated in colon and lung cancer (Wang S.S, et al., 1998). A study in HEK293 cells showed that a 50% reduction in the PP2A scaffolding isoform (Aα) levels reduced the PP2A regulatory isoform (B'γ) holoenzyme activity, which enhanced the activity of Akt/PKB that subsequently enhanced tumour formation in immune-deficient mice (Chen, et al., 2005). Another regulatory subunit isoform (B55α) is important in the regulation of Akt/PKB by facilitating its dephosphorylation at T308. The suppression of B55α in cancer leads to consistent activation of Akt/PKB which increases proliferation (Ruvolo, et al., 2011). The

isoform B56γ interacts with p53 and mediates its dephosphorylation at Thr55 enhancing p53 tumour suppression (Shouse, et al., 2010).

PP1 regulation in cardiac function

Type 1 Protein Phosphatase (PP1) is a highly conserved serine/threonine phosphatase involved in various biological functions (Tournebize, et al., 1997). Alterations in the activity of PP1 had been associated with myocardial infarction. One of the target substrates of PP1 is phospholamban (PLN), a phospho-protein regulator of sarco/endoplasmic reticulum Ca^{2+} - ATPase (SERCA) which is vital for muscle contraction (MacDougall, et al., 1991). In other words, PLN regulates calcium pump activity in the cardiac muscle cells. PP1 is reported to dephosphorylate PLN and negatively regulate cardiac contractility. Thus, inhibition of PP1 leads to increased phosphorylation of PLN and contractility (Steenaart, et al., 1992). Studies using non-specific inhibitors, reported that treatment with okadaic acid in isolated guinea-pig ventricular muscle effectively enhanced contractility. Okadaic also inhibits PP2A, therefore it could also be implicated (Kodama, et al., 1986). Furthermore, treatment with calyculin A or cantharidin also increased contractility in both isolated guinea pig ventricular myocytes and in human cardiac preparations. As with okadaic acid, calyculin inhibits both PP1 and PP2A, so there could be an association with PP2A as well (Ishihara, et al., 1989).

PP1 regulation in hypoxia and apoptosis

A study by Lee et al. (2007) demonstrated the role of PP1α in the regulation of p53 and mouse double minute 2 homolog (MDM2) under hypoxic conditions. They observed that to induce p53, hypoxia induced the expression of protein phosphatase-1 nuclear targeting subunit (PNUTS), a negative regulator of PP1. PNUTS disrupted PP1 binding with p53, thus interfering with the dephosphorylation of p53 and consequently resulting in increasing the amount of phospho-p53 (Lee, et al., 2007). These results were confirmed by treatment with desferrioxamine, a hypoxia-mimetic agent. They concluded that HIF-1α is necessary for the activation of PNUTS under hypoxic conditions which in turn reduces the activity of PP1 (Lee, et al., 2007).

A study by Li et al. also showed the association between PP1 and p53. They demonstrated that PP1 can dephosphorylate p53 at Ser15 and Ser37, changing the transcriptional activity and apoptotic capacity of p53 in human lens epithelial cells (Li, et al., 2006). These results suggest the importance of the regulation of the phosphorylation state and the function of p53 by PP1.

PP1 regulation in cellular metabolism

As mentioned, PP1 regulates diverse biological events including metabolism. In eukaryotes, PP1 contributes to regulating appropriate substrate utilization for energy production during nutrient abundance as well as cellular recovery following metabolic stress (Ceulemans & Bollen, 2004). Hypoxia has been shown to decrease PP1 to facilitate a metabolic shift in response to hypoxic stress. PP1 promotes a shift to the more energy-efficient fuels when nutrients are abundant and stimulates the storage of energy in the form of glycogen. There are three mechanisms proposed to explain the impact of PP1 activity on mediating a metabolic shift. These includes:1) activation of AMP activated kinase (AMPK), an enzyme which acts as an energy sensor (Carling, 2004); 2) Glycogen synthase kinase (GSK) dephosphorylation and activation which promotes glycogen synthesis when there is abundance of nutrients (Ceulemans & Bollen, 2004); and 3) cAMP response element binding protein (CREB) which is critically involved in the regulation of the gene expression of several proteins involved in metabolic activity (Mayr & Montminy, 2001). In fact, approximately 25% of the genes regulated by CREB are involved in metabolism (Mayr & Montminy, 2001). A study by Comerford et al. (2006) further demonstrated a mechanism by which hypoxia downregulates PP1 activity through association with the specific inhibitory subunit, nuclear inhibitor of PP1 (NIPP1) (Comerford, et al., 2006).

PP2B (calcineurin) regulation by cardiomyocytes

In 1993, Griffiths and Halestrap observed that cyclosporine A (CsA), an immunosuppressant and PP2B (calcineurin) inhibitor improved post-ischemic left ventricular function in isolated rat hearts. Moreover, they discovered that CsA also inhibits the opening of the Mitochondrial Permeability Transition Pore (MPTP). To date, the mechanism by which CsA protects the heart is still controversial. Some researchers suggest that CsA protects via the inhibition of PP2B, whereas others urge it is via the inhibition of MPTP opening (Griffiths & Halestrap, 1993; Lui, et al., 1991). In 1991 Griffiths attempted to address this controversy by treating rabbit hearts with two PP2B inhibitors, CsA and FK-506. The design of this experiment was based on the fact that the mitochondrial cyclophilin D (CyPD) isoform which is implicated in the opening of the MPTP can bind CsA but not FK-506. Their results showed that both CsA and FK-506 protected the heart (Griffiths & Halestrap, 1991). Furthermore, in 2003 Hausenloy et al. further investigated this controversy using Sanglifehrin A, a drug that inhibits mitochondrial CyPD without an effect on PP2B and found that Sanglifehrin A also protected the heart. All these findings suggest that both the inhibition of PP2B as well as closing the MPTP elicits protective effects (Hausenloy, et al., 2003). These observations lead to the interesting hypothesis that PP2B indirectly regulates MPTP. Immunosuppression studies have shown that there is an association between

PP2B and the cytoplasmic cyclophilin family. These studies suggest that CsA inhibits cytosolic cyclophilin peptidylprolyl isomerase (PPIase) activity, via binding and inhibition of cytosolic PP2B (Griffiths & Halestrap, 1993). Therefore, it could be possible that in the mitochondria, CsA inhibits the opening of the MPTP via an association between PP2B and the cyclophilin isoform, CyPD. Alternatively, it could however also be that PP2B inhibition protects through a different pathway.

PP2B (calcineurin) regulation by cancer

PP2B (calcineurin) plays a central role in immunity. This was demonstrated by using PP2B inhibitors cyclosporine A and tacrolimus (FK506) as immunosuppressants (Woo, et al., 1997). PP2B is activated by an intracellular increase in Ca^{2+} levels which can be induced by hypoxic conditions, inflammation, and vascular endothelial growth factor signalling (Hogan, et al., 2003). These conditionings have also been shown to increase the activation of PP2B in malignant cells. Activation of PP2B is associated with signalling pathways which promote proliferation, migration, and metastasis. One of the substrates of PP2B, NFAT has been implicated in intestinal tumour growth in both a genetic model, as well as a colitis-associated model of colorectal cancer (Peuker, et al., 2016). In this study, the deletion of the Ppp3r1 gene which encoded for the PP2B regulatory B1 subunit (Cnb1) led to the reduction (size and number) of tumours in colon cancer epithelial cells of the ApcMin/+ mouse model. Similarly, treatment with colitis-inducing dextran sulfate along with the carcinogen azoxymethane in an intestinal epithelial cell-specific deletion of Ppp3r1 mice model, reduced the tumour size by reducing epithelial proliferation and increasing apoptosis. Peuker et al. (2016) further investigated the PP2B downstream target NFATc3, an -NFAT isoform which is ubiquitously expressed in normal intestinal epithelial cells. The deletion of NFATc3 in intestinal epithelial cells resulted in reduced tumour size and number. Inhibition of PP2B decreases cancer stem cell survival and proliferation.

Paradoxically, the chronic use of immunosuppressants such as cyclosporine A and tacrolimus, both inhibitors of PP2B increases cancer incidence. Research reported that the transplant population has a twofold increased risk of cancer. It is suggested that immunosuppressants increase the risk of cancer in three possible ways: 1) by increasing the risk of virus induced tumorigenesis; 2) by impairing immune surveillance of transformed cells; and 3) by specific effects of the drugs used for immunosuppression. The first two are directly related to disruption of the immune system. Therefore, PP2B inhibitors may directly promote tumorigenesis in an autonomous manner through modulation of the immune system (Hojo, et al., 1999).

PP2B (calcineurin) regulation by hypoxia

HIF-1α O_2 -dependent degradation is facilitated by von Hippel-Lindau (VHL) while receptor of activated protein kinase 1 (RACK1) facilitate HIF-1α degradation in an O_2 -independent pathway. The binding of RACK1 to HIF-1α recruits an Elongin-C/E3 ubiquitin ligase complex to HIF-1α leading to the ubiquitination and degradation of HIF-1α. RACK1 can also bind to the catalytic domain of activated PP2B, whereby it inhibits the ubiquitination and degradation of HIF-1α. Phosphorylation of RACK1 promotes dimerization whereas, dephosphorylation by PP2B inhibits dimerization. Therefore, PP2B promotes HIF-1α expression by dephosphorylating and blocking RACK1 dimerization. Inhibition of PP2B by cyclosporine A induced the degradation of HIF-1α (Liu, et al., 2007).

Summary

Acute myocardial infarction is one of the leading causes of death worldwide. Murry et al. (1986) made an incredible discovery in the form of ischemic preconditioning. In ischemic preconditioning it has been shown that the exposure of the heart to brief episodes of ischemia followed by reperfusion, confers protection against a prolonged ischemic insult. This concept has been employed by many researchers to illuminate the fundamental principles underlying acute myocardial infarction due to both ischemia and ischemia/reperfusion injury. In conditioning, protection is achieved immediately but lasts only a few hours. This is then followed by what is called the second window of protection which last approximately 48 hours. The immediate protection is facilitated by differential protein modulation and post-translational modification, whereas the second window of protection involves differential gene expression. These mechanisms show that the heart has the inherent ability to adapt to ischemia, with the limitations that such adaptation is transient.

Cancer and heart cells differ in many ways, such as: 1) cancer cells are terminally proliferative, whereas adult cardiomyocytes are terminally differentiated with limited proliferative capacity; 2) the metabolic preference of cancer cells is glycolysis, whereas cardiomyocytes prefer OXPHOS; 3) cancer is more concerned with replicating itself therefore it prefers anabolic metabolism to catabolic metabolism, whereas cardiomyocytes prefer large amount of ATP production via catabolic metabolism; and 4) cancer cells prove to be more resistant to death whereas cardiomyocytes are susceptible. Our interest in cancer relates to its ability to adapt to stressors such as hypoxia.

Cellular metabolism within a tumour can be heterogeneous. Tumour cells concomitantly increase glucose metabolism, leading to generation of ATP, NADPH, lactate, and nucleic acids (Gatenby & Gawlinski, 2003). On the other hand, they can also utilize glutamine fuelled OXPHOS leading to generation of ATP, amino acids, nucleic acids, and lipids through the pentose phosphate pathway (Eagle, 1955). It appears certain cancer-associated mutations allow cancer cells to acquire and

metabolize nutrients in a manner conducive for proliferation rather than efficient ATP production (Vander, et al., 2009). Metabolism in cardiomyocytes is mostly to favour high ATP production through OXPHOS utilizing mostly lipids and carbohydrates (D'Souza, et al., 2016).

Reversible phosphorylation has been implicated as a major regulator of molecules in signal transduction. Protein kinases catalyse the phosphorylation reaction, whereas protein phosphatases catalyse the dephosphorylation reaction (Voet, et al., 2006).

Most studies have shown PP2A to be a tumour suppressor (cell death promotor) in cancer studies and its inhibition to promote cell survival in cardiomyocytes (Mumby, 2007; Weinbrenner, 1998). In studies in the context of cancer cells and cardiomyocytes, the inhibition of PP2A always leads to cell survival, whereas its activation induces cell death (Weinbrenner, 1998). However, other studies in cancer show that PP2A can also act as a tumour promotor where its inhibition leads to cell death (Janssens, et al., 2016). Therefore, PP2A plays a dual role in cell death. More research must be done to hocument the PP2A holoenzymes and how they influence cell death or survival, since PP2A might be a therapeutic drug target. PP1 is found to be involved in cardiac contractility and metabolic adaptation during hypoxia (MacDougall, et al., 1991). PP1 has also been shown to dephosphorylate p53, leading to a reduction in phosphorylated p53 and a subsequent reduction in cell death (Lee, et al., 2007). In the heart, the inhibition of PP2B reduces cell death, whereas in cancer, PP2B has been found to either induce, or reduce tumorigenesis (Griffiths & Halestrap, 1991; Hojo, et al., 1999). Therefore, there isn't a clear effect of PP2B in cancer signalling. There is still more research to be done on the role of phosphatases in cellular signalling. In our research we aim to investigate and compare the effect of ischemia on phosphatases in cancer and heart cells.

Aim, Objectives and Hypothesis

Our previous study was an investigation on protein phosphatase activity and expression in H9c2 cells exposed to SI. In this study we were interested to see how cancer cells may regulate phosphatases in the same conditions.

We aim to investigate:

1) **The effect of 2 hours simulated ischemia with metabolic inhibition on cell viability in a cancer cell line (MDA-MB 231) and a heart cell line (H9c2).**

Objectives:

i. Measure ATP levels following 2 hours simulated ischemia.
ii. Measure Mitochondrial function and integrity using JC-1 stain following 2 hours SI and 30 minutes reperfusion.

iii. Measure necrosis by propidium iodide (PI) staining following 2 hours SI and 30 minutes reperfusion.

2) The effect of simulated ischemia on the activity and expression of phosphatases at 2 hours SI with metabolic inhibition between H9c2 and MDA- MB 231 cell line.

Objectives:

i. Use a para-Nitrophenylphosphate (pNPP) assay, as well as a 6,8-Difluoro-4-Methylumbelliferyl Phosphate (DifMUP) assay to measure the activity of different phosphatases.

ii. The use of inhibitors in conjugation with the phosphatase activity assays to distinguish between different phosphatases.

iii. Use Western blotting to measure the expression of phosphatases (PP1α, PP2Ac and PP2B).

3) The effect of pharmacological manipulation of PP2A on heart cell line (H9c2) versus cancer cell line (MDA-MB231) after 2 hours simulated ischemia, followed by 30 minutes reperfusion in terms of cell injury and death.

Objectives:

i. Use cantharidin (2 µM and 5 µM) to inhibit PP2A and PP1

ii. Use FTY 720 (1 µM and 5 µM) to activate PP2A

iii. Measure ATP levels

iv. Measure mitochondrial function and integrity using JC-1 stain

v. Measure necrosis using PI stain

Hypothesis:

The null hypothesis states that SI will not exert effects on protein phosphatase activity and expression in either cancer cells or heart cells. The alternative hypothesis states that SI will exert an effect on phosphatases in cancer and/or heart cells. If this is indeed the case, we propose that there will be a difference in the effect of SI on phosphatase activity and expression in these two types of cells.

CHAPTER 2: Methodology

Cell lines

In this study, two cell lines: H9c2 and MDA-MB 231 were used to compare the effect of SI on phosphatases.

H9c2 cells

H9c2(2-1) is a subclone of the original clonal cell line derived from embryonic BD1X rat heart tissue by B. Kimes and B. Brandt and exhibits many of the properties of skeletal muscle. It is however commonly used as a model for heart cell (ATCC® CRL-1446™). Myoblastic cells in this line can fuse to form multinucleated myotubes and can respond to acetylcholine stimulation. Fusion occurs faster if the serum concentration in the medium is reduced to one percent (Kimes & Brandt, 1976).

MDA-MB 231

The MDA-MB-231 cell line is an epithelial, human breast cancer cell line that was established from a pleural effusion of a 51-year-old caucasian female with a metastatic mammary adenocarcinoma and is one of the most commonly used breast cancer cell lines in medical research laboratories. MDA-MB-231 is a highly aggressive, invasive and poorly differentiated breast cancer cell line (Cailleau, et al., 1978).

Cell culture

To investigate the effect of SI on phosphatases in H9c2 and MDA-MB 231 cells, cells were cultured in Dulbecco's Modified Eagle Medium (DMEM) containing L-glutamine and 4.5 g/L of glucose (Lonza; BE12-604F) with 10 % Fetal Bovine Serum (FBS) (Sigma F6178) and 1 % Penicilin Streptomycin (Pen Strep) (Sigma, P4333). 0.25 % Trypsin left on the cells for 4 minutes was used to detach cells during routine subculturing. The resulting cell suspension was centrifuged at 125 xg for 4 minutes for H9c2, and 300xg for 3 minutes for MDA-MB 231 cells. Culturing was done in a sterile environment with incubation in 95 % atmospheric air, and 5 % CO_2 at 37 °C in a humidified atmosphere. For experimentation in 96 well plates, cells were counted using the haemocytometer. For H9c2 1 x 10^4 cells/100 µl/well were seeded, while for MDA-MB 231 25 x 10^3 cells/100 µl/well were seeded. This was done 24 hours before experimentation to ensure an optimal cell density for 96 well plate experiments. At 70 % - 80 % confluence, ischemia was simulated by the Modified Esumi buffer (Esumi, et al., 1991).

Experiments for Simulated Ischemia

For control, normal growth medium was used for treatment whereas for SI (SI), a buffer solution called the Modified Esumi buffer was used (Esumi, et al., 1991). The Modified Esumi buffer mimics the conditions of cells within the system when exposed to ischemia. The Modified Esumi buffer was prepared containing: 137 mM NaCl, 12 mM KCl, 0.5 mM $MgCl_2$, 0.9 mM $CaCl_2$-$2H_2O$, 4 mM HEPES

(4-(2- hydroxyethyl)-1-piperazineethanesulfonic acid), 20 mM Lactate, 0.5 mM sodium dithionate (SDT), 20 mM 2 deoxy-glucose (2-DG) and 2 % fetal bovine serum (FBS) at pH 6.4. The Modified Esumi buffer contains 0.5 mM SDT to inhibit the electron transport chain and 20 mM 2-DG to inhibit glycolysis. In comparison to a standard HEPES cell culture buffer, KCl was increased to 12 mM, HEPES was reduced to 4 mM, while 20 mM of Lactate was added (Esumi, et al., 1991). The Modified Esumi buffer was used in conjunction with a hypoxic gas mixture (0 % O_2 /95 % N_2/5 % CO_2) incubation. Hypoxic gas flush through the hypoxic chamber was allowed for 10 minutes. SI incubation was done at 37°C for a period of 2 hours.

Optimization for hypoxia

We made use of both a home-made and a commercial hypoxic chamber and added resazurin to the chambers for the 2 hours incubation period to confirm hypoxia. Resazurin (7-Hydroxy-3H-phenoxazin-3-one 10-oxide) is a blue dye under normoxic conditions, which can be reduced to a pink coloured fluorescent resorufin under low oxygen conditions and can be further reduced to a colourless hydroresorufin in the absence of oxygen. Three different concentrations of resazurin were tested: 0.01 g/L, 0.001 g/L and 0.0001 g/L, with 0.001g/L being a recommended concentration from literature for this type of experiment. The absorbance for resazurin was measured at 600 nm and resofurin, the reduced form of resazurin was measured at 570 nm wavelength using a BMG Labtech FLUOstar Omega Plate reader. A ratio was calculated and used for statistical analysis. Colour change from blue to pink to clear was also used as a visual indication of hypoxia.

Thereafter, to test how long it takes for oxygen to fully saturate the buffer system immediately after opening the hypoxic chamber, we also measured resazurin absorbance as an oxygen indicator. This was done monitored at 5 minutes intervals over period of 25 minutes reoxygenation.

Pharmacologic manipulation of PP2A

In order to inhibit Protein Phosphatase 2A (PP2A), cantharidin (purchased from Sigma, #C7632) was used at 2 µM and 5 µM, and to increase the activity of PP2A, FTY 720 (purchased from Cayman chemical, #10006292) was used at 1 µM and 5 µM. Cantharidin is a natural toxin produced by blister beetles that inhibits PP2A at low concentrations and both PP1 and PP2A at high concentrations (Honkanen, 1993). Cantharidin was prepared as follows: 25 mg of Cantharidin was dissolved into 1.27 ml of DMSO to make up a stock solution of 100 mM. Serial dilutions were titrated to make up the final concentrations of 2 µM and 5 µM which inhibits both PP1 and PP2A (Fan , et al., 2010). FTY 720, Fingolimod (Hydrochloride) is a derivative of ISP-1 (myriocin), a fungal metabolite of a Chinese herb (the fungus *Isaria sinclairii*), as well a structural analog of sphingosine. It is a novel immune modulator that prolongs allograft transplant survival in numerous models by inhibiting lymphocyte emigration from lymphoid organs (Brinkmann, et al., 2001). FTY 720 was prepared as follows: 50mg of FTY was dissolved into 2900 µl of DMSO to make up the stock solution of 50 mM. Serial dilutions were titrated

to make up final concentrations of 1 µM and 5 µM. Appropriate DMSO controls were included in the experimentals.

Cell harvesting for Western blotting and phosphatase activity.

For phosphatase activity and expression, twelve 100mm culture dishes were allowed to reach 80 % confluency. Six plates were used as controls and 6 were treated with SI. All 12 plates were washed twice with 10 ml PBS. New 10 ml growth medium was replaced into the 6 control plates, while the other 6 plates received 10ml of Modified Esumi buffer. The Modified Esumi treated cells were placed in the hypoxic chamber, flushed with (0 % O_2/5 % CO_2/95 % N_2) gas for 10 minutes then incubated for a period of 2 hours. After 2 hours incubation cells were scraped, and the resulting cell suspension centrifuged at 125 xg at 4 °C for 4 minutes (for H9c2); or 300 xg, 4 °C for 3 minutes (for MDA-MB 231). Following this the resulting pellet was used to prepare lysates.

Preparing Lysates for Western blotting and phosphatase activity

The cell lysates generated for Western blotting were prepared by using a different lysis buffer than used for lysate preparations for the pNPP and DiFMUP based phosphatase activity assays. Lysis buffer preparation was done on ice. The components and concentrations for the lysis buffer are shown in Table 2.1 for Western blotting and Table 2.2 for pNPP and DiFMUP.

Table 2.1: The components of the lysis buffer used for the preparation of the lysates for western blotting.

WESTERN BLOTTING LYSIS BUFFER

COMPONENTS	CONCENTRATION
TRIS-HCL +	20 mM
EGTA	1 mM
EDTA	1 mM
NACL	150 mM
B GLYCEROPHOSPHATE	1 mM
TETRA-NA- PIROPHOSPHATE	2.5 mM
NA_3VO_4	1 mM
PMSF	50 µg/ml
LEUPEPTIN	10 µg/ml
APROTININ	10 µg/ml
TRIXON X-100	1 %

[1] The buffer was made up to 10 ml with distilled water.

1

Table 2.2: The components of the lysis buffer used for the preparation of the lysates for pNPP and DiFMUP.

PNPP AND DIFMUP ASSAY BUFFER

COMPONENTS	CONCENTRATION
TRITON X-100	1 %
GLYCEROL	5 %
BENZAMIDINE	1.3 µM
APROTININ	0.01 µl
NACL	150 mM
HEPES	50 mM
EGTA	0,01 µM
B-MERCAPTOETHANOL	0.1 %
PMSF	10 mM

[2] The buffer was made up to 10 ml with distilled water.

For cell lysis, 0.5 mM zirconium beads and lysis buffer were added to the pellet and subjected to the bullet blender (Next Advance Bullet Blender) at 4ºC for three cycles of 1 minute at speed 4, with 5 minutes rest periods between cycles. After three repeats, the lysates were left in ice for 20 minutes for the foam to settle then centrifuged for 20 minutes at 300 xg. After 20 minutes centrifugation, the supernatant was transferred into new eppendorff tubes and either stored at -80 ℃ for enzyme activity measurements, or protein content determined for samples that were prepared for Western blotting.

Bradford Assay

Bradford protein assay in a method used to determine total protein concentration of a sample, whereby a colorimetric dye Coomassie Brilliant Blue G-250 proportionally binds to proteins and as the concentration of protein increases the colour of the test sample becomes darker (Bradford, 1976). Coomassie absorbs at 595 nm. The protein concentration of a test sample is determined by comparison to that of a series of protein standards known to reproducibly exhibit a linear absorbance profile in this assay. The protein standard used in our laboratory is Bovine Serum Albumin (BSA). After protein determination, a spread sheet was used to deduce the amount of sample and lysis buffer required to acquire equal amounts of protein is all the assays: Western blotting, pNPP assay and DiFMUP assay.

Phosphatase Activity Assay

Phosphatase activity was measured using to different techniques: colomeric pNPP and fluorescence DiFMUP. The two techniques were used to appreciate confirmation studies.

[2]

p-nitrophenol phosphate (pNPP) Phosphatase Activity Assay

The colometric assay using pNPP (Sigma, #71768) as a substrate for phosphatase activity was performed in transparent 96 well flat bottom plate in a final volume of 100 µl. pNPP is a synthetic non-specific protein phosphatase substrate that is dephosphorylated by active phosphatases into a yellow product p-nitrophenolate, which absorbs light at 405 nm. An increase in absorbance at 405 nm corresponds to the turnover of pNPP to p-nitrophenolate (Chernoff & LI, 1983). The pNPP substrate was prepared as a 20 mM stock dissolved in 5ml assay buffer (AB) (50 mM of HEPES + 5 mM $MgCl_2$, 0.02 % Mercaptoethanol, 1,5 µM BSA and distilled H_2O).

Equal amounts of 55 µg protein/sample were used. Phosphatase inhibitors were used to distinguish between specific protein phosphatases: NaF was used to inhibit all serine/threonine phosphatases, EGTA to inhibit PP2B, Na_3VO_4 to inhibit tyrosine and dual specificity phosphatase and cantharidin at different concentrations for PP1 and PP2A. For the 96-well plate, the phosphatase activity assay was prepared as follows: 30 µl of Assay Buffer (AB) or AB + inhibitors (NaF, EGTA, Na_3VO_4 & cantharidin), 50 µl of sample and 20 µl of pNPP. All the conditions were performed in duplicate. The blanks, containing only buffers and pNPP, were also performed in duplicate. After addition of the inhibitors, the plate was shaken and allowed to equilibrate at room temperature for 20 minutes. After incubation, 20 µl of pNPP was dispensed into the respective wells (containing 50 µl protein mixture, 30 µl AB +/- inhibitor) using a 50- 200 µl eight-channel pipette. Before the readings were taken, the plate was shaken again and bubbles inside the wells were removed using a sterile hypodermic needle. The colorimetric measurements were taken using a BMG Labtech FLUOstar Omega Plate reader at 37 °C. The absorbance readings were measured 5 minutes after pNPP was added at 405 nm. Readings were taken every 5 minutes until the incubation period of 60 minutes in total had expired. The readings taken at 45 minutes were used for statistical analysis.

DiFMUP (6,8-difluoro-4-methylumbelliferyl phosphate) Phosphatase Activity Assay

An EnzCheck® phosphatase assay kit was purchased from Molecular Probes (E12020). The fluorescence assays were carried out in a black flat bottom 96 well plate in a final volume of 100 µl. The fluorogenic substrate, 6,8-Difluoro-4-Methylumbelliferyl Phosphate (DiFMUP) was prepared in 5 ml assay buffer (50 mM of HEPES + 5 mM $MgCl_2$, 0.02 % Mercaptoethanol, 1,5 µM BSA and distilled H_2O). Reactions were initiated by addition of 50ul assay buffer containing DiFMUP (200 µM), resulting in a final concentration of 100 µM. The fluorescence intensity of hydrolysed DiFMUP, a fluorogenic product DiFMU has an excitation/emission maximum of ~ 360/460 nm. Fluorescence was used as a measure of phosphatase activity, where a decrease (or increase) in fluorescence indicated phosphatase activity. A 6,8-difluoro-7-hydroxy-4-methylcoumarin standard curved was prepared to determine the moles of product produced. A concentration of 10 mM 6,8-difluoro-7-hydroxy-4-methylcoumarin was diluted into 1X reaction buffer to yield 6,8-difluoro-7-hydroxy-4-methylcoumarin solutions ranging in concentration from 0-100 µM. Final volume of 100 µl was pipetted into 96 well plate and fluorescence

measured with the BMG Labtech FLUOstar Omega Plate reader at 37 °C. The phosphatase assay with inhibitors was prepared in a similar way as the pNPP assay. The fluorescence readings were measured 5 minutes after DiFMUP was added, at an excitation wavelength of 360 nm and emission at 460 nm. Readings were taken every 5 minutes until the incubation period of 60 minutes in total had expired. The readings taken at 45 minutes were used for statistical analysis.

Optimization for Phosphatase inhibitors for phosphatase activity

To know the best concentrations of inhibitors to block phosphatase activity, different concentrations of inhibitors were tested. All protein serine/threonine phosphatases (PSP) share a signature motif that can allow for generic binding of several ligands such as sodium fluoride (NaF). NaF is a known nonspecific PSP inhibitor. It is usually used to distinguish PSP from protein tyrosine phosphatase (PTP) (Morgan, et al., 1976). Both PTPs and dual specificity phosphatases (DuSPs) retain a conserved consensus binding site that contains a cysteine residue at the catalytic site, which forms a thiol-phosphate intermediate during catalysis (Cho, et al., 1992). Sodium orthovanadate (Na_3VO_4) is a phosphate analog that is generally thought to bind as a transition state analog to the phosphoryl transfer enzymes which it inhibits. This characteristic makes Na_3VO_4 a general inhibitor of PTPs (DuSP included) (Swarup, et al., 1982). Na_3VO_4 inhibition capacity can be completely reversed by EDTA, a metal chelater with affinity to Mg^{2+} (Guroff,, 1991). Other inhibitors used were EGTA, an inhibitor of PP2B and cantharidin, an inhibitor of PP2A at low concentrations and both PP2A and PP1 at higher concentrations. To evaluate the appropriate concentrations to use for our inhibitors, three different concentrations were used for each inhibitor (Table 2.2). The optimization was done for both pNPP and DiFMUP. For both the assays specific concentrations were chosen for experiments based on their optimal inhibition capacity. For NaF, 10 mM was chosen; for EGTA,1 mM, for Na_3VO_4 1 mM; and for cantharidin 0.2 µM was chosen for PP2A inhibition and 2 µM chosen for PP1 inhibition.

Table 2.3: Different concentrations used for optimizing the different inhibitors.

INHIBITORS	CONCENTRATIONS		
NAF	5 mM	10 mM	20 mM
NA_3VO_4	1 mM	5 mM	10 mM
EGTA	1 mM	5 mM	10 mM
CANTHARIDIN	0.25 µM	2 µM	20 mM

Phosphatase Expression- Western Blotting

Protein Extraction

Proteins were extracted, and lysates were made as described above under harvesting cells and preparing lysates respectively.

Protein Separation

Samples were first boiled in Laemmli sample buffer for 5 minutes, followed by brief centrifugation (4-5 minutes), before being loaded in BioRad Criterion pre-cast 4-20 % gradient gels (Bio-rad, 5678095). Proteins in the lysate samples were separated using sodium dodecyl sulfate-polyacrylamide gel electrophoresis (SDS-PAGE). Gels were run for 10 minutes at 100 V (voltage), 200 A (ampere) followed by 50 minutes at 200 V, 200 A. Running buffer used contained: Tris 25 mM; glycine 192 mM and sodium dodecyl sulfate (SDS) 3.5 mM. For each SDS-PAGE experiment, an equal amount of 9 µl of 30µg protein per sample was loaded.

Western Blotting

After SDS-PAGE separation, proteins were transferred from the polyacrylamide gel to a polyvinylidene fluoride (PVDF) membrane (Immobilon™ P, Millipore) using a wet tank-transfer system (35 minutes at 200 V, 200 A). For transfer, the membrane-gel stack was immersed in transfer buffer containing: Tris 25mM; glycine 192nM and 20 % methanol.

Blocking the membrane

Following transfer, non-specific protein binding sites on the PVDF membranes were blocked by incubating the membrane in 5 % fat-free milk in washing buffer (Tris-buffered saline (TBS)-0.1 % Tween 20 solution), under constant agitation, for at least one hour.

Incubation with antibodies

Between blocking and antibody incubation the membranes were thoroughly washed with three rapid changes of TBS-Tween, followed by at least 4 cycles of 5 minutes each washing with TBS-Tween. This washing was repeated after primary antibody incubation, as well as after secondary antibody incubation, which was the last step before visualisation. Following the wash, the membranes were incubated with the relevant primary antibody overnight at 4 °C under constant agitation. Antibodies were diluted in TBS-Tween with the appropriate dilution factor (1:1000). This was again followed by a washing cycle, after which the membranes were incubated with appropriate horseradish peroxidase-linked secondary antibody for an hour at room temperature at constant agitation. Primary antibodies and secondary antibodies are shown in Table 2.3.

Table 2.4: Information about antibodies used for Western blotting.

ANTIBODY TARGET PROTEIN	SOURCE	MOLECULAR WEIGHT	DILUTION FACTOR	SECONDARY ANTIBODY	MANUFACTURER & PRODUCT NO
PP1- ALPHA	Rabbit	38kDa	1:1000	Goat anti-rabbit IgG, HRP-linked Antibody	Cell signalling Primary: #2582S Secondary: #7074
PHOSPHO PAN SERINE/ THREONINE	Rabbit	-	1:1000	Goat anti-rabbit IgG, HRP-linked Antibody	Abcam Primary: #ab17646 Cell signalling Secondary: #7074
PAN-CALCINEURIN (PP2B)	Rabbit	59kDa	1:1000	Goat anti-rabbit IgG, HRP-linked Antibody	Cell signalling Primary: #2614 Secondary: #7074
HIF-1ALPHA	Rabbit	120kDa	1:1000	Goat anti-rabbit IgG, HRP-linked Antibody	Cell signalling Primary: #3716 Secondary: #7074
PTEN PHOSPHO & TOTAL	Rabbit	54kDa	1:1000	Goat anti-rabbit IgG, HRP-linked Antibody	Cell signalling Primary: #9552 Secondary: #7074
PP2A-C	Rabbit	36.38kDa	1:1000	Goat anti-rabbit IgG, HRP-linked Antibody	Cell signalling Primary: #2038 Secondary: #7074
AKT/PKB PHOSPHO & TOTAL	Rabbit	60kDa	1:1000	Goat anti-rabbit IgG, HRP-linked Antibody	Cell signalling Primary: #4060 Secondary: #7074

Visualization and analysis

Membranes were covered with ECL™ detection reagents for 2 minutes and were visualised using the ChemiHoc MP System in association with stain free technology (Bio Rad, 2017). The stain-free technology is a total protein staining method whereby the acrylamide gel solution is mixed with a compound called trihalocompound. When this compound is exposed to UV light it covalently binds to tryptophan residues in the protein to give a strong fluorescent signal that can be visualized and

quantified in a stain-free enabled imager such as the ChemiHoc MP system. The stain-free technology allows one to visualise protein separation quality, to verify the transfer efficiency, and most importantly, to validate any changes in the protein of interest by using total protein quantification as a reliable loading control (Posch, et al., 2013). Normalization was done using image lab Bio Rad. Target protein levels were normalised using the stain free total protein measurement as a loading control. Normalisation was done by measuring the total protein directly on the membrane, or 'transfer image. To obtain the total density of each lane, normalisation of blots was expressed as pixel values which were then expressed relative to control. The resulting values were expressed as arbitrary units (AU) and used for statistical analysis.

Cell Viability test

For cell viability, three assays were used: 1) An ATP assay which measures the intracellular energy levels of the cells, 2) Propidium Iodide (PI) which measures cell death accompanied by cell membrane disruption and 3) JC-1 stain which measures the integrity and function of the mitochondria. The experiments were repeated 3 times on three different days. 25000 cells/100µl MDA-MB 231 and 10 000 cells/100µl H9c2 cells were seeded into a 96 well plate. 80 % confluence was reached after 24 hours incubation. Thereafter, cells were exposed to SI (Esumi buffer) in combination with hypoxic gas mixture (0 % O_2/5 % CO_2/95 % N_2) for 2 hours. Immediately after exposure to SI ATP was measured and for the rest of the cells 30 minutes reperfusion was done, which thereafter was followed by PI and JC-1 staining. The calcium reperfusion buffer contained:137 mM NaCl, 4 mM KCl, 0.5 mM $MgCl_2$, 0.9 mM $CaCl_2.2H_2O$, 4 mM HEPES, 20 mM Lactate and 5.5 mM Glucose at pH 6.4. DMSO was used as a vehicle control and dH_2O and 1% Triton as a positive control for H9c2 and MDA-MB 231 respectively.

ATP assay

The ATP assay (CellTiter-Glo® Luminescent Cell Viability Assay from Promega, #G7571) measures the intracellular energy state. ATP is a marker for cell viability because it is present in all metabolically active cells. The ATP concentration declines very rapidly when cells undergo necrosis or apoptosis. The ATP assay system is based on the production of light caused by the reaction of ATP with added luciferase and d-luciferin (ATP + d-Luciferin + O2 Luciferase Oxyluciferin + Mg^{2+} AMP + PPi + CO_2 + Light). The emitted light is proportional to the ATP concentration within certain limits. Cells are the source of ATP in the luciferase reaction. Thus, luminescence produced is proportional to the number of viable cells. The procedure as supplied by the manufacturer was followed. The CellTiter-Glo® Assay was performed in white clear bottom 96 well plates. Cells were treated with appropriate drugs and DMSO controls, followed by 2 hours SI incubation and lysis of the cells immediately thereafter with CellTiter-Glo® Reagent, which was added directly to the cells in the serum-supplemented medium or Modified Esumi buffer. This was followed by 10 minutes incubation to stabilize the luminescent signal. The homogenous "add-mix-measure" format results in cell lysis and generation of luminescent signal

proportional to the amount of ATP present (Crouch, 1993). An ATP standard curve was prepared in duplicate. 10 µM ATP was prepared in PBS with serial dilutions ranging from 1 µM – 10 µM. 100 µl of CellTiter-Glo® reagent was added and allowed to incubate for 10 minutes at room temperature. Luminescence was read in the BMG Labtech FLUOstar Omega Plate reader.

Propidium Iodide (PI)

Propidium iodide (PI) measures cell death. PI is a membrane impermeant fluorescence dye, which stains non-viable cells with broken membranes. Live cells have intact membranes that exclude a variety of dyes that easily penetrate the damaged, permeable membranes of non-viable cells. When there is cellular damage, PI binds to double stranded DNA by intercalating between base pairs. PI was excited at 544 nm and emission measured at a maximum wavelength of 640 nm.

For PI staining, 10000 cells/100 µl/well for H9c2 cells and 25000 cells/100 µl/well for MDA-MB 231 were cultured in clear flat bottom black 96 well plates. Cells were treated with appropriate drugs, followed by 2 hours SI incubation. Thereafter, upon reoxygenation cells were rinsed 3X with PBS and media was replaced with calcium containing reperfusion buffer. Cells with calcium reperfusion buffer were allowed to incubate for 30 minutes in a non-CO_2 incubator. After reperfusion, cells were stained with 0.5 mg/ml PI and allowed to incubate for 10 minutes. Cells were washed 3X with calcium containing reperfusion buffer. After the wash, the fluorescence signal was read in a BMG Labtech FLUOstar Omega Plate reader at the excitation wavelength of 544 nm and emission wavelength of 640 nm. The stained cells couldn't be properly observed under the fluorescence microscopy (NIKON); thus, no images were captured.

JC-1 stain

A distinctive feature of the early stages of programmed cell death is the disruption of active mitochondria. This mitochondrial disruption includes changes in the membrane potential and alterations to the oxidation–reduction potential of the mitochondria (Cossarizza, et al., 1993). JC-1 measures the integrity and function of the mitochondria, as an indicator for mitochondrial membrane potential. JC-1 stain is a positively charged molecular probe which is used as a membrane permeant fluorescent dye to measure apoptosis by monitoring mitochondrial health. At low mitochondrial concentrations (due to low mitochondrial membrane potential), JC-1 is predominantly a monomer that yields green fluorescence with emission of 520 nm. Whereas, at high mitochondrial concentrations (due to high mitochondrial membrane potential), the dye aggregates yielding a red to orange coloured emission of 590 nm. Consequently, a decrease in the aggregate fluorescent count is indicative of depolarization whereas an increase is indicative of hyperpolarization (abcam).

For JC-1 staining,1 x 10^4 cells/100 µl/well for H9c2 and 25 x 10^3 cells/100 µl/well for MDA-MB 231 cells were cultured in clear flat bottom black 96 well plates. Cells were treated as explained above with appropriate drugs and DMSO controls, followed by 2 hours SI incubation. After incubation, cells were

rinsed 3X with PBS and media was replaced with calcium containing reperfusion buffer. Cells with calcium reperfusion buffer were allowed to incubate for 30 minutes in a non-CO_2 incubator. After reperfusion, cells were stained with 10 µM JC-1 stain and allowed to incubate for 10 minutes. Cells were washed 3X with calcium containing reperfusion buffer. After this the fluorescence signal was read in a BMG Labtech FLUOstar Omega Plate reader with fluorescence emission from green (~520 nm) to red (~590 nm). The aggregate dye can be excited at 535 nm, the monomer and aggregate together at 475 nm. Stained cells were viewed under 10X magnification fluorescence microscopy (NIKON) and images were captured and analysed with ImageJ. Two wells were captured per treatment by microscopic camera and 20 cells per image were analysed by Image J.

Statistics

All the experiments were repeated three or four times on three or four different days. The data was analysed using Graphpad Prism version 5. All data is expressed as mean +/- SEM. The student T-test was used when comparing two groups. For more than two variables the one-way analysis of variance (ANOVA) with Bonferroni post hoc test was used. The statistical test was considered significant at $p < 0.05$.

Normalisation was done for all data by expressing all data relative to relevant control values.

CHAPTER 3: Optimization of hypoxia

Testing the efficacy of hypoxic chambers (commercial vs home-made) to induce hypoxia: using resazurin as an oxygen sensor and the effect of reoxygenation over time.

The effect of hypoxia on resazurin

To test the efficacy of the hypoxic chamber and the hypoxic gas mixture to induce hypoxia, resazurin was used as an oxygen sensor at different concentrations: 0.0001 g/L, 0.001 g/L and 0.01 g/L. Resazurin can be used as a colorimetric oxidation-reduction indicator in cell viability assays for both aerobic and anaerobic respiration (Chen, et al., 2015). Resazurin is a blue powder that can be diluted into solution using distilled water. The resultant blue solution can be reduced to pink-coloured resofurin which can be further reduced to clear hydroresofurin. Resazurin is an oxygen indicator, when the solution is dark blue it indicates the presence of oxygen, while when it is pink or clear it shows there is low or no oxygen present. Different concentrations of resazurin was dispensed into a 96 well Costar plate, then flushed with hypoxic gas mixture (0% O_2 /5% CO_2 /95% N_2) for 10 minutes. After 2 hours incubation, the plate was removed from the hypoxic chamber. Empty wells reserved for normoxic resazurin solution were then filled to be used as control. Absorbance was measured using a BMG Labtech FLUOstar Omega plate reader for resofurin at 570 nm and resazurin at 600 nm wavelength.

Our lab has two hypoxic chambers: a commercial chamber (Billups-Rothenberg Inc) and a home-made chamber. The commercial chambers are expensive, and we have only one available in our lab. We were therefore interested in constructing our own hypoxic chambers in order to save costs, while increasing our capacity for high throughput experimentation. The hypoxic air-tight chamber is designed with inflow and out-flow pipes (Figure 3.1). During hypoxic gas flush, the inflow pipe is connected to the gas cylinder pipe, while the outflow pipe is left open to flush out the gas inside the container for 10 minutes to ensure an equilibrated hypoxic environment. Immediately after 10 minutes flush, both the pipes were clipped to prevent air coming in or out of the chamber. To ensure sterility, the chamber was exposed to UV light before the experiment and sprayed with 80% ethanol before incubation. Initial experimental observation on the home-made chamber suggested that they are effective to maintain a hypoxic environment (not published).

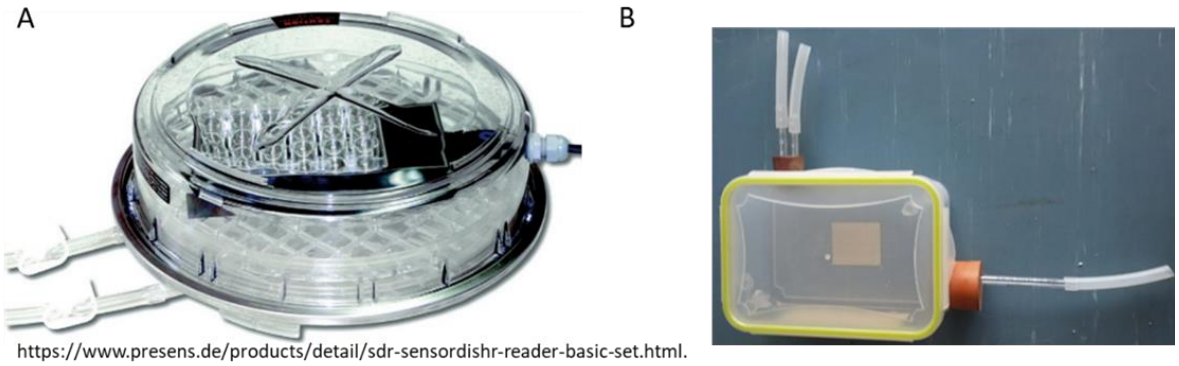

Figure 3.1: Chambers tested for their ability to maintain hypoxia. A. is the sealed commercial hypoxic chamber and B. is the sealed home-made hypoxic chamber. The inlet valve is used to receive hypoxic gas while the outlet valve releases the gas from the chamber.

The hypoxic chambers were flushed with an anoxic gas mixture (0 % O_2/ 5 CO_2/ 95% N_2) followed by incubation in the same gas mixture for 2 hours.

In Figure 3.2, the absorbance of 0.001 g/L and 0.01 g/L resazurin in the home-made hypoxic chamber showed statistically significant reduction in resazurin absorbance after 2 hours SI. Moreover, significant colour change was visually observed in both 0.001 g/L and 0.01 g/L resazurin. The colour of the normoxic resazurin solution was clear in the lowest resazurin concentration (0.0001 g/L) and thus had the lowest absorbance of 1.039 ± 0.0118 Arbitrary Units (AU). A 10-fold increase in resazurin to 0.001 g/L caused the solution to appear light blue, consequently causing the absorbance to increase to 1.248 ± 0.1130 AU. A further 10-fold increase in resazurin (0.01g/L) made the solution dark blue and understandably increased the absorbance to a high of 1.419 ± 0.0169 AU. Comparison of the three different resazurin concentrations during hypoxia shows that the absorbance values are all low, displaying a light pink colour to clear due to the reduction of resazurin to resorufin and clear due to the reduction of resorufin to hydroresorufin. Interestingly, the colour and absorbance of all three hypoxic resazurin solutions were like that of 0.0001 g/L resazurin during normoxia, which makes it impossible for the lowest resazurin concentration to undergo any colour and absorbance changes due to hypoxia. Thus, the lowest resazurin concentration was not found to be effective in detecting hypoxia. Only the two higher resazurin concentrations showed colour and absorbance differences between normoxia and hypoxia and were thus found to be able to detect hypoxia. Statistical analysis of normalised data shows that this colour change due to hypoxia was of significant difference in absorbance for 0.001 g/L (control: 1.000 ± 0.0000 AU vs hypoxia: 0.700 ± 0.063 AU; n= 3; $p < 0.001$) and 0.01 g/L (control: 1.000 ± 0.0000 AU vs hypoxia: 0.7240 ± 0.065 AU; n= 3; $p < 0.001$) respectively.

The commercial chamber showed a statistical reduction in all the different concentrations of resazurin exposed to 2 hours hypoxia. At the concentration of 0.0001 g/L there was a statistical reduction (control: 1.000 ± 0.000 AU vs Hypoxia: 0.951± 0.010 AU; n= 3; $p < 0.05$). The concentration of 0.001 g/L also

showed a statistical reduction in the absorbance (control: 1.000 ± 0.000 AU vs Hypoxia: 0.757 ± 0,006 AU; n = 3; $p < 0.001$). The highest concentration of 0.01 g/L also showed a statistical reduction in the absorbance (control: 1.000 ± 0.000 AU vs Hypoxia: 0.723 ± 0.020 AU); n= 3; $p < 0.001$) (Figure 3.3). Figure 3.4 compares hypoxia in the home-made and commercial chamber. The absorbance reading shows that there is no difference on the effect of hypoxia between the two chambers. However, it is interesting that individual statistics showed that only the commercial hypoxic chamber was associated with a reduction in colour absorbance due to 2 hours hypoxia.

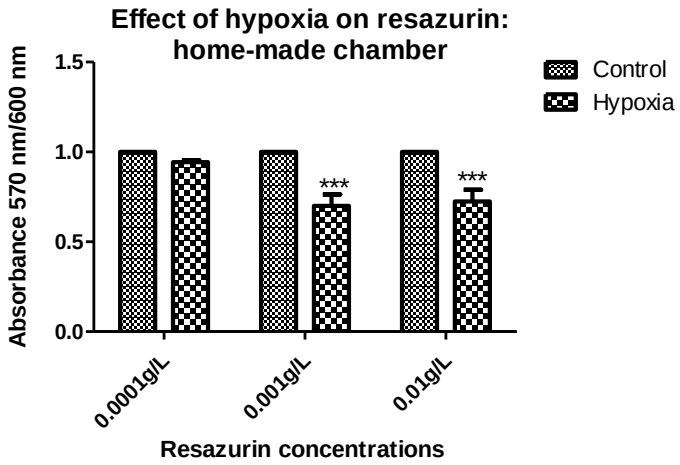

Figure 3.2: The effect of hypoxia on resazurin in the home-made hypoxic chamber at 2 hours incubation period at 37°C. The colour change observed in 0.01 g/L & 0.001 g/L showed a statistical reduction in the absorbance. Statistical analysis was done using one-way ANOVA with Bonferroni post hoc test, n = 3. Statistical significance was measured at ***$p < 0.001$. All data was normalized by expressing it relative to control values.

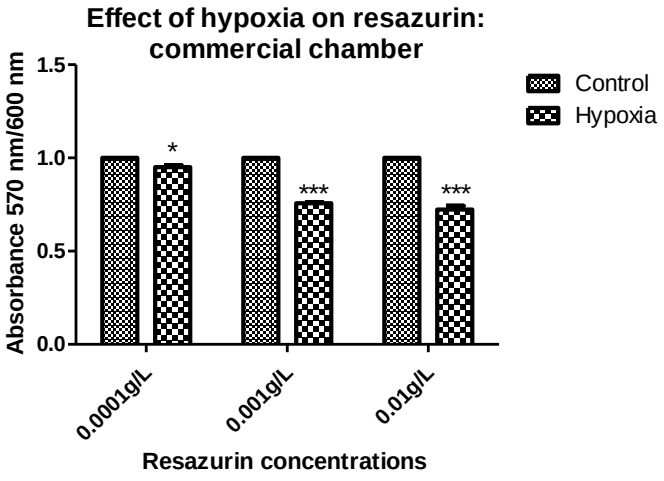

Figure 3.3: The effect of hypoxia on resazurin in the commercial hypoxic chamber at 2 hours incubation period at 37°C. All the concentrations showed statistically significant reduction due to 2 hours hypoxia including 0.0001 g/L. The statistical test used was the student T-test, n = 3. Statistical significance was measured at *$p < 0.05$, and ***$p < 0.001$. All data was normalized by expressing it relative to control values.

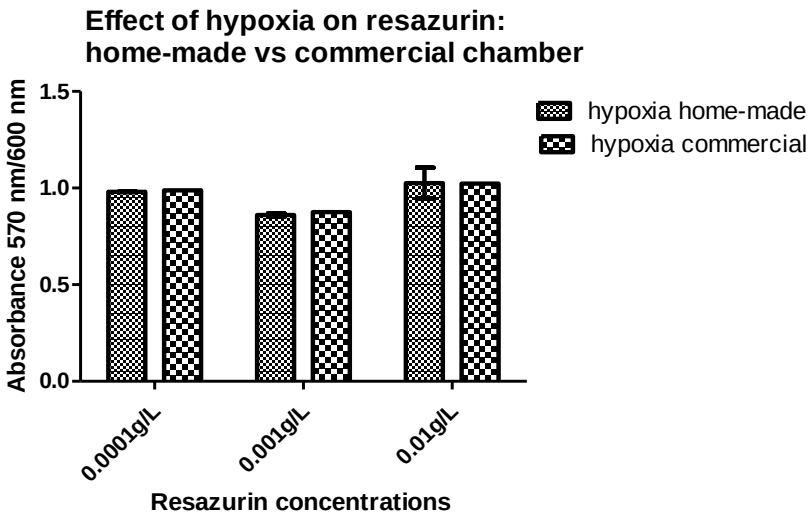

Figure 3.4: Comparing the effect of hypoxia on resazurin (0.01g/L, 0.001g/L & 0.0001g/L) between the home-made vs commercial hypoxic chambers. There were no differences between the two hypoxic chambers. Statistical testing was done using the student T-test, n = 3.

The effect of reoxygenation on resazurin

To test how long it takes for resazurin to be oxidized back when the hypoxic chamber is opened after 2 hours hypoxic incubation, we measured the absorbance over time during the initial reoxygenation. This was a different set of experiments with the aim to measure reoxygenation over time. We repeated the experiments three times on three different days using the home-made chamber. The resazurin solution was exposed to hypoxia for 2 hours. After two hours hypoxic incubation, the plate was removed from the chamber. The empty wells reserved for normoxic resazurin solution were filled up immediately after hypoxic incubation. To limit the reoxygenation time before measurements, the hypoxic chamber was opened near the BMG Labtech FLUOstar Omega plate reader. Measurements were taken from time 0, every five minutes for 25 minutes and a statistical analysis was done between control and hypoxia for each time point. Figure 3.5 shows that there was a significant reduction in absorbance ($p < 0.05$) from 0 to 20 minutes of reperfusion. This difference disappeared at 25 minutes reperfusion.

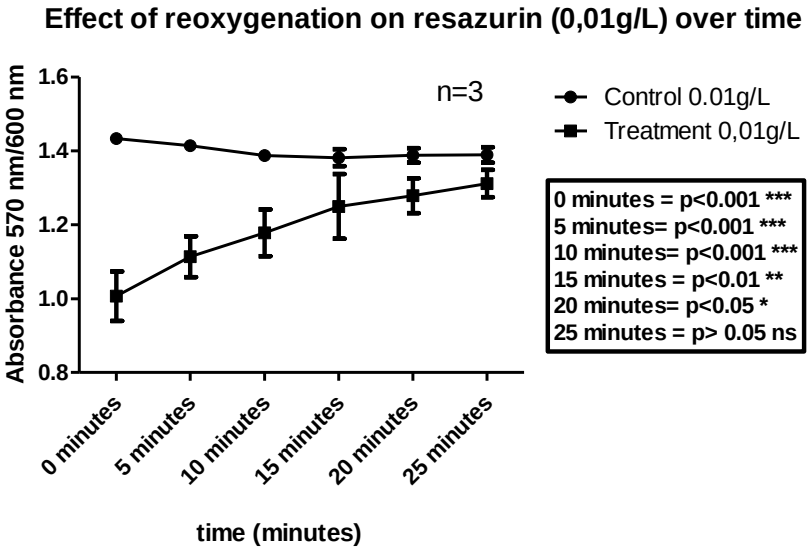

Figure 3.5: The effect of reoxygenation on resazurin (0.01 g/L) over a period of 25 minutes. The control group had a steady absorbance throughout the timeline, whereas, in the treatment groups (hypoxia), reperfusion lead to a reversed colour change and absorbance from pink back to its original blue colour within 25 minutes. There was a significant reduction in absorbance. from 0 to 20 minutes of reperfusion. This difference disappeared at 25 minutes of reperfusion. Statistical analysis was done using one -way ANOVA, n = 3. Statistical significance was measured at *p < 0.05, **p < 0.1 and ***p < 0.001.

In Figure 3.6, the absorbance of the 0.001 g/L resazurin solution was steady with minimal colour reversal after reoxygenation. After adding dH_2O to dilute resazurin to the concentration of 0. 001 g/L, resazurin was pink. After 2 hours hypoxic incubation, resazurin became clear. From time 0 minutes to 25 minutes of reoxygenation, the colour was light pink. The statistical difference in 0.001 g/L due to hypoxia was steady throughout 25 minutes. As mentioned before, 0.0001 g/L resazurin solution was clear before and after hypoxia. Thus, there was no significant difference in 0.0001 g/L resazurin due to reperfusion (Figure 3.7). Please note that the significant increase in normoxic absorbance at 10 minutes is an outlier.

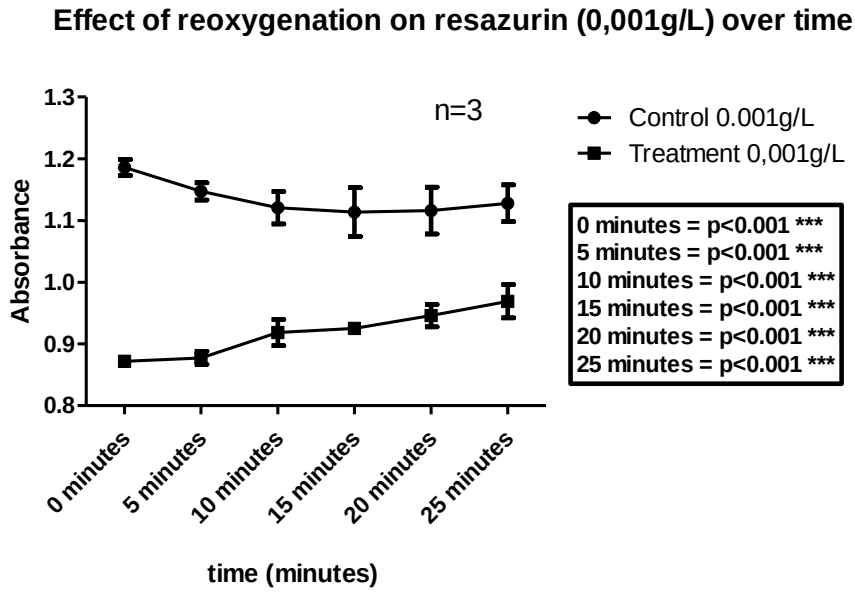

Figure 3.6: The effect of reoxygenation on resazurin (0.001 g/L) over a period of 25 minutes. During a 2 hours hypoxia incubation period, the colour changed from pink to clear. The control group had a steady absorbance throughout the timeline. Also, in the treatment group (hypoxia), the colour change is quite steady throughout with little reversal into light pink colour. There was a significant change in colour due to hypoxia (***p < 0.001) from 0 – 25 minutes. Statistical analysis was done using one -way ANOVA, n = 3.

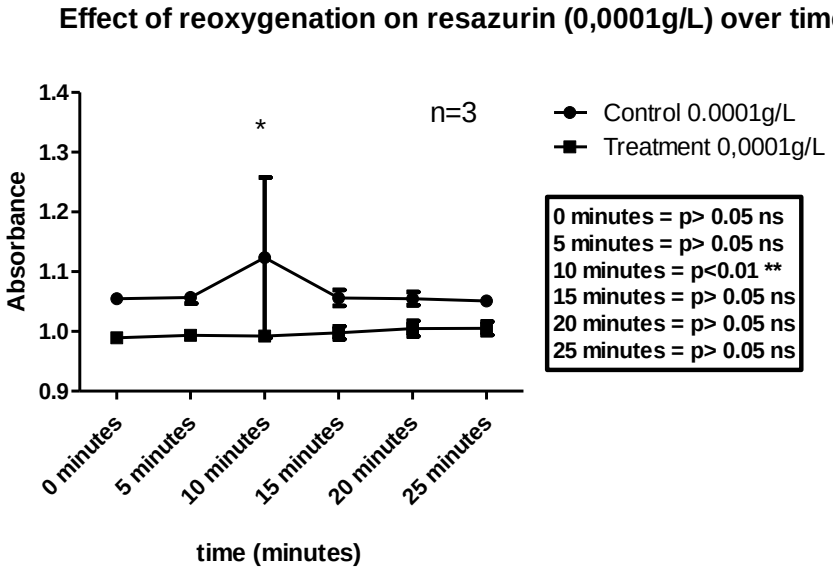

Figure 3.7: The effect of reoxygenation on resazurin (0.0001 g/L) over a period of 25 minutes. Resazurin at the concentration of 0.0001 g/L is already clear before exposure to hypoxia. During a 2 hours hypoxia incubation period, the colour remained clear. The treatment group (hypoxia) remains steady throughout the timeline with no noticeable colour change. Therefore, there was no significant colour difference due to hypoxia or reoxygenation. At 10 minutes, the statistical difference observed is an outlier. Statistical analysis was done using one -way ANOVA, n = 3.

Discussion and Conclusion

We aimed to investigate the efficacy of our hypoxic intervention using a hypoxic gas mixture in conjunction with both a home-made and commercial hypoxic chamber to induce hypoxic conditions. The effect of reoxygenation over time was also assessed.

Three different concentrations of resazurin were used: 0.0001 g/L, 0.001 g/L and 0.01 g/L. The colour of 0.0001 g/L resazurin was clear before incubation in the hypoxic environment. Therefore, the colour observed after exposure to hypoxia was the same as before. Surprisingly, statistics on the data collected from the commercial hypoxic chamber eluded that colour change due to hypoxia was significant for 0.0001 g/L resazurin; which is impossible since there was no visual colour change observed at this concentration. Looking at Figure 3.2, the home-made chamber suggests there was measurable colour change on 0.001 g/L and 0.01g/L resazurin in terms of absorbance; colour change was also observed from pink to clear and blue to pink respectively. Literature suggests that the blue colour change of resazurin to pink resorufin is evidence of hypoxia (Bueno, et al., 2002). Moreover, the data analysed from the commercial chamber also suggested that the colour change observed resulted in a significant reduction in absorbance; even for 0.0001 g/L resazurin.

Similar statistical results were obtained for the both commercial chamber and home-made chamber. Moreover, the visual colour change was similar, and a direct hypoxia absorbance as shown in Figure 3.4 showed that the hypoxic effect on both the chambers was not different from each other. Moreover, re-oxygenation over time showed significant difference between normoxia and hypoxia in the home-made chamber.

We have empirical evidence showing that, immediately after you open a hypoxic chamber, atmospheric oxygen diffuses back into the system. This can be observed in Figure 3.5, where after time 0 minutes, the hypoxia absorbance increases towards the normoxia until it saturates at 25 minutes. What was advantageous about the colour change due to lack of oxygen was that, reoxygenation reversed the reduction process, oxidizing resofurin back to resazurin. However, hydroresofurin indicated by the clear colour did not reverse the colour back to resofurin in the presence of oxygen. The colour reversal allowed us to measure the absorbance over time using the BMG Labtech FLUOstar Omega Plate reader. The analysed data from 0.01 g/L resazurin showed that colour reversal due to reoxygenation was statistically significant between hypoxia and normoxia. However, at 25 minutes when the colour reversal was complete, there was no difference between hypoxia and normoxia, indicating an oxygen saturated system. Reoxygenation and colour reversal in the concentration of 0.001 g/L resazurin was steady and the reversal was not complete at 25 minutes. Whereas, resazurin concentration of 0.0001 g/L was too low to cause any colour change before and after hypoxia: the colour appeared clear upon dilution with dH_2O and remained clear after exposure to hypoxia and reoxygenation.

It is possible that this reoxygenation effect would not have any noticeable physiological changes, or it might change the physiological response by the cells. We still do not know the level of hypoxia in the medium around the cells. This could have been measured by testing resazurin in growth medium (or Esumi buffer) with cells. However, we only investigated resazurin in dH_2O without the cells or media. Literature shows that the absence of oxygen during the hypoxic period creates a condition in which the restoration of oxygen results in inflammation and oxidative damage through the induction of oxidative stress rather than (or along with) restoration of normal function (Carden & Granger, 2000). PI and JC-1 protocol in our experiments for testing cell viability required that we reperfused after SI. This was especially due to that PI and JC-1 stain requires washing steps and this increases the period undergone since the hypoxic chamber is opened, and thus automatic reperfusion occurs.

With regards to our experiments where we assessed the levels of oxygen in the chambers using resazurin, it is evident that indeed hypoxia was achieved. Our data also confirmed that 0.001 g/L and 0.01 g/L are the recommended concentrations of resazurin to measure hypoxia. We also compared the effectiveness of our home-made versus the commercial hypoxic chamber: in both the home-made chamber and commercial chamber we have visually confirmed changes in colour, and significant reduction in absorbance due to hypoxia. Therefore, a comparison of the two chambers shows no differences. Reoxygenation was observed to reverse resazurin colour change from pink to blue. This change could affect the physiological response of cells to hypoxia; however, we did not confirm this speculation. Regulated reperfusion can be performed to account for this event. For Western blotting and phosphatase activity assay, the commercial chamber was used. Whereas, for cell viability studies, the home-made chamber was preferred.

Chapter 4: The effect of simulated ischemia on cell viability

Aim 1: The effect of 2 hours simulated ischemia with metabolic inhibition on cell viability, in cancer (MDA-MB 231) and heart cell lines (H9c2).

SI was induced by the Modified Esumi buffer with metabolic inhibition plus hypoxia in H9c2 and MDA-MB 231 cells. To inhibit glycolysis 20 mM of deoxy-glucose (2-DG) was used, while 0.5 mM of sodium dithionite (SDT) was used to inhibit the electron transport chain. To test for cell viability due to SI: ATP assay, JC-1 stain and propidium iodide (PI) were used.

ATP assay viability test

H9c2 and MDA-MB 231 cells were subjected to 2 hours of SI incubated in 0% O_2/5% CO_2/95% N_2 and 0.5%O_2/5% CO_2/balance N_2 respectively. Unfortunately, due to logistical and availability issues, we had to use different gas mixtures. 10000cells/100µl H9c2 and 25000cells/100µl MDA -MB 231 cells were seeded to reach 80% confluence after 24 hours. ATP assay was performed on both cell lines to assess the energetic state of the cells at the end of SI compared to normoxia. As shown in Figure 4.1A, statistical analysis by student T-test on H9c2 cells shows that SI reduced ATP levels relative to control (control: 1,000 ± 0,000 Arbitrary Unit (AU) vs SI: 0,597 ± 0,042 AU; n = 3; $p < 0.001$). MDA-MB 231 also showed a reduction in ATP levels due to SI (control: 1,000 ± 0,000 vs SI: 0,458 ± 0,025 vs; n = 4; $p < 0.01$).

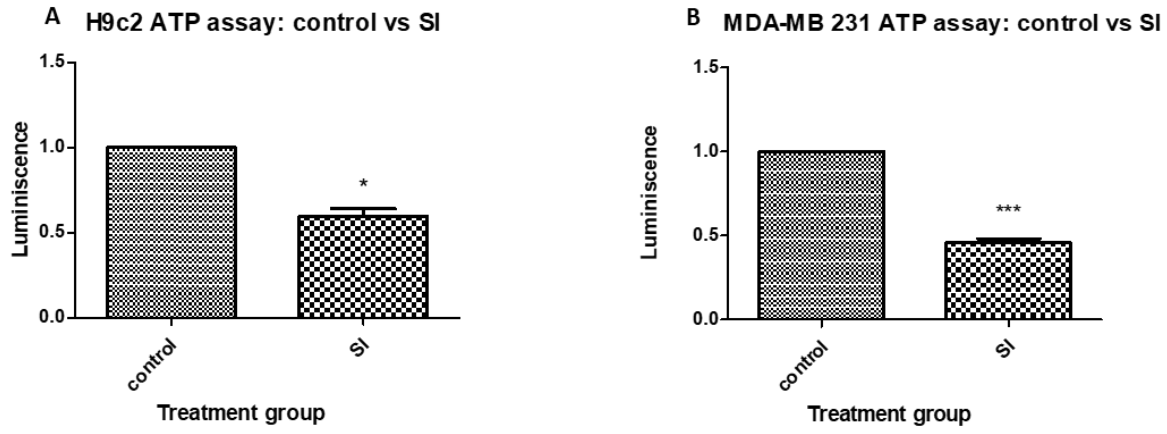

Figure 4.1: ATP assay analysis on H9c2 and MDA-MB 231 at the end of 2 hours SI. Following exposure of both MDA-MB 231 and H9c2 cells to SI and a hypoxic gas mixture (0.5 % O_2/5 % CO_2/balance N_2 for MDA-MB 231 and 0 % O_2/5 % CO_2/95 % N_2 for H9c2), cell viability was determenined in terms of ATP content. SI reduced ATP levels in both A. H9c2 and B. MDA-MB 231 cells indicating that both cell lines were under energetic stress. Comparisons were done using a student T-test, n = 3 to 4, *$p < 0.05$, ***$p < 0.001$.

Propidium Iodide stain viability test

Propidium Iodide is a cell membrane impermeable stain that stains DNA and only penetrates the cell membrane when it is broken, indicative of cell death. After H9c2 and MDA-MB 231 cells were treated with 2 hours SI followed by 30 minutes reperfusion, and then the cells were stained by PI for a period of 10 minutes. Statistical analysis showed no measurable change in PI fluorescence due to SI in both cell lines (Figure 4.2).

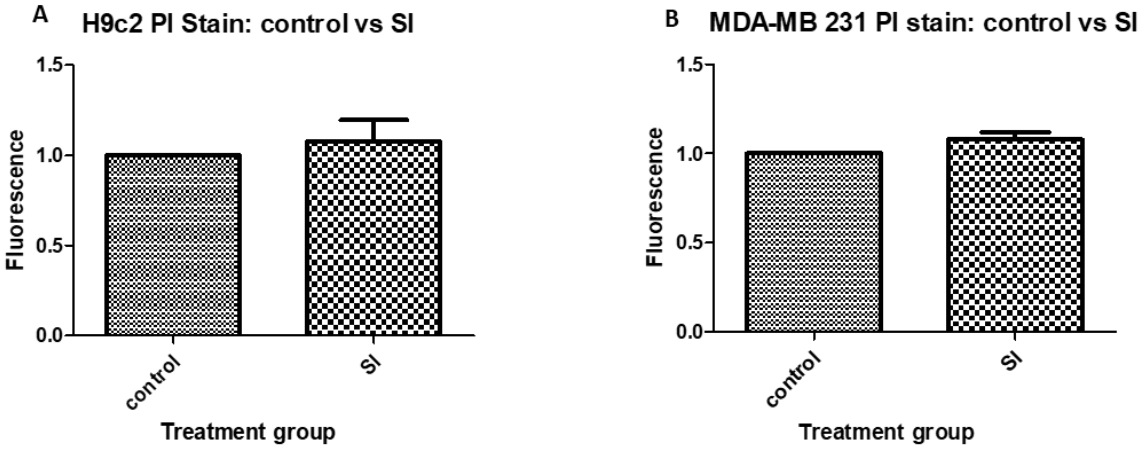

Figure 4.2: Propidium iodide stain was used to test cell death due to 2 hours SI followed by 30 minutes reperfusion in H9c2 and MDA-MB 231 cells. After exposing cells to SI and a hypoxic gas mixture (0.5%O2/5% CO2/balance N2 for MDA-MB 231 and 0% O2/5% CO2/95% N2 for H9c2), they were then exposed to 30 minutes reperfusion followed by a 10 minutes PI staining. SI did not induce necrotic death on both cell lines. Comparison was done using a student T-test, n = 3 to 4, $p > 0.05$.

JC-1 stain viability test measured by the plate reader

JC-1 stain is another cell viability test that indicates the integrity and function of the mitochondria which in turn relates to cellular viability. Cells were subjected to the same SI intervention as described above followed by 30 minutes reperfusion, and then an additional 10 minutes of JC-1 staining. The samples were subjected to the plate reader and fluorescence microscopy. Statistical analysis from the plate reader showed that SI and reperfusion exerted no effect on mitochondria in either H9c2 or MDA-MB 231 cell lines (Figure 4.3).

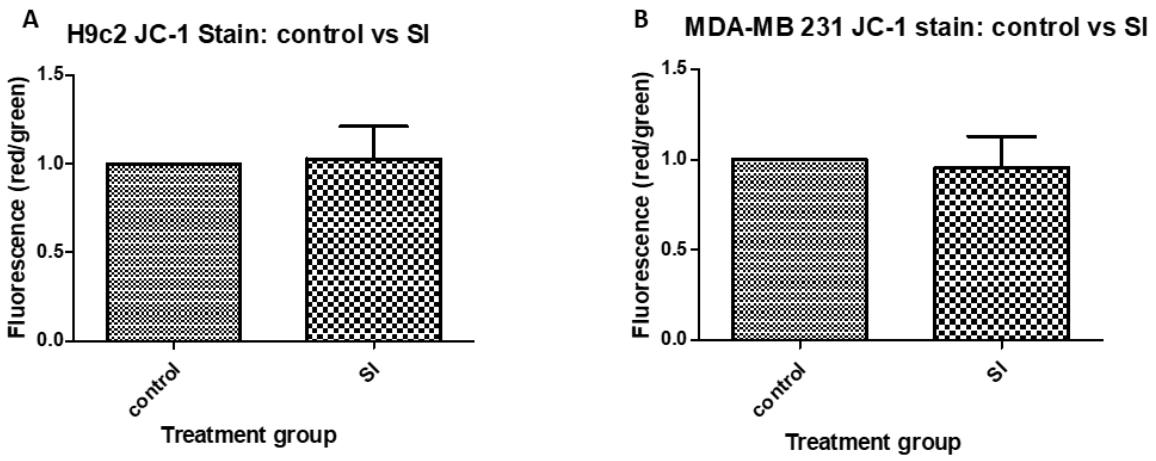

Figure 4.3: JC-1 stain was used to test mitochondrial fucntion in response to 2 hours SI followed by 30 minutes reperfusion on H9c2 and MDA-MB 231 cells. After cells were exposed to SI and a hypoxic gas mixture (0.5 % O_2/5 % CO_2/balance N_2 for MDA-MB 231 and 0 % O_2/5 % CO_2/95 % N_2 for H9c2), cells were exposed to simulated reperfusion for 30 minutes, whereafter 10 minutes JC-1 staining was perfomed and measured in the plate reader. SI and reperfusion had no significant effect on mitondondrial functionand integrity in both cell lines. Comparision was done using student T- test, n = 3 to 4. $p > 0.05$.

JC-1 image analysis cell viability test

As mentioned, JC-1 staining was subjected to two analyses: the plate reader and fluorescence microscopy. The images obtained were analysed using imageJ. Unfortunately, the images obtained were not of high quality, making analysis difficult. Twenty cells were selected per image and analysed to obtain an average. The red/green ratio was calculated, and this was used for statistical analysis. Statistics reported that there was no measurable change due to SI and reperfusion in either cell lines (Figure 4.4 A and B). Viable cells stain red whereas damaged cells (with a lack of mitochondrial integrity and function) stain green. However, green staining was difficult to observe in our samples. We therefore split the red/green/blue composition (RGB) images into separate channels. The style used here is a montage where we show the colour RGB image, the red channel and the green channel. As described above, there were no differences between H9c2 and MDA-MB 231 cells. When one observes the images one can see that indeed the intensity of the green channel is low compared to the red channel showing faint staining mainly because most cells were still viable. Typically, SI would cause a morphological change from spindle to spherical shape. However, the morphology of the H9c2 cell line was intact (Figure 4.4C), whereas MDA-MB 231 assumed a spherical shape. Paradoxically, the normoxic MDA-MB 231 showed a spherical shape, likely due to cell detachment from the plate induced by washing and reperfusion (Figure 4.4D). According to the American Type Culture Collection (ATCC), normal MDA-MB 231 is spindled shaped (Figure 4.5). MDA-MB 231 treated with normoxic buffer and SI/reperfusion were also exposed to washing Phosphate Buffered Saline (PBS) and calcium-based acid reperfusion buffer (pH 6.4), which could have more likely caused the morphological transition.

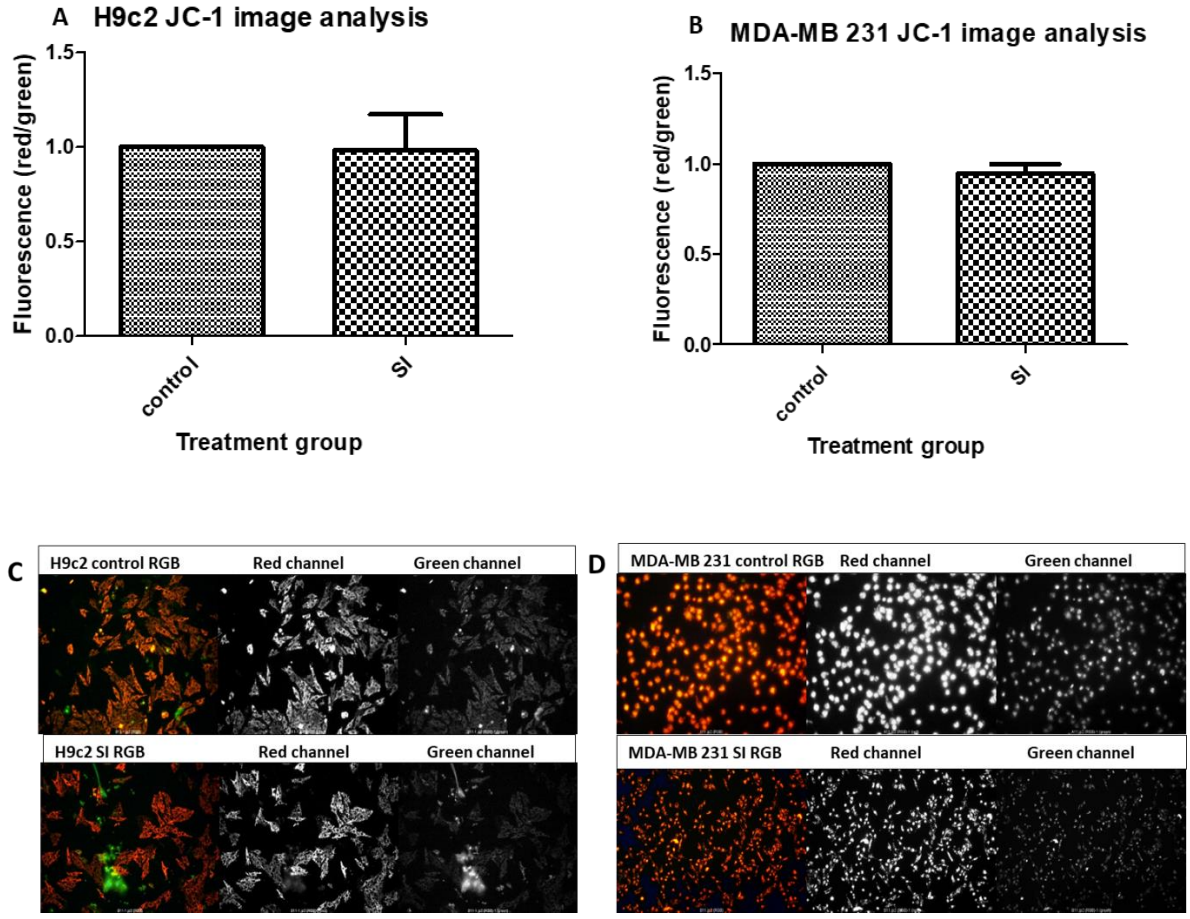

Figure 4.4: JC-1 stain image analysis showing the effect of 2 hour SI followed by 30 minutes reperfusion on H9c2 and MDA-MB 231 cells. After SI and exposure to a hypoxic gas mixture (0.5 % O_2/5 % CO_2/balance N_2 (MDA-MB 231) and 0 % O_2/5 % CO_2/ 95% N_2 (H9c2)), cells were reperfused and then stained with JC- 1 for 10 minutes. Cells were then viewed under the fluorensence microscope and images were taken. Images were then anlysed using Image J. Data showed that there was no significant change in the red/green ratio due to SI and reperfusion. Statistical analsis was perfomed by student T-test, n = 3 to 4. JC-1 stain red/green/blue composition (RGB) montage showing the red and green channel of both H9c2 and MDA-MB 231 cells. These are the representatve images of cells stained with JC-1. C. H9c2 cells images reveales no visible change due to SI. D. However, MDA-MB 231 cells (normoxic and SI) showed a transition in morphology from spindle shape to spherical with is most likely due to detachment from the plate induced by washing or reperfusion. The green stain was faint, mostly due to the abundance of viable cells strongly stained by red. Normalisation was done for all data by comparing treatment against relevant control which is always 1.

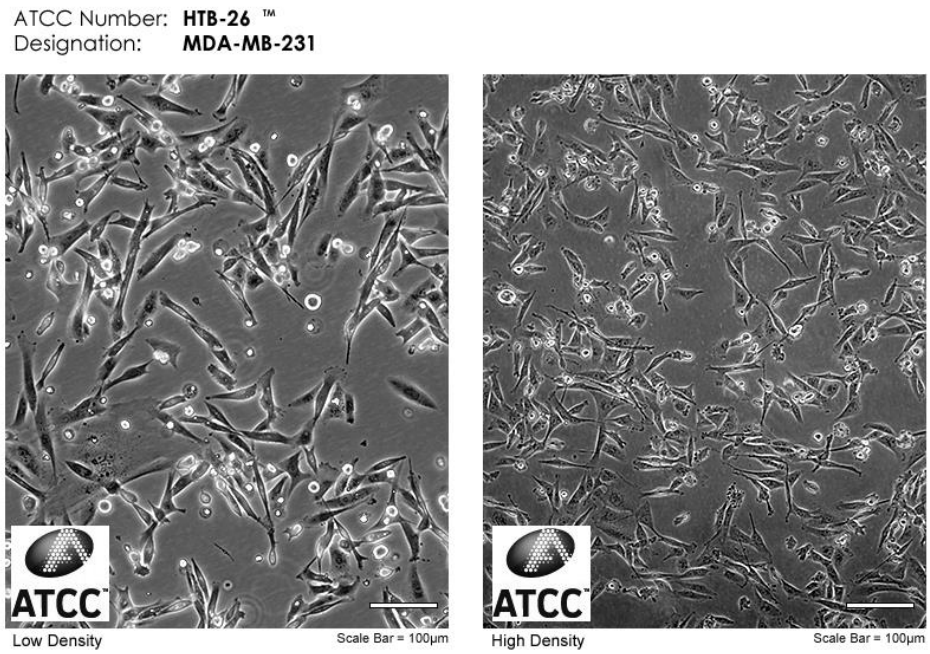

Figure 4.5: The American Type Culture Collection (ATCC) of MDA-MB 231 cultured in ATCC-formulated Leibovitz's L-15 Medium with 10 % fetal bovine serum (FBS) in a free gas exchange with atmospheric air. Normally MDA-MB 231 assumed a spindle shape.

Chapter 5: The effect of simulated ischemia on the activity and expression of protein phosphatases

Aim 2: The effect of 2 hours simulated ischemia with metabolic inhibition on the activity and expression of protein phosphatases in H9c2 and MDA- MB 231 cell lines.

H9c2 and MDA-MB 231 cells were exposed to 2 hours SI with a hypoxic gas mixture [0.5% O_2/5% CO_2/balance N_2 (MDA-MB 231) and 0% O_2/5% CO_2/95% N_2 (H9c2)]. Lysates were collected for both phosphatase activity (pNPP and DiFMUP) and Western blotting. For both the pNPP and DiFMUP assays 55 µg of protein per cell supernatant were used in a 96 well plate. pNPP and DiFMUP are recommended to be used in the presence of inhibitors. Inhibitors were used in combination with the phosphatase assays to distinguish between different phosphatases in the lysates. These inhibitors are widely used; nonetheless, they are non-specific. Inhibitors inhibit a group of phosphatases allowing the uninhibited phosphatases to hydrolyse the synthetic phosphate pNPP or DiFMUP, giving off a colorimetric and fluorescence product respectively. Phosphatases catalyse the hydrolysis of pNPP liberating inorganic phosphate and colorimetric para-nitrophenol (pNP). Upon phosphatase-induced hydrolysis, DiFMUP generates fluorinated 4-methylumbelliferyl fluorophore. Assay buffer (AB) contains no inhibitors and represents total phosphatase activity. In the presence of inhibitors, it is assumed that the signal generated is by the uninhibited phosphatases. Inhibitors were diluted in the assay buffer (AB). These inhibitors include: NaF which inhibits serine/threonine phosphatases, Na_3VO_4 which inhibits tyrosine and dual specificity phosphatases, EGTA which inhibits PP2B, and cantharidin which inhibits PP2A at low dosage as well as PP1 at high dosage. Inhibitors were allowed to incubate for 20 minutes before measurements were taken in a plate reader. For Western blotting, equal amounts of 30 µg of samples were loaded into the gel wells. Normalisation of the blots was performed to compare the relative abundance of a specific protein across the lanes of a blot. The experiments for both phosphatase activity and expression were repeated three times on three different days.

Phosphatase activity

Previously in our laboratory, we investigated the effect of SI on the activity and expression of phosphatases in the heart using the H9c2 cell line. We measured protein phosphatase activity using para-Nitrophenylphosphate (pNPP) in the presence of inhibitors. Statistical analysis showed that inhibitors (Assay Buffer (AB) vs NaF and AB vs Na_3VO_4) significantly reduced phosphatase activity under both normoxic and SI conditions. However, SI did not cause any change in phosphatase activity compared to control. Western blotting was used to measure the expression of all phosphorylated proteins at serine/threonine residues (pan phosphor ser/thr), PP1 alpha, PP2B and PP2Ac; however, no differences were found between control and SI. For this study, we compared the activity and expression of phosphatases between the previously studied H9c2 cells (not repeated) and MDA-MB 231 cells. For MDA-MB 231 we used both para-Nitrophenylphosphate (pNPP colorimetric assay) and 6,8-Difluoro-

4-Methylumbelliferyl Phosphate (DiFMUP fluorescence assay) both of which are synthetic non-specific phosphatase substrate used for measuring phosphatase activity.

pNPP assay showed that the inhibition of protein tyrosine phosphatase with 1 mM Na_3VO_4 statistically reduced the phosphatase activity against assay buffer (AB) under normoxic conditions (AB: 1.000 ± 0.000 Arbitrary Unit (AU) vs Na_3VO_4: 0.350 ± 0.011 AU; n= 9; $p < 0.001$) as well as SI conditions (AB: 1.000 ± 0.000 AU vs Na_3VO_4: 0.358 ± 0.009 AU; n= 9; $p < 0.001$). The inhibition of protein serine/threonine phosphatases with 10 mM NaF showed no statistically significant effect on phosphatase activity under normoxic conditions, whereas there was a significant reduction under SI conditions (AB: 1.000 ± 0.000 AU vs NaF: 0.920 ± 0.025 AU; n= 9; $p < 0.05$). The inhibition of PP2B with 1 mM EGTA showed a significant reduction in phosphatase activity under normoxic conditions (AB: 1.000 ± 0.000 AU vs EGTA: 0.896 ± 0.027 AU; n = 9; $p < 0.01$) as well as SI conditions (AB: 1.000 ± 0.000 AU vs EGTA: 0.900 ± 0.016 AU; n= 9; $p < 0.01$). Whereas, the inhibition of PP2A with 0.2 µM cantharidin (CN1) showed a significant reduction in phosphatase activity only under normoxic conditions (AB: 1.000 ± 0.000 AU vs CN1: 0.906 ± 0.023 AU; n= 9; $p < 0.05$). Surprisingly, the inhibition of both PP1 and PP2A with 2 µM cantharidin (CN2) did not influence phosphatase activity under both normoxic and SI conditions (Figure 5.1). The activity of phosphatases treated with inhibitors was also measured by a fluorescence DiFMUP assay under both normoxic and SI conditions. Only the inhibition of protein tyrosine phosphatases with 1 mM Na_3VO_4 showed a reduction in phosphatase activity under normoxic (AB: 1.000 ± 0.000 AU vs Na_3VO_4: 0.375 ± 0.080 AU; n= 9; $p < 0.001$) as well as SI conditions (AB: 1.000 ± 0.000 AU vs Na_3VO_4: 0.267 ± 0.018 AU; n =9; $p < 0.001$).

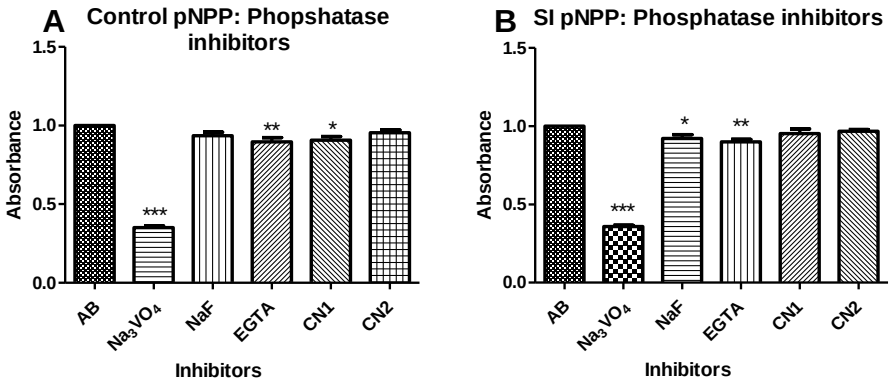

Figure 5.1: pNPP measurements of the effect of phosphatase inhibitors on MDA-MB 231 phosphatase activity under both A. normoxic and B. SI conditions. 1 mM Na_3VO_4 was used to inhibit protein tyrosine phosphatase, 10 mM NaF was used to inhibit protein serine/threonine phosphatases, 1 mM EGTA was used to inhibit PP2B, 0.2 µM cantharidin (CN1) was used to inhibit PP2A and 2 µM cantharidin (CN2) was used to inhibit PP1. Phosphatase activity in the presence of inhibitors was measured against total phosphatase activity containing only assay buffer (AB). Na_3VO_4 and EGTA showed a statistical reduction in phosphatase activity under both normoxic and SI conditions. NaF only showed reduction in phosphatase activity under SI conditions. 0.2 µM cantharidin showed a reduction in phosphatase activity under normoxic conditions. Surprisingly, 2 µM cantharidin did not influence phosphatase activity. the Statistical test was done using one-way ANOVA with Bonferroni post

hoc test, n = 3. Statistical significance was measured at *p < 0.05, **p < 0.01 and ***p < 0.001. Normalisation was done for all data by comparing treatment against relevant control which is always 1.

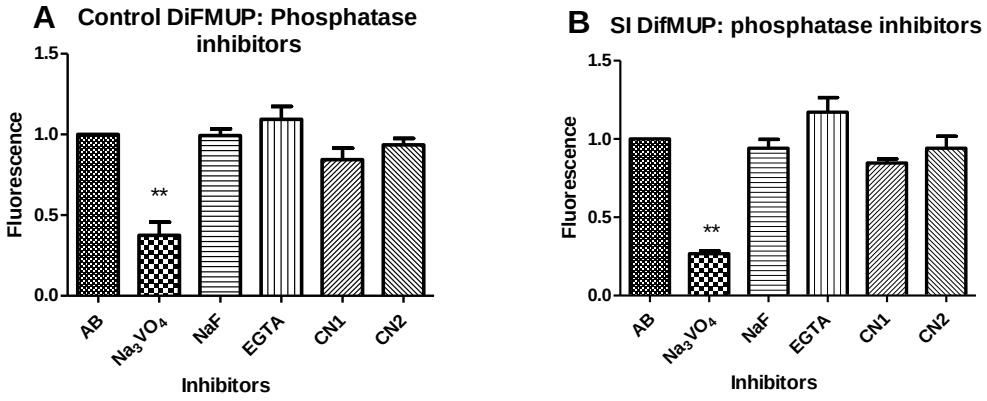

Figure 5.2: DifMUP measurements of the effect of phosphatase inhibitors on MDA-MB 231 phosphatase activity under both normoxic and SI conditions. 1 mm Na3VO4 was used to inhibit protein tyrosine phosphatase, 10 mm Naf was used to inhibit protein serine/threonine phosphatases, 1 mm EGTA was used to inhibit PP2B, 0.2 µm cantharidin (CN1) was used to inhibit PP2A and 2 µm cantharidin (CN2) was used to inhibit PP1. Phosphatase activity in the presence of inhibitors was measured against total phosphatase activity containing only assay buffer (AB). Only inhibition with Na3VO4 showed a statistically significant reduction in phosphatase activity under both normoxic and SI conditions. Statistical test was done using one-way ANOVA with Bonferroni post hoc test, n = 3. Statistical significance was measured at ***p< 0.001. Normalisation was done for all data by comparing treatment against relevant control which is always 1.

As previously mentioned, phosphatase activity was measured in MDA-MB 231 cells exposed to 2 hours SI using the pNPP assay. The inhibitors inhibit a group of phosphatases, leaving the uninhibited phosphatases to dephosphorylate the synthetic pNPP substrate to para-nitrophenol (pNP) product which directly measure the activity of the respective phosphatases. There are three named categories of phosphatases catalogued: protein serine/threonine phosphatases (PSPs), protein tyrosine phosphatases (PTPs) and dual specificity phosphatases (DuSPs). PTPs and DuSPs are both inhibited by Na_3VO_4. When Na_3VO_4 inhibits both PTPs and DuSPs, provided that the inhibition is 100%, it is then appropriate to assume that the remaining phosphatases activity measured is mainly due to PSPs. On the other hand, when NaF inhibition of PSPs is complete, the remaining phosphatase activity is due to PTPs and DuSPs. 2 hours SI had no effect on phosphatase activity due to PTPs and DuSPs as well as PSPs. When EGTA inhibits PP2B, it subtracts the activity of PP2B from the total phosphatase activity. Also, when cantharidin inhibits PP2A (0.2 µM) or both PP1 and PP2A (2 µM), it subtracts the activity of PP2A or both PP1 and PP2A from the total phosphatase activity respectively. pNPP assay showed that when either PP2B, PP2A or both PP1 and PP2A are subtracted from the total phosphatase activity during SI, they have no influence on the activity of the remaining phosphatases activity (Figure 5.3). Phosphatase activity as measured by DiFMUP in MDA-MB 231 also showed that there was no significant difference in total phosphatase activity (AB) due to SI. Moreover, SI did not influence the activity of the uninhibited phosphatases (Figure 5.4).

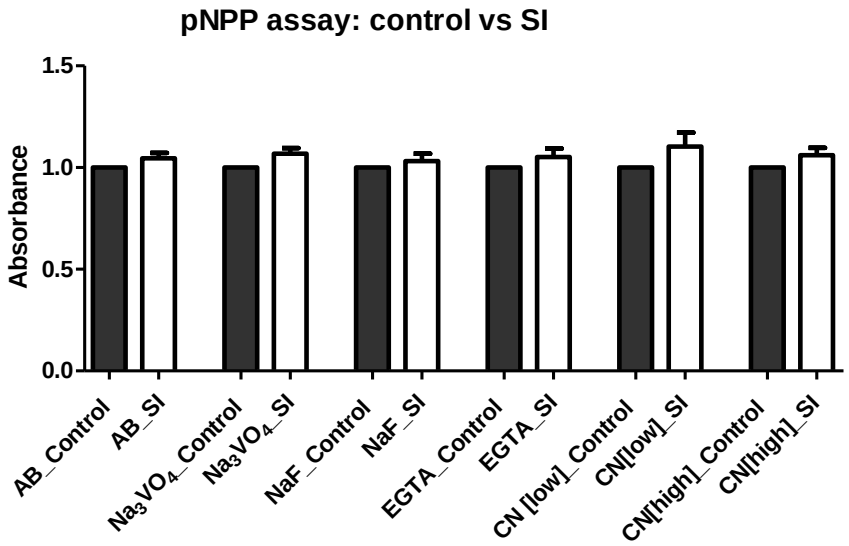

Figure 5.3: Results on the activity of phosphatases in MDA-MB 231 following 2 hours SI using the pNPP assay in the presence of inhibitors. SI did not influence either total phosphatase activity or the activity of uninhibited phosphatases. Statistical testing was done using one-way ANOVA with Bonferroni post hoc test, n= 3. Normalisation was done for all data by comparing treatment against relevant control which is always 1.

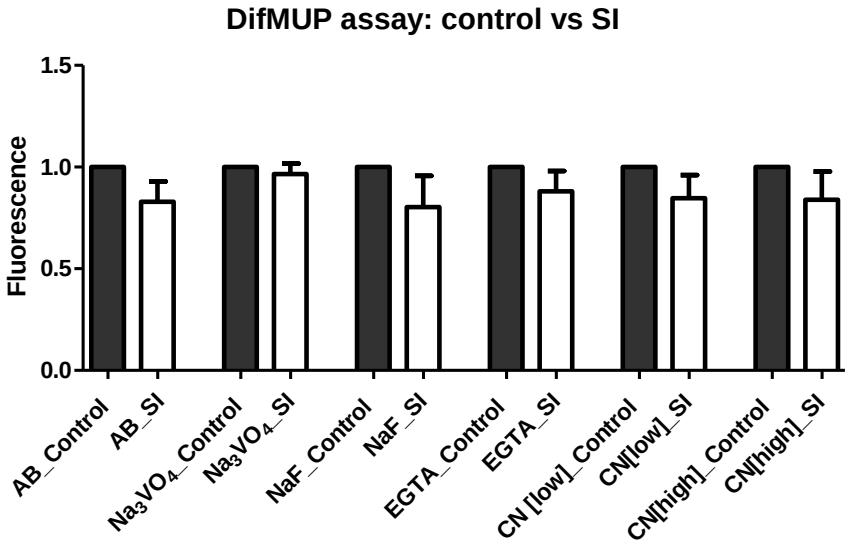

Figure 5.4: Results on the activity of phosphatases in MDA-MB 231 following 2 hours SI using the DiFMUP assay in the presence of inhibitors. SI did not influence either total phosphatase activity or the activity of uninhibited phosphatases. Statistical testing was done using one-way ANOVA with Bonferroni post hoc test, n= 3. Normalisation was done for all data by comparing treatment against relevant control which is always 1.

Phosphatase Expression

Equal amounts of 30 µg protein were loaded into the gel wells. Western blotting results showed no statistically significant difference in the expression of all serine/threonine phosphorylated proteins (pan phosphor ser/thr) between control and SI. However, the expression of proteins with a molecular weight of between 72kDa and 55kDa showed a heightened intensity in phosphorylation (Figure 5.5). Our

protein separation and the pan phospho serine/threonine antibodies are not sensitive enough to distinguish specific proteins. Each protein band observed using the pan phospho serine/threonine antibody represent all the protein fragments in that size range. The increased phosphorylation signal could therefore be due to several other phosphorylated proteins. We, however, speculate that Akt/PKB (60kDa) is the possible phosphorylated protein in this location. Akt/PKB has two phosphorylation sites: one is at Threonine T308 (T308), while the other is at Serine S473 (S473). We blotted for both phosphorylated Akt/PKB S473 and total-Akt/PKB. The data showed that the expression of phosphorylated Akt/PKB at serine 473 was inconclusive. However, we did not confirm for the expression of phosphorylated Akt/PKB T308. Using a paired student T-test, the expression of total-Akt/PKB showed a statistically significant reduction following 2 hours SI (control: 1.000 $\pm$ 0.000 vs SI: 0.556 $\pm$ 0.027; n = 3; $p < 0.01$) (Figure 5.6). PTEN is a negative regulator of Akt/PKB. If PTEN is negative in this cell line, there would be expected to be a high phosphorylation of Akt/PKB (Carnero & Paramio, 2014). When PTEN is phosphorylated in its C-terminal it is inactive. The expression of phosphorylated PTEN showed inconclusive results. Whereas, the expression of total-PTEN showed no statistically significant difference between control and SI (Figure 5.7). We also measured the expression of HIF-1 alpha, PP2B, PP2Ac and PP1 alpha. HIF-1 alpha, PP1 alpha and PP2B showed no statistically significant differences between control and SI. However, unpaired student T- test showed that the expression of PP2Ac significantly increased following 2 hours SI (control: 1482 x 10^4 $\pm$ 8715 x 10^2 vs SI: 1964 x 10^4 $\pm$ 1406 x 10^3; n = 3; $p < 0.05$). Whereas, a paired student T- test of normalised data suggests that the increase in PP2Ac due to SI is not of statistical significance (control: 1.000 $\pm$ 0.0000 AU vs SI: 1.330 $\pm$ 0.100 AU; n = 3; $p > 0{,}05$) (Figure 5.8, 5.9, 5.10 & 5.11A and 5.11B respectively).

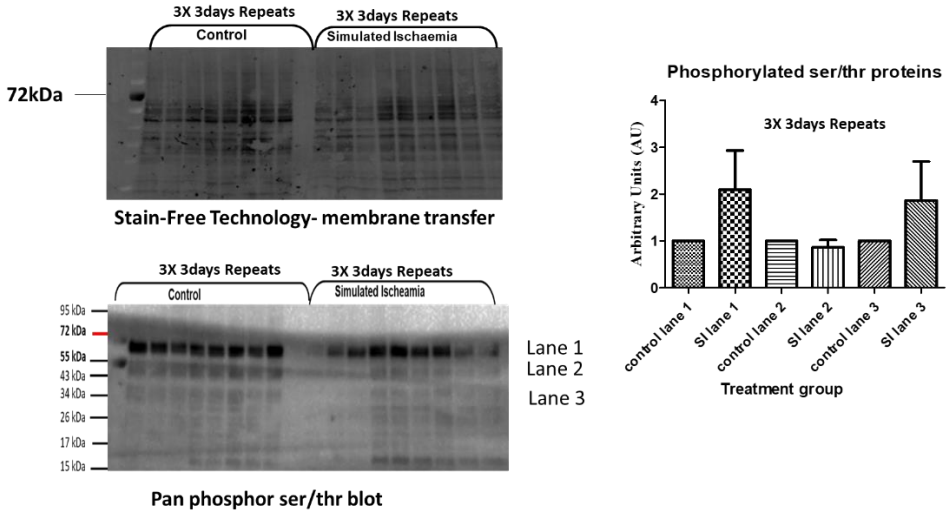

Figure 5.5: Western blot results of MDA-MB 231 exposed to 2 hours SI showing the expression of all phosphorylated proteins at serine/threonine residues (pan phospho ser/thr). Proteins with a molecular weight of between 72kDa and 55kDa showed high intensity in phosphorylation. However, there was no difference in phosphorylation between control and SI. Statistical test was done using student T-test, n = 3.

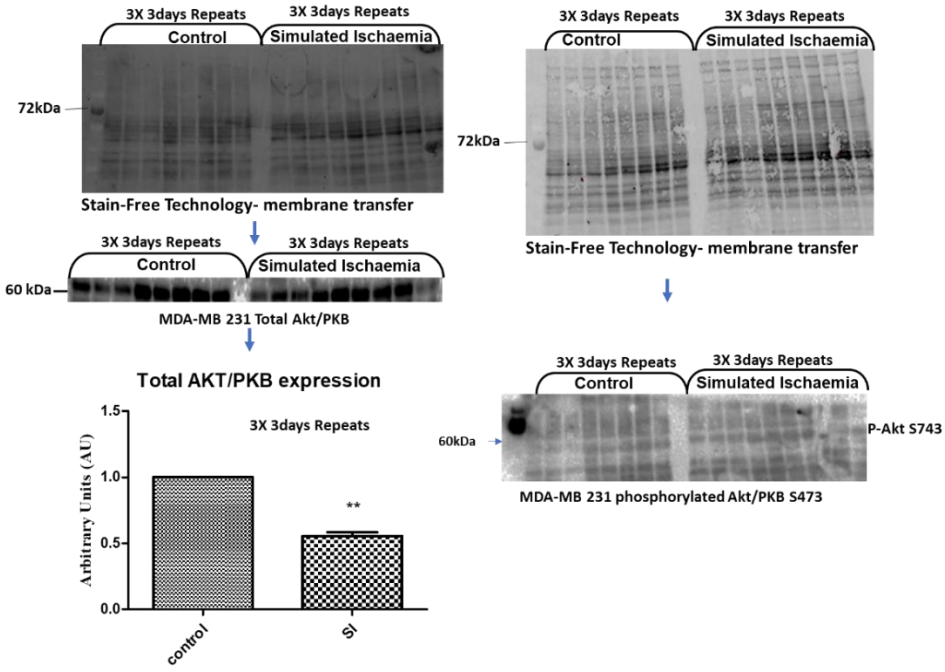

Figure 5.6: Western blot results of MDA-MB 231 exposed to 2 hours SI showing the expression of phosphorylated Akt/PKB S743 and total-Akt/PKB. The data shows a statistically significant reduction in the expression of T-Akt/PKB at **p value < 0.01 following 2 hours SI. A statistical test was done using student T-test, n = 3. The expression of phosphorylated AKt/PKB S743 was not conclusive.

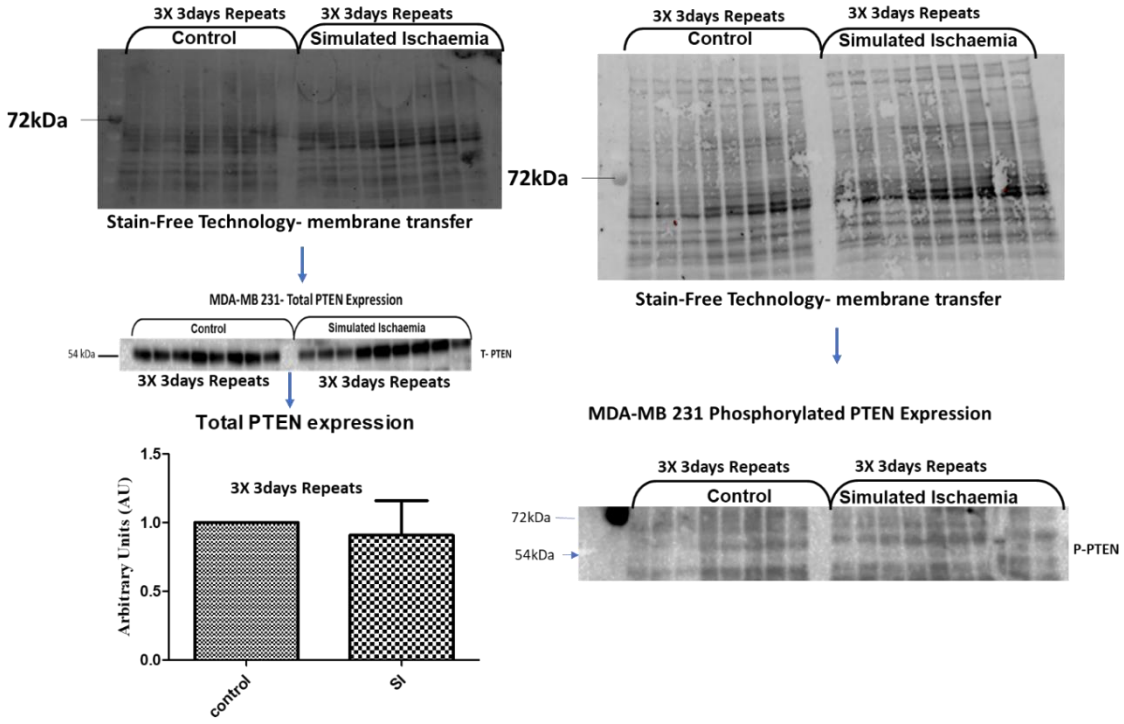

Figure 5.7: Western blot results of MDA-MB 231 exposed to 2 hours SI showing the expression of phosphorylated PTEN and total-PTEN. There was no statistically significant difference in the expression of PTEN following 2 hours SI. A statistical test was done using student T-test, n= 3. The expression of phosphorylated PTEN was inconclusive.

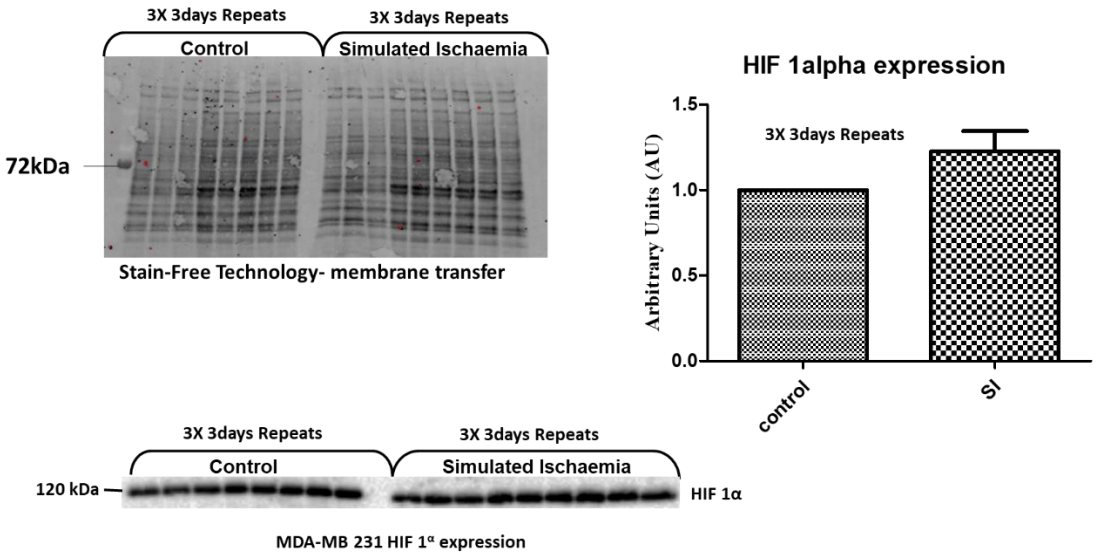

Figure 5.8: Western blot results showing protein expression of HIF-1 alpha on MDA-MB 231 following 2 hours SI. The expression of HIF-1 alpha showed no statistically significant differences in expression between the control and SI. A statistical test was done using student T-test, n =3.

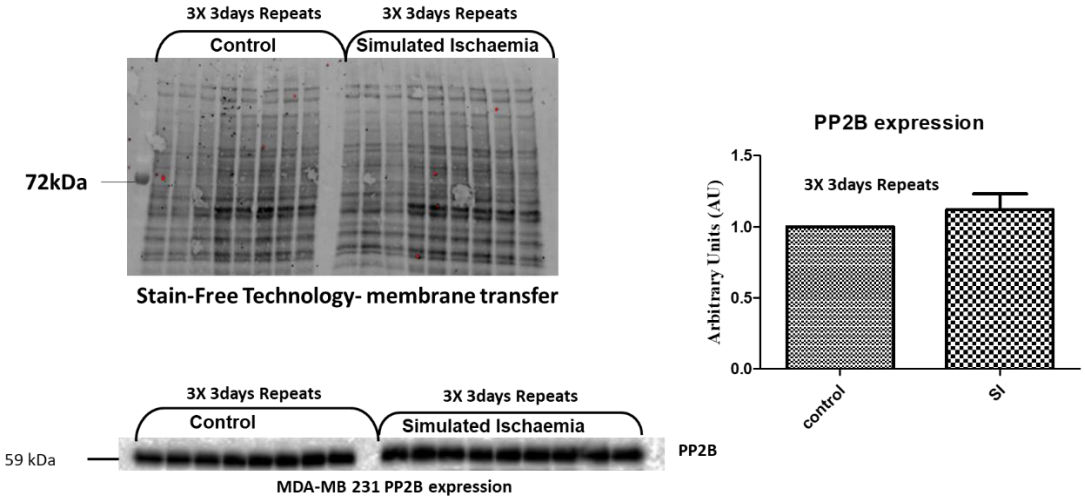

Figure 5.9: Western blot results showing protein expression of HIF-1 alpha on MDA-MB 231 following 2 hours SI. PP2B showed no difference in expression between control and SI. A statistically test was done using student T-test, n =3.

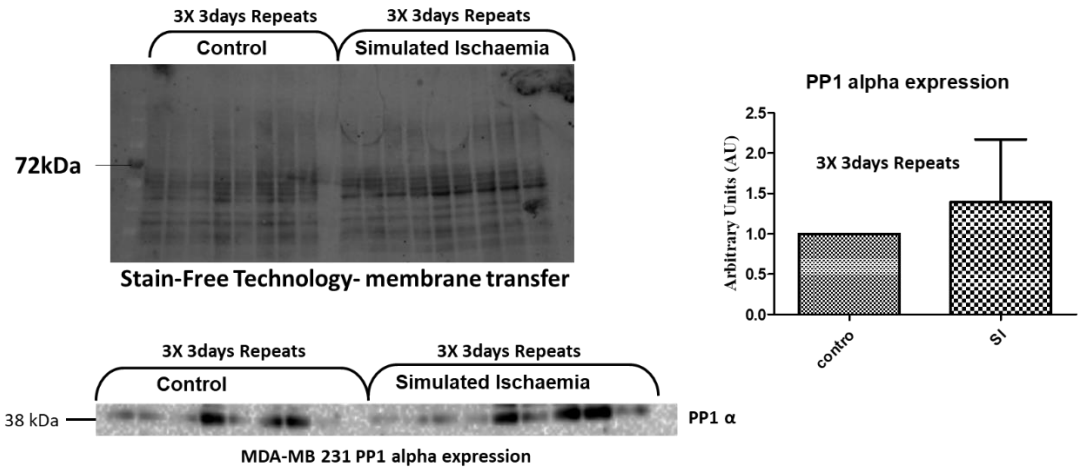

Figure 5.10: Western blot results showing protein expression of PP 1alpha on MDA-MB 231 following 2 hours SI. The expression of PP 1alpha was inconclusive. A statistical test was done using student T-test, n =3.

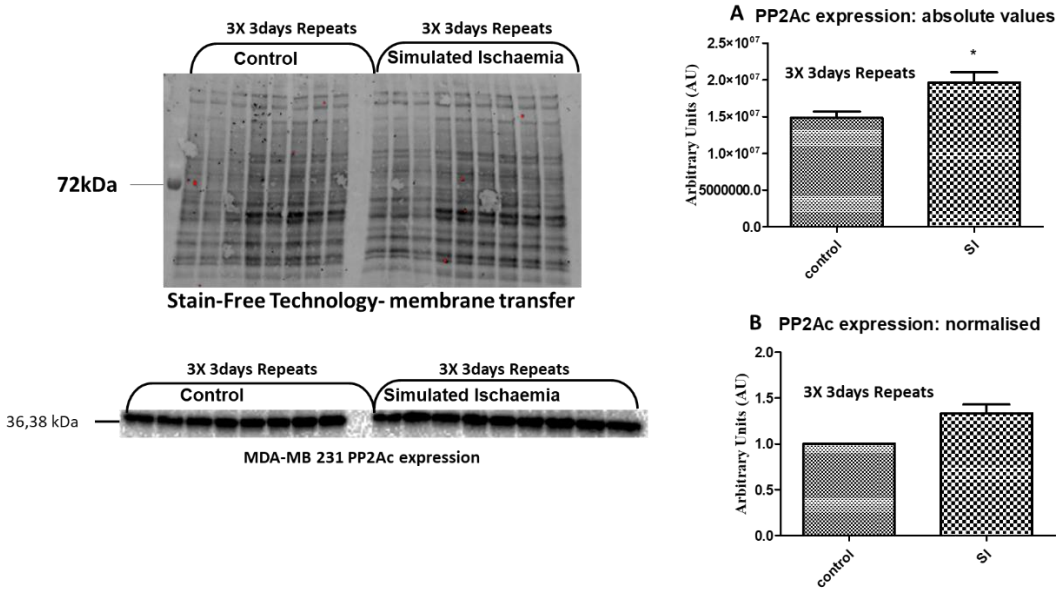

Figure 5.11: Western blot results showing protein expression of PP2Ac on MDA-MB 231 following 2 hours SI. A. unpaired student T-test of absolute values of PP2Ac expression showed an increase in expression at *p < 0.05 following SI. Whereas, B. paired student T-test of normalised data showed no significance, n =3.

Chapter 6: Pharmacological modulation of PP2A

Aim 3: The effect of pharmacological manipulation of PP2A in the heart (H9c2) and cancer (MDA-MB 231) cell lines following 2 hours simulated ischemia and 30 minutes reperfusion.

While investigating the effect of SI on the expression and activity of protein phosphatases, it was found that PP2A was slightly increased following 2 hours SI in MDA-MB 231 cells. In order to determine the importance, if any, of this increase, we set out to pharmacologically modulate PP2A in H9c2 and MDA-MB 231 cells. Cantharidin (2 µM and 5 µM), an inhibitor of both PP2A and PP1, and FTY 720 (1 µM and 5 µM), an activator of PP2A were chosen for the modulation. Drugs were prepared in DMSO. Dilutions were done using either DMEM (normal growth media) or Esumi buffer (SI media). Normoxic control and SI were incubated in 5 % CO_2 at 37 °C in a humidified atmosphere for 2 hours. Following 2 hours incubation, cells prepared for ATP assay were transferred to a white bottom clear plate for reading, whereas the remaining cells were exposed to 30 minutes reperfusion with a calcium reperfusion buffer in a non-CO_2 incubator for the purpose of PI and JC-1 staining. Simulated reperfusion was included to control for automatic reperfusion. Results from the optimization for hypoxia as described in chapter 3 showed that automatic reperfusion occurs immediately after opening the hypoxic chamber. For the ATP assay, cells were lysed immediately after we opened the hypoxic chamber, whereas, the PI and JC-1 stain procedure is lengthy and guarantees automatic reperfusion. More than 1 mM calcium was added to the reperfusion buffer to represent the elevation of calcium in the extracellular fluid due to ischemia, which is still present during reperfusion. Since our reperfusion buffer did not contain bicarbonate it was not necessary to incubate in a CO_2 incubator, thus we used a non-CO_2 incubator. After 30 minutes of reperfusion, cells were stained with either PI or JC-1 for 10 minutes. After washing, cells subjected to PI staining were analysed using the BMG Labtech FLUOstar Omega Plate reader. JC-1 stained cells were subjected to both the BMG Labtech FLUOstar Omega Plate reader and fluorescence microscopy. Images for JC-1 were analysed using Image J.

ATP assay viability results

An ATP assay was performed to asses cell viability in normoxic cells and cells exposed to SI in the presence and absence of PP2A inhibition (cantharidin) or activation (FTY 720). H9c2 normoxic cells treated with 2 µM cantharidin and 5 µM cantharidin had no statistically significant difference in ATP levels compared to control. Controls contained only growth medium without DMSO. Additionally, H9c2 cells treated with SI + 2 µM cantharidin and 5 µM cantharidin had no effect on ATP levels compared to SI controls (Figure 6.1A). Normoxic treatment with 1 µM FTY 720 and 5 µM FTY 720 showed no statistically significant difference compared to control. Both treatments with SI + 1 µM FTY 720 and SI + 5 µM FTY had no effect on ATP levels (Figure 6.1B). MDA-MB 231 normoxic samples treated with 2 µM and 5 µM cantharidin showed no effect on ATP levels against normoxia with “no drugs”. Moreover, SI treatment with 2 µM and 5 µM cantharidin had no effect on ATP levels against

SI with "no drugs" (Figure 6.2A). MDA-MB 231 normoxic cells treated with 1 µM and 5 µM FTY 720 showed no statistically significant difference in ATP levels against normoxic with "no drugs". 1 µM and 5 µM FTY 720 treatment under SI conditions had no statistical difference on ATP levels against SI with "no drugs" (Figure 6.2B).

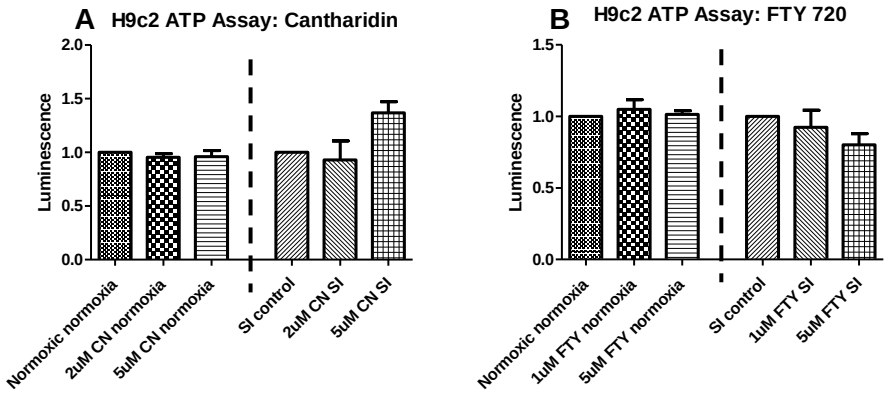

Figure 6.1: A. H9c2 cells treated with cantharidin (2 µM and 5 µM) and B. FTY 720 (1 µM and 5 µM) were compared using one-way ANOVA with Bonferroni post hoc test against both normoxia and SI. Drug treatment in both normoxic and SI samples had no effect on the levels of ATP, n = 3.

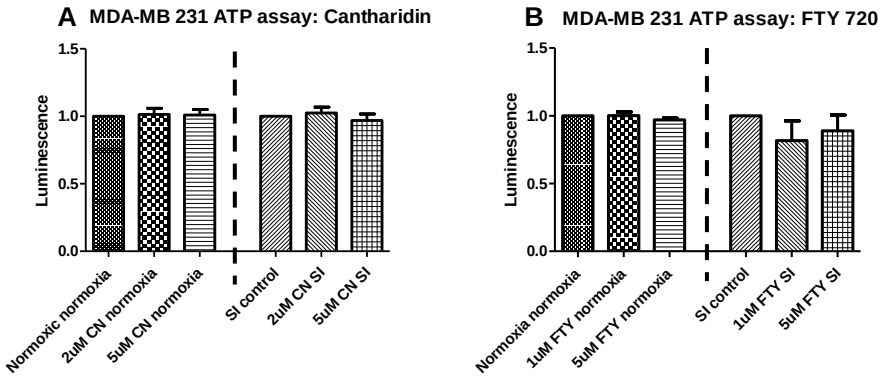

Figure 6.2: A. MDA-MB 231 cells treated with cantharidin (2 µM and 5 µM) and B. FTY 720 (1 µM and 5 µM) were compared using one-way ANOVA with Bonferroni post hoc test following 2 hours SI; also comparing the effect of the drugs under normoxic conditions. All the samples treated with drugs under both normoxic and SI conditions drugs showed no effect on the levels of ATP; n= 4. The normoxia data was expressed relative to normoxia control values, while the SI data was expressed relative to the SI drug control.

DMSO exerted no significant effect on ATP levels in H9c2 cells (Figure 6.3A). dH_2O was used as a positive control which confirmed cell death (normoxia: 1.000 ± 0.000 AU vs normoxia + dH_2O: 0.0118 ± 0.003 AU; n= 3; $p < 0.001$) and (SI: 1.000 ± 0.000 AU vs SI + dH_2O: 0.052 ± 0.011 AU; n= 3; $p < 0.001$) (Figure 6.3B). DMSO exerted no significant effect on the ATP levels of MDA-MB 231 cells (Figure 6.4A). 1 % Triton X-100 treatment was used as a positive control for cell death in the MDA-MB 231 cells both under normoxic conditions (normoxia: 1.000 ± 0.000 AU vs normoxia + 1 % Triton

X-100: 0.073 ± 0.026 AU; n= 4; $p < 0.001$), as well as SI conditions (SI: 1.000 ± 0.000 AU vs SI + 1 % Triton X-100: 0.278 ± 0.086 AU; n= 4; $p < 0.05$) (Figure 4.5B).

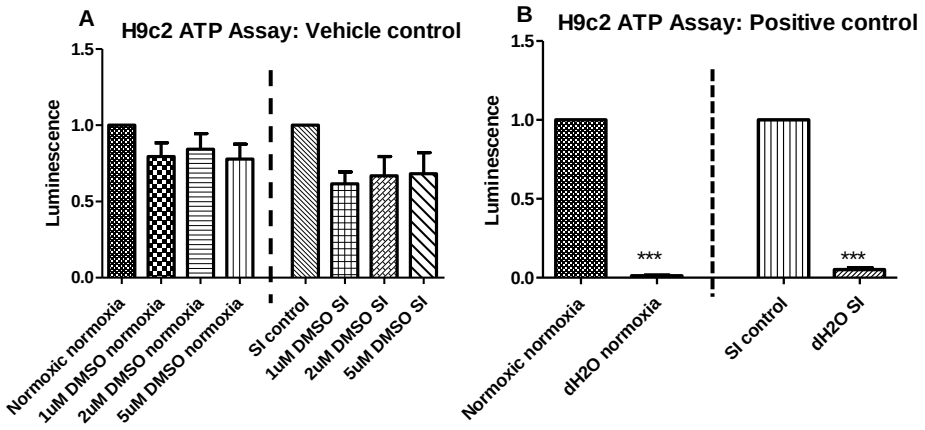

Figure 6.3: A. One- way ANOVA analysis on H9c2 cells treated with DMSO as a vehicle control and B. dH_2O as a positive control. A. shows that 1 µM, 2 µM and 5 µM DMSO exerted no significant effect on H9c2 cell line. However, B. showed dH_2O positive control to have confirmed cell death, n= 3. Statistical significance was measured at ***$p < 0.001$.

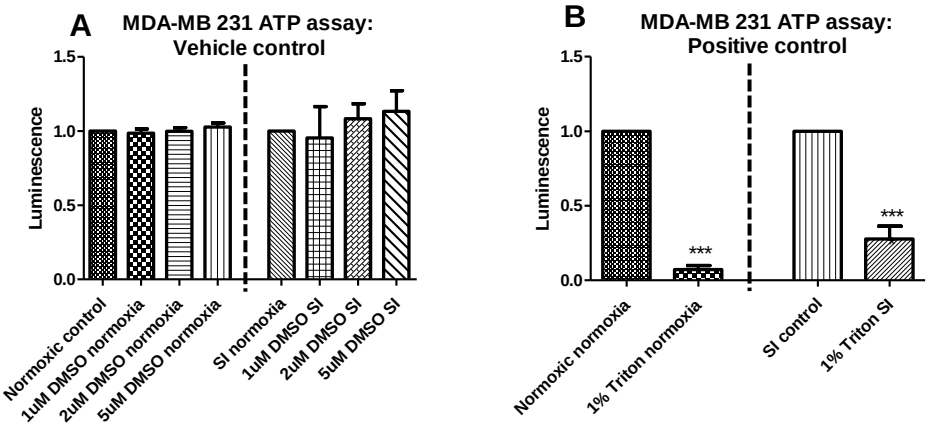

Figure 6.4: One-way ANOVA analysis on MDA-MB 231 cells treated with DMSO and 1 % Triton. A. DMSO exerted no effect on MDA-MB 231 cells. B. 1 % Triton X-100 induced a reduction in ATP levels under both normoxic and SI conditions, n = 4. Statistical significance was measured at *$p < 0.05$ and *** $p < 0.001$.

Propidium Iodide stained cell viability results

Propidium iodide is a cell membrane impermeable dye that penetrates the cell membrane when it is damaged, thereby staining the intracellular DNA. It is therefore used to measure cell death by necrosis. H9c2 and MDA-MB 231 cells were exposed to 2 hours SI followed by 30 minutes reperfusion. Cantharidin (2 µM and 5 µM) were used to inhibit PP2A whereas to activate PP2A, FTY 720 (1 µM

and 5 µM) was used. Table 6.1 shows the mean±SEM for both normoxia and SI with different concentrations of DMSO. DMSO did not induce significant cell death as assessed by PI (table 6.1).

Table 6.1. The effect DMSO (1, 2 µM and 5 µM) on MDA-MB 231 cells subjected to both normoxia and 2 hours SI followed by 30 minutes reperfusion.

PROPIDIUM IODIDE (PI) STAINING

	RELATIVE FLUORESCENCE UNITS (RFU)			
	H9C2 CELL		MDA-MB 231	
TREATMENT GROUPS	Normoxia	Simulated ischemia (SI)	Normoxia	Simulated ischemia (SI)
	Mean ± SEM	**Mean ± SEM**	**Mean ± SEM**	**Mean ± SEM**
Normoxia	157.8 ± 10.92	167.5 ± 8.520	199.5 ± 8.381	214.1 ± 1.192
Positive control	193.6 ± 12.61	244.2 ± 80.93	370.6 ± 67.62	454.2 ± 87.27
1 µM DMSO	165.3 ± 6.623	156.3 ± 156.3	209.0 ± 8.24	229.8 ± 12.96
2 µM DMSO	256.0 ± 48.99	185.8 ± 13.18	201.3 ± 15.73	218.0 ± 10.91
5 µM DMSO	194.7 ± 6.366	183.7 ± 14.68	190.9 ± 15.95	202.3 ± 7.29

[3] Cells were stained with Propidium Iodide at the end of 30 minutes reperfusion for 10 minutes. One-way ANOVA with Bonferroni post hoc test showed that DMSO did not induce cell death on both H9c2 and MDA-MB 231 cell lines, n= 3 to 4. The mean ± SEM are dipicted in the table.Positive control for H9c2 cell line used was dH_2O whereas, for MDA-MB231 Triton X100.

Figure 6.5 shows how dH_2O which was used as a positive control for H9c2 cell line failed to confirm cell death when measured by PI. Whereas, triton X-100 was used to induce cell death in MDA-MB 231 cell line under both normoxic (normoxia: 1.000 ± 0.000 RFU vs normoxia + 0.5 % Triton X-100: 1.384 ± 0.1431 RFU vs normoxia + 1 % Triton X-100: 2.547 ± 0.4194;n =3; p <0.01) and SI conditions (SI:1.000 ± 0.000 RFU vs SI + 0.5 % Triton X-100: 1.820 ± 0.154 RFU vs SI + 1 % Triton X-100: 2.649 ± 0.399 RFU n =3; p <0.01)).

One-way ANOVA statistical analysis evaluated the effect of cantharidin (2 µM and 5 µM) on normoxic H9c2 cells and those exposed to 2 hours SI followed by 30 minutes reperfusion. No cell death, as measured by PI stain, was observed (Figure 6.6A). FTY 720 (1 µM and 5 µM) treatment of normoxic H9c2 cells which received only DMEM normal growth media and those exposed to 2 hours SI followed by 30 minutes reperfusion also showed no effect on cell death (Figure 6.6B).

MDA-MB 231 cell line treatment with cantharidin (2 µM and 5 µM) under normoxic conditions did not induce cell death as measured by PI (Figure 6.7A). Although the treatment with 1 µM FTY 720 under normoxic conditions induced cell death, which was indicated by a significant increase in PI fluorescence (normoxia:1.000 ± 0.000 RFU vs normoxia + 1 µM FTY 720: 1.149 ± 0.044 RFU; n= 4;

[3]

p < 0.05), 5 µM FTY 720 showed no effect. Moreover, both treatment with FTY 720 (1 µM and 5 µM) under SI conditions showed no effect on cell death (Figure 6.7B).

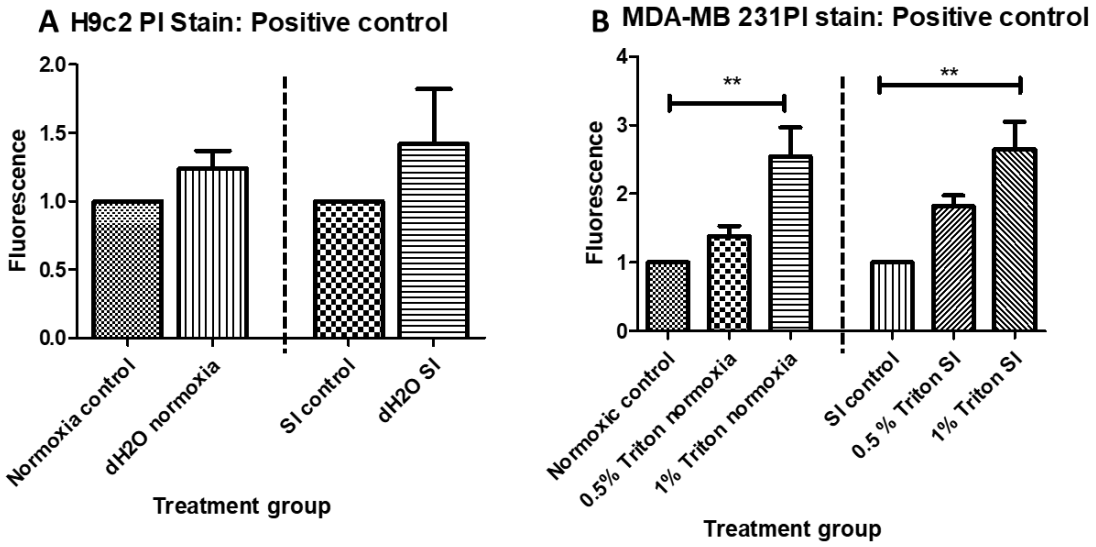

Figure 6.5: The effect of positive control on H9c2 and MDA-MB 231 cells exposed to both normoxia and 2 hours simulated SI followed by 30 minutes reperfusion. Propidium Iodide did not detect cell death when H9c2 cells were treated with dH_2O (A), whereas, Triton X-100 showed significant cell death in MDA-MB 231 cells (B), n = 3 to 4. Statistical significance was measured at *p < 0.05 and **p < 0.01.

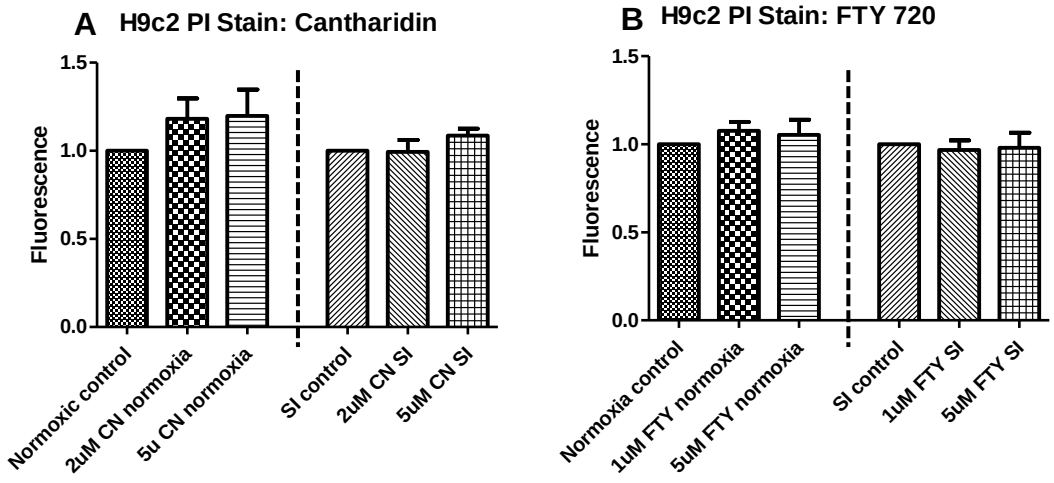

Figure 6.6: The effect of cantharidin (2 µM and 5 µM) and FTY 720 (1 µM and 5 µM) on H9c2 exposed to both normoxia and 2 hours SI followed by 30 minutes reperfusion. One-way ANOVA with Bonferroni post hoc test showed that none of the interventions induced necrosis as assessed by PI staining, n= 3.

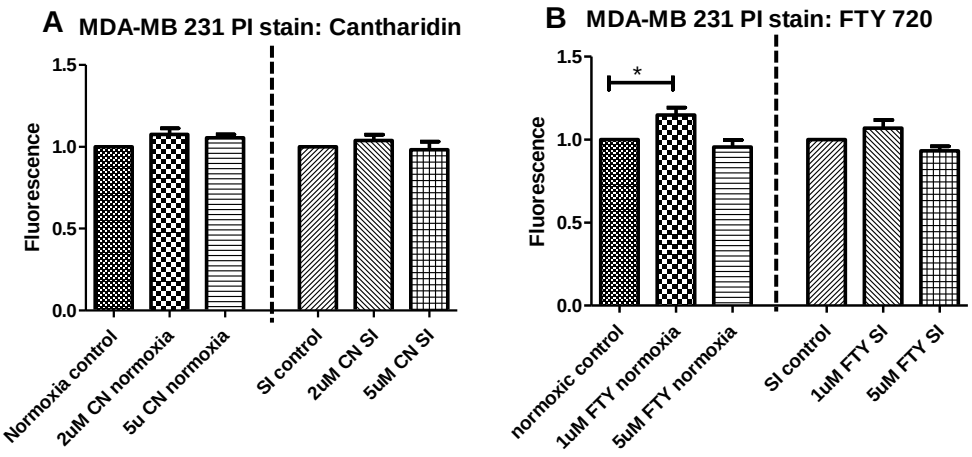

Figure 6.7: The effect of cantharidin (2 µM and 5 µM) and FTY 720 (1 µM and 5 µM) on MDA-MB 231 cells exposed to both normoxia and 2 hours SI followed by 30 minutes reperfusion. One-way ANOVA with Bonferroni post hoc test showed that cantharidin treatment had no effect on normoxia and SI as measured by PI stain. However, normoxic MDA-MB 231 treated with 1 µM FTY 720 showed an induction of cell death by necrosis indicated by an increase in PI fluorescence, n = 4. Statistical significance was measured at * $p < 0.05$.

JC-1 stain viability test measured by the plate reader

JC-1 stain was performed to assess the integrity and function of the mitochondria in both H9c2 and MDA-MB 231 cells exposed to both normoxia and 2 hours SI in the presence and absence of drug intervention followed by 30 minutes reperfusion. Cells stained with JC-1 were subjected to the plate reader and fluorescence microscopy. As mentioned previously, cantharidin (2 µM and 5 µM) and FTY 720 (1 µM and 5 µM) were used to inhibit and activate PP2A respectively. DMSO vehicle did not induce any damage to the mitochondria. H9c2 and MDA-MB 231 treatment with different concentrations of DMSO did not cause any damage to the mitochondria as measured by the plate reader (Table 6.2).

Table 6.2: The effect of DMSO in H9c2 and MDA-MB 231 cells exposed to both normoxia and SI followed by 30 minutes reperfusion on.

JC-1 STAINING

RELATIVE FLUORESCENCE UNITS (RFU)				
	H9C2 CELLS		**MDA-MB 231**	
TREATMENT GROUPS	Normoxia	Simulated ischemia (SI)	Normoxia	Simulated ischemia (SI)
	Mean ± SEM	**Mean ± SEM**	**Mean ± SEM**	**Mean ± SEM**
Normoxia	0.4212 ± 0.063	0,4336 ± 0.1078	0.5336 ± 0.1754	0.5113 ± 0,165
Positive control	0.1415 ± 0.056	0.1260 ± 0.039	0.097 ± 0.013	0.088 ± 0.004
1 µM DMSO	0,4628 ± 0,156	0,2504 ±0,098	0,5514 ± 0,178	0,4456 ± 0,111
2 µM DMSO	0,4544 ± 0,161	0,3468 ±0,347	0,5001 ± 0,144	0,5050 ± 0,149
5 µM DMSO	0,4674 ± 0,160	0,4853 ±0,056	0,5262 ± 0,159	0,5228 ± 0,154

[4] There was no statistical significant difference in any of the treatments with different DMSO concentrations. Cells were stained with JC-1 immediately after reperfusion and allowed to incubate for 10 minutes. One-way ANOVA with Bonferroni post hoc test was used to compare between normoxia and SI, n= 3 for H9c2 and n= 4 for MDA-MB 231. The table reports mean±SEM of all DMSO treatment groups.

dH_2O served as a positive control to induce mitochondrial damaged in H9c2 line under both normoxia (normoxia: 1.000 ± 0.000 RFU vs normoxia + dH_2O: 0.3388 ± 0.1356 RFU) and SI conditions (SI: 1.000 ± 0.000 RFU vs SI + dH_2O: 0.3661 ± 0.1927 RFU) as measured by JC-1 stain in the plate reader. Whereas, triton X-100 was used to confirm mitochondrial damage in MDA-MB 231 cell line under both normoxia (normoxia: 1.000 ± 0.000 RFU vs normoxia + 0.5 % TritonX-100: 0.2371 ± 0.0859 RFU vs normoxia + 1 % Triton X-100: 0.2424 ± 0.0918 RFU) and SI conditions (SI: 1.000 ± 0.000 RFU vs SI + 0.5 % TritonX-100: 0.2027 ± 0.0498 RFU vs SI + 1 % Triton X-100: 0.2081 ± 0.0557 RFU) (Figure 6.8). Both Cantharidin (2 µM and 5 µM) and FTY 720 (1 µM and 5 µM) treatment in H9c2 under both normoxic and SI conditions did not cause any changes in the function and integrity of mitochondria (Figure 6.9). Only 5 µM Cantharidin treatment under SI conditions reduced the mitochondrial function and integrity, as assessed by JC-1 staining in MDA-MB 231 cell line (SI: 1.000 ± 0.000 RFU vs 5µM cantharidin: 0.625 ± 0.112 RFU; n= 4; $p < 0.01$). Whereas, FTY 720 (1 µM and 5 µM) treatment under both normoxic and SI conditions did not influence mitochondrial function and integrity (Figure 6.11).

[4]

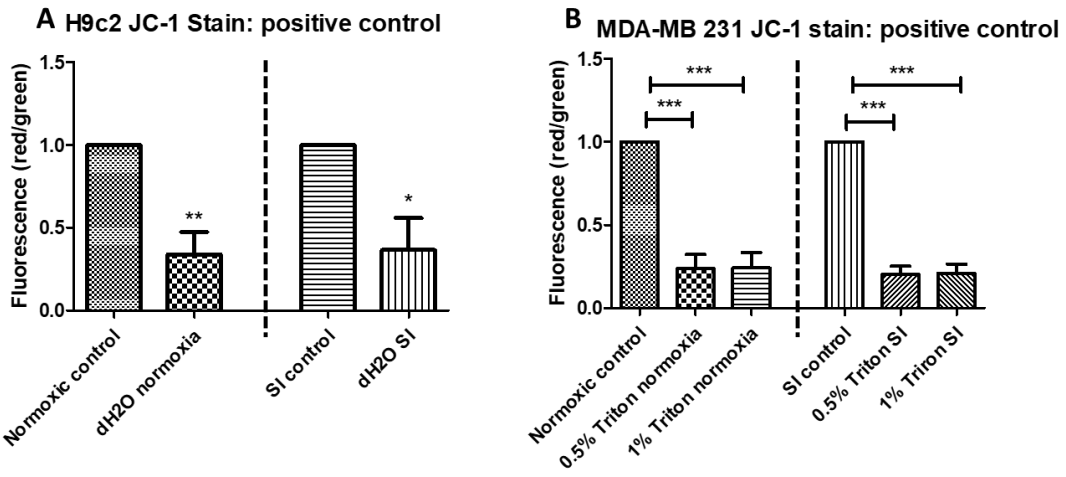

Figure 6.8: The effect of positive control on A. H9c2 and B. MDA-MB 231 cells exposed to both normoxia and 2 hours SI followed by 30 minutes reperfusion as assessed by JC-1 stain and measured in the plate reader. dH_2O reduced mitochondrial function and integrity of H9c2 cells, whereas Triton X-100 reduced the mitochondrial function and integrity of MDA-MB 231, n = 3 to 4. Statistical significance was determined by One-way ANOVA at *p < 0.05, **p < 0.01 and ***p< 0.001.

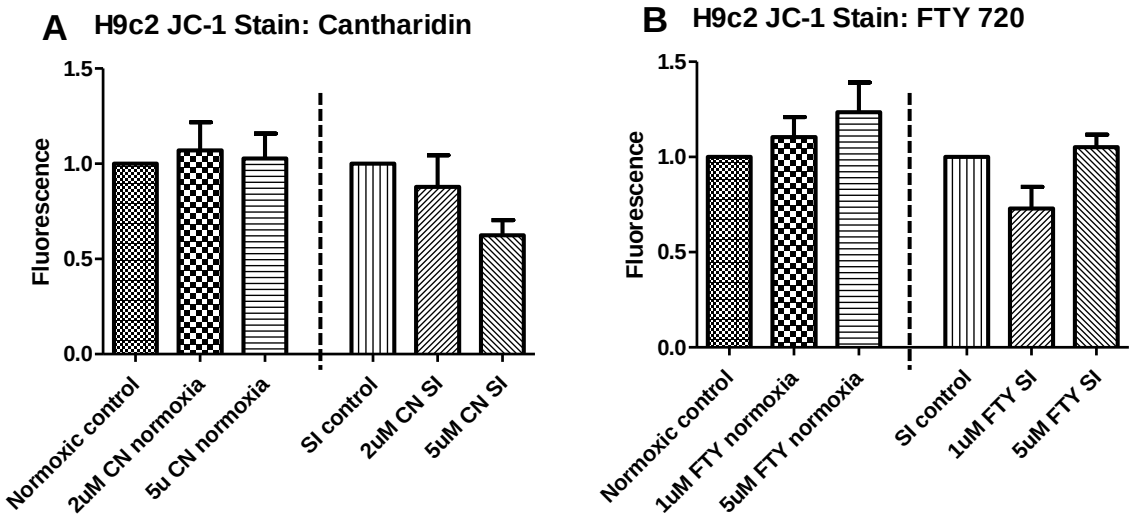

Figure 6.9: The effect of Cantharidin and FTY 720 on H9c2 cells treated with both normoxia and 2 hours SI followed by 30 minutes reperfusion. After reperfusion, cells were stained with JC-1 for 10 minutes. One-way ANOVA with Bonferroni showed that neither cantharidin nor FTY 720 caused any damage to the mitochondria of H9c2 cells, n= 3.

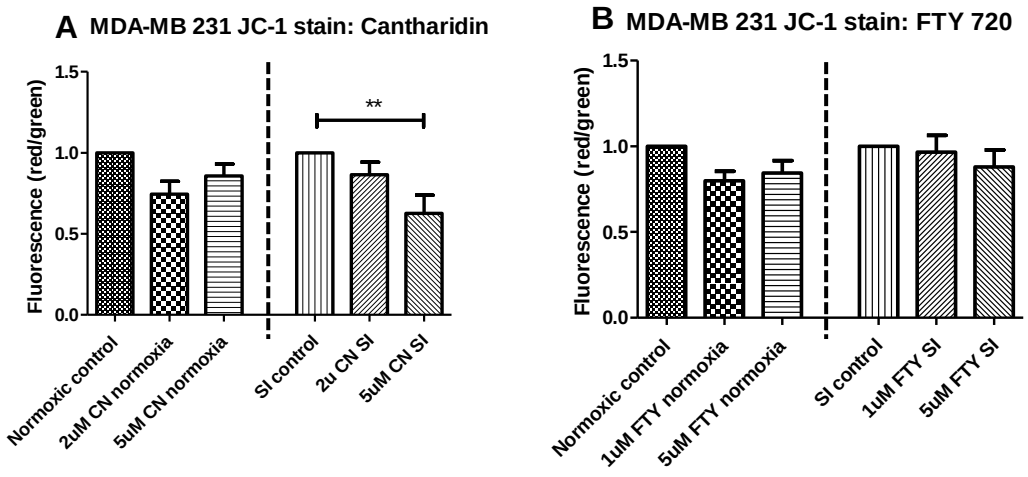

Figure 6.10: The effect of Cantharidin and FTY 720 on MDA-MB 231 cells treated with both normoxia and 2 hours SI followed by 30 minutes reperfusion. Cells were stained with JC-1 after 30 minutes reperfusion and incubated for 10 minutes. One-way ANOVA with Bonferroni post hoc test reported that only 5 µM cantharidin under SI conditions reduced mitochondrial function and integrity. FTY 720 treatment did not induced any mitochondrial damage under neither normoxia nor SI conditions, n= 4. Statistical significance was measured at *p < 0.01.

JC-1 image statistical analysis

H9c2 and MDA-MB 231 cells were exposed to both normoxia and 2 hours SI followed by 30 minutes reperfusion. As mentioned earlier, cells stained with JC-1 were subjected to the plate reader and fluorescence microscopy. Although the plate reader is deemed more accurate, image analysis was used as a confirmation technique. Two images were taken per group per 4x experimental repeats. Images obtained from the microscope were analysed by imageJ where 20 cells were selected per image for analysis and the mean was calculated. Thereafter, the red/green ratio was calculated, and used for further statistical analysis. The quality of the images captured from the microscopy was not superb. However, visual presentation of these data may supply additional information to the plate reader. The images were highly cropped to fit, therefore the scale bar of a 100 was used at 20X magnification. We noted the lack of visibility of green on the colour image, which is likely due to most cells being viable. However, imageJ has an option to split channels into red and green to visualise which cells stained red and which stained green. The cells that stained red indicate viable cells whereas those that stained green indicates compromised mitochondria. Images were stacked to make a montage as represented below. Some cells were overpopulated, some had changed their morphology, and some were washed away. This made analyses for these images a bit difficult.

JC-1 image analysis using one-way ANOVA with Bonferroni post hoc test shows that 2 µM cantharidin had no effect on H9c2 mitochondrial integrity and function under both normoxia and SI conditions (Figure 6.11A). RGB (red, green & blue) image of H9c2 cells treated with 2 µM cantharidin under normoxic conditions was heavily stained red and showed no difference compared to the normoxic

control. The split channel showed that the green channel has faded or weak staining on both the nomoxia and normoxia + 2 µM cantharidin. There appear to be no visible distinction between SI and SI + 2µM cantharidin in terms of cell population size, staining intensity and morphology Figure 6.11C). 5 µM cantharidin treatment under SI conditions led to a reduction in the JC-1 red/green ratio, indicative of the reduction in the function and integrity of the mitochondria (SI: 1.000 $\pm$ 0.000 RFU vs SI + 5 µM cantharidin: 0.285 ± 0.059 RFU; n= 3; $p < 0.01$) (Figure 6.11A). RGB image of H9c2 cells treated with 5 µM cantharidin under normoxic conditions showed fainted staining for the red stain compared to H9c2 RGB normoxic control. The green channel showed lighter intensity compared to the red channel in the colour split channel. H9c2 cells treated with 5 µM cantharidin under SI conditions showed shredded pieces of cells stained both red and green compared to SI (Figure 6.11C). JC-1 image analysis of FTY 720 (1 µM and 5 µM) treatment on normoxic and SI H9c2 cell line revealed that FTY 720 exerted no effect on the mitochondria (Figure 6.11B). Fluorescence imaging showed that H9c2 cells treated with 2 µM FTY 720 under both normoxic and SI conditions showed no visible change compared to normoxic and SI control respectively. The green channel showed faded stain compared to the red channel. Additionally, the JC-1 image of H9c2 cells treated with 5 µM FTY 720 under both normoxic and SI conditions showed no visible change observed compared to normoxic and SI respectively control (Figure 6.11D).

One-way ANOVA analysis of MDA-MB 231 cell fluorescent image showed that cantharidin at both 2 µM and 5 µM did not exert an effect on JC-1 staining under both normoxic and SI conditions (Figure 6.12A). Microscopic images obtained from MDA-MB 231 cells showed the morphology to be circular instead of the standard elongated spindle shape, possibly due to detachment via washing or reperfusion. This was mostly observed in cells containing the normoxic growth medium (DMEM) compared to those exposed to SI (Esumi buffer). Cells treated with 2 µM cantharidin under normoxic conditions showed a reduction in cell population size compared to the mormoxic control. The RGB images showed that the MDA-MB 231 cells of both normoxic control and normoxia + 2 µM cantharidin were intensly stained with red and almost no green staining. The split channel revealed that green stained weakly. Cells treated with 2 µM cantharidin under SI conditions showed a visible reduction in population size in comparison to SI. The green stain stained weakly. MDA-MB 231 cells treated with 5µM cantharidin under both normoxic and SI conditions had changed morphology from elongated spindle shape of the typical MDA-MB 231 cell line to circular. The green channel was stained lighter than the red channel in the colour split channel (Figure 6.12C). Moreover FTY 720 treatment at both 1µM and 5µM had no effect on MDA-MB 231 mitochondria under both normoxic and SI conditions (Figure 6.12B). MDA-MB 231 cells treated with 2 µM FTY 720 under normoxic conditions seemed to have fewer cells compared to normoxic control. There was no visible change observed in MDA-MB 231 cells treated with 2 µM FTY 720 under SI conditions. The green channel in all images was weakly stained relative to the red channel. MDA-MB 231 treated with 5 µM FTY 720 under both normoxic and SI conditions

appeared to have reduced number of cells compared to normoxic control and SI respectively (Figure 6.12D).

Statistical test for H9c2 cells treated with DMSO vehicle under both normoxic and SI conditions showed no effect on the function and integrity of the mitochondria (Figure 6.13A). This report only showed the JC-1 images of DMSO with the highest concentration of 5 µM. H9c2 cells treated with 5 µM DMSO under both normoxic and SI conditions showed no visible change between all groups, most of the cells were stained red (Figure 6.13C). Positive control confirmed reduction in mitochondrial function and integrity of H9c2 cells (SI: 10.97 $\pm$ 1.774 RFU vs dH_2O + SI: 0.5825 $\pm$ 0.3313 RFU; n= 3; $p < 0.001$) (Figure 6.13B). H9c2 cells treated with dH_2O under both normoxic and SI conditions showed high levels of green staining in the RGB colour image; there was a significant reduction in number of cells and the cells had shrunk in morphological size (Figure 6.13D).

Statistical analysis showed that MDA-MB 231 cells treated with DMSO vehicle control under normoxic conditions had no effect on the mitochondria. Moreover, MDA-MB 231 cells treated with DMSO vehicle control under SI conditions had no effect on the integrity and function of the mitochondria, indicated by no noticeable change in the JC-1 red/green ratio (Figure 6.14A). MDA-MB 231 cells treated with 5 µM DMSO under both normoxic and SI conditions showed no visible change in staining between all groups (Figure 6.14C). One-way ANOVA showed that positive control indeed reduced the integrity and function of MDA-MB 231 mitochondria under normoxic conditions (normoxia: 1.000 ± 0.000 RFU vs normoxia + 1% Triton X-100: 0.351 ± 0.166 RFU; n= 4; $p < 0.05$). Also, 0.5 % and 1 % Triton treatment under SI conditions reduced the function and the integrity of the mitochondria respectively (SI: 1.000 ± 0.000 RFU vs SI + 0.5% Triton X-100: 0.241 ± 0.070 RFU; n= 4; $p < 0.01$) and (SI: 1.000 ± 0.000 RFU vs 1% Triton X-100 + SI: 0.186 ± 0.007 RFU; n= 4; $p < 0.01$) (Figure 6.14B). MDA-MB 231 treated with 1% Triton under normoxic conditions showed a significant reduction in cell number. RGB image of 1% Triton treatment under SI conditions showed all green stain, but the morphology of the cells was still intact. Thus, the green channel was more strongly stained than the red channel, indicative of severe mitochondrial damage (Figure 6.14D).

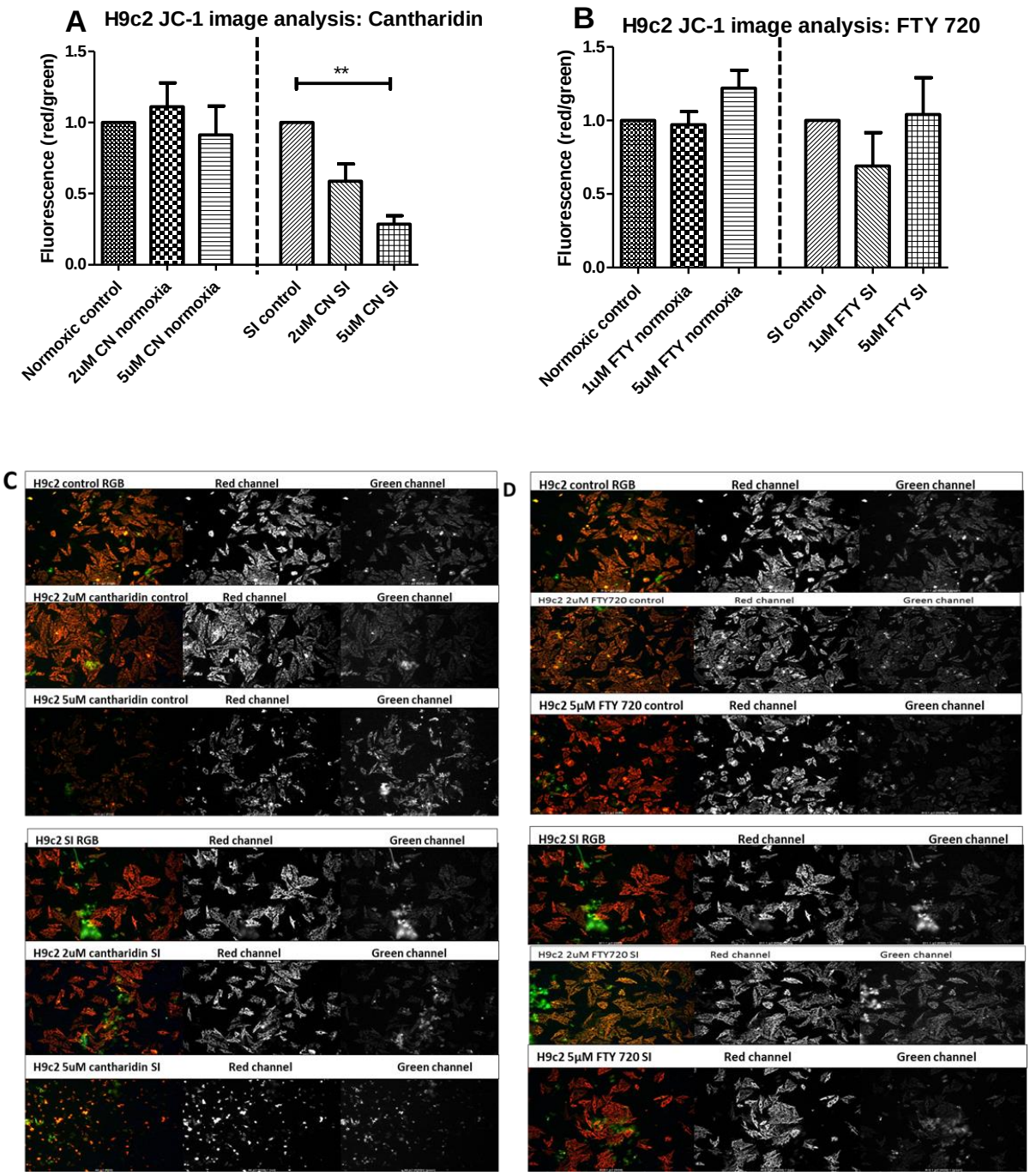

Figure 6.11: The effect of JC-1 stain on H9c2 cells cells treated with cantharidin (2 µM and 5 µM) and FTY 720 (1 µM and 5 µM) exposed to both normoxia and 2 hours SI followed by 30 minutes reperfusion. A. One-way ANOVA with Bonferroni post hoc test revealed that 5 µM cantharidin under SI conditions led to a reduction in mitochondrisal function and integrity. B. FTY 720 showed no effect on mitochobdria, n = 3. Statistical significance was measured at **p < 0.01. C. Montage JC-1 images from ImageJ showing H9c2 cells treated with 2 µM and 5 µM cantharidin under normoxic and SI conditions. JC-1 image analysis showed that 2 µM cantharidin treatment did not exert any effect on the mitochondrial integrity and function. However, Image analysis showed that 5 µM cantharidin under SI conditions negatively influenced the mitochondrial function and integrity with shredded pieces of cells stained red and green for H9c2 cells. D. H9c2 cells treated with 2 µM and 5 µM FTY 720 under both normoxic and SI conditions showed no visible changes in the mitochondrial function and integrity.

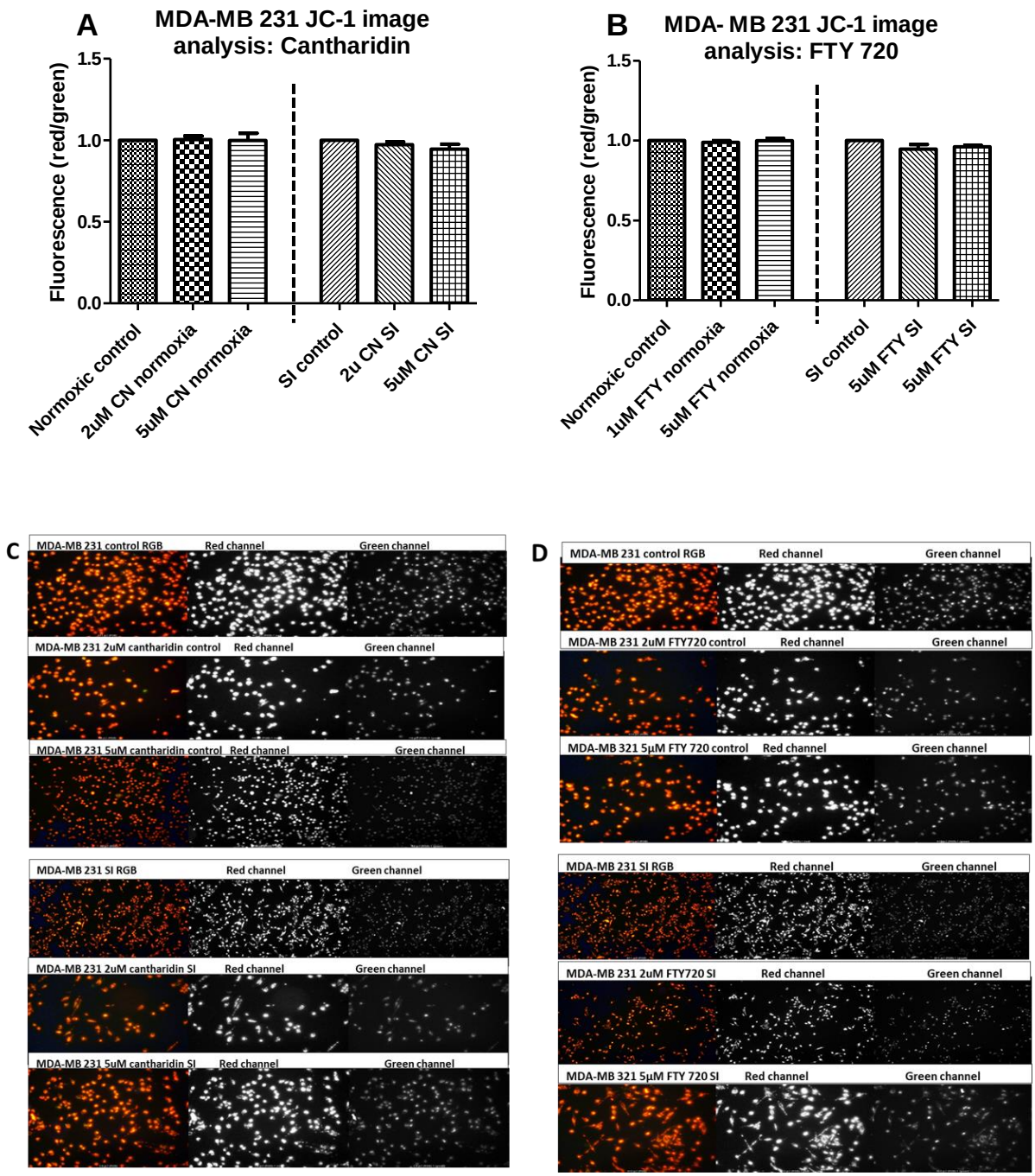

Figure 6.12: The effect of JC-1 stain on MDA-MB 231 cells treated with cantharidin (2 µM and 5 µM) and FTY 720 (1 µM and 5 µM) exposed to both normoxia and 2 hours SI followed by 30 minutes reperfusion. A. One-way ANOVA with Bonferroni post hoc test showed that cantharidin had no effect on the mitochondria. B. Statistical analysis showed that FTY 720 had no effect on the function and integrity of the mitochondria, n = 3. C. Montage JC-1 images from ImageJ showing MDA-MB 231 cells treated with 2 µM and 5 µM cantharidin under normoxic and SI conditions. JC-1 image analysis showed that cantharidin did not exert any effect on the mitochondrial integrity and function under both normoxic and SI conditions. D. MDA-MB 231 cells treated with 2 µM and 5 µM FTY 720 seem to show a reduction in population size under normoxic and SI conditions.

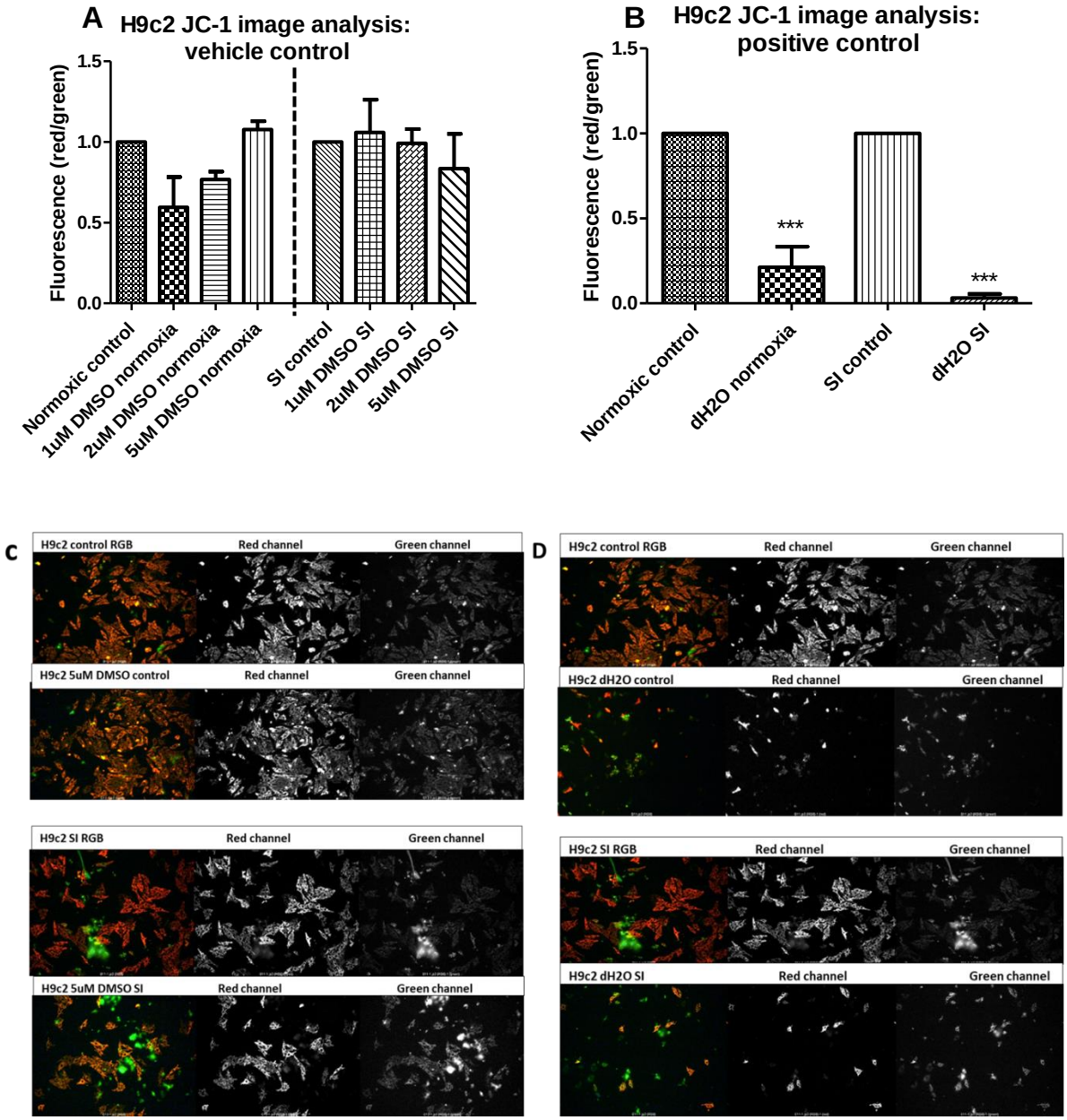

Figure 6.13: The effect of H9c2 cells treated with DMSO and dH_2O exposed to both normoxia and 2 hours SI followed by 30 minutes reperfusion. A. One-way ANOVA with Bonferroni post hoc test showed that DMSO vehicle control had no effect under both normoxic and SI conditions. B. dH2O under normoxic conditions showed no significant difference, whereas, in SI conditions it led to a significant reduction in the integrity and function of the mitochondria, n = 3. Statisticsl significance was measured at ***$p < 0.001$. C. Montage JC-1 images from ImageJ showing H9c2 cells treated with 5 µM DMSO under normoxic and SI conditions. Image analysis shows that 5 µM DMSO had no effect on the function and integrity of the mitochondria. D. Image analysis showed that H9c2 cells treated with dH_2O had a negative effect on the function and integrity of the mitochondria.

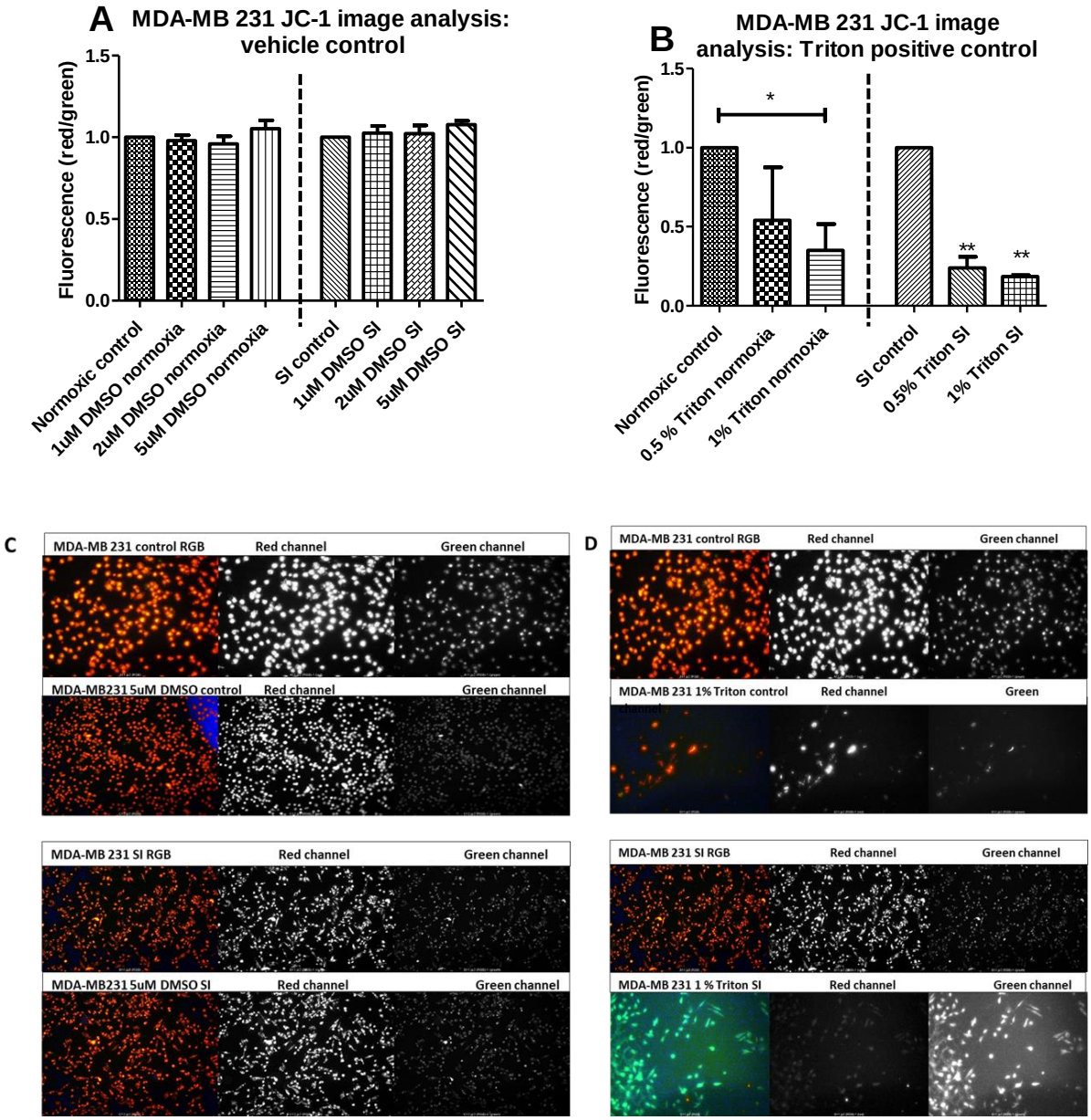

Figure 6.14: The effect of MDA-MB 231 cells treated with DMSO exposed to both normoxia and 2 hours SI followed by 30 minutes reperfusion. A. One- way ANOVA with Bonferroni post hoc test showed that DMSO vehicle control exerted no effect on the function and integrity of the mitochondria under both normoxia and SI conditions. B. 1 % Triton X-100 under normoxic conditions showed a statistical reduction in in the function and integrity of mitochondria at *p< 0.05, whereas, 0.5 % and 1 % Triton X-100 under SI conditions led to a reduction in red/green ratio at **p < 0.01 and **p < 0.01 respectively. C. Montage JC-1 images from ImageJ showing MDA-MB 231 cells treated with 5 µM DMSO under normoxic and SI conditions. Image analysis shows that 5 µM DMSO had no effect on the function and integrity of the mitochondria. D. Image analysis showed that 1 % Triton X-100 negatively affected the mitochondrial integrity and function of MDA-MB 231 cells as indicated by the green staining.

Chapter 7: Discussion and conclusion

Aim 1: The effect of 2 hours simulated ischemia with metabolic inhibition on cell viability in cancer (MDA-MB 231) and the heart cell lines (H9c2).

What is the effect of 2 hours SI on cell viability in H9c2 and MDA-MB 231 cell lines? For evaluation, H9c2 and MDA-MB 231 cells were exposed to 2 hours SI with metabolic inhibition in the presence of a hypoxic gas mixture (0 % O_2/5 % CO_2/95 % N_2 (H9c2) and 0.5 % O_2/5 % CO_2 and balance N_2 (MDA-MB 231)). Three cell viability tests were used: an ATP assay, propidium iodide (PI) and JC-1 staining. Within minutes after a loss of membrane integrity, cells lose their ability to synthesize ATP, and endogenous ATPases destroy any remaining ATP, thus the levels of ATP fall rapidly (Riss, et al., 2003). ATP determination showed that 2 hours SI significantly reduced ATP levels in H9c2 and MDA-MB 231 cell lines. The ATP assay confirmed that both the cell lines responded to ischemic insult by showing metabolic stress. It could however also be argued that the ATP merely indicates energy levels, not necessarily cell death. To quantify whether the significant reduction in ATP levels had led to cell death, JC-1 and Propidium Iodide staining were used to assess mitochondrial damage and cell death respectively.

To evaluate whether the reduction in ATP levels were associated with cell death, cells were reperfused for 30 minutes using calcium acidic reperfusion buffer followed by JC-1 and PI stain to measure cell death. JC-1 stain measures the integrity and function of the mitochondria, whereas, PI stain indicates cell death. JC-1 and PI stain showed that 2 hours SI did not cause mitochondrial damage or cell death. We had expected that the significant drop in ATP levels in association with reperfusion would result in cell death. We suspect that had SI been prolonged for more than two hours we would have observed cell death. Another possibility to have ensured cell death would have been the use of reperfusion buffered at pH 7 instead of the acidic reperfusion at pH 6.4. However, based on the report from a study by Inserte et al. (2008) we think acidic reperfusion could not have prevented cell death. In this study, they investigated the effect of acidic reperfusion on prolongation of intracellular acidosis and myocardial salvage. They reported that 40 minutes of prolonged ischemia followed by 30 minutes acidic reperfusion delayed pH normalisation, improved phosphocreatine recovery, and markedly reduced lactate dehydrogenase release and infarct size for the initial 3 minutes. After the first 15- or 30-minutes of reperfusion, there was no further delay of pH normalization and the protection afforded by the initial 3 minutes of acidic reperfusion was abolished (Inserte, et al., 2008). Therefore, even though we had used acidic reperfusion in our study; since it was prolonged for the duration of 30 minutes it could have not been protective, thus it could not have been the cause of the lack of observed cell death in our study. In so saying, the more likely cause is that 2 hours SI was not enough to induce cell death. Although we could not find supporting literature that administered the very same conditions as we applied in our lab, the studies we have found using hypoxia alone had a longer duration of hypoxic exposure of about 6 to

48 hours to observe a significant increase in cell death. In these studies, apoptosis was measured using Annexin V and PI apoptosis detection kit (Ma, et al., 2018; Wang, et al., 2017). In another study where apoptosis was measured using Annexin V and PI apoptosis detection kit, H9c2 cells were exposed to 50 minutes SI induced by Esumi buffer with metabolic inhibition followed by 4 hours reperfusion. The results showed that SI increased the percentage of apoptosis (Li, et al., 2017). The study on the effect of hypoxia on MDA-MB 231 where cells were exposed to hypoxia (1 % O_2) found that the percentage of apoptotic cells were significantly reduced after 48 hours (Xie, et al., 2016).

Regarding the lack of observable cell death, the Esumi buffer used to simulate ischemia had inhibited both glycolysis and the electron transport chain, which should have induced more metabolic stress to injure the cells. Despite the remarkable reduction in ATP levels observed, MDA-MB 231 and H9c2 cells remained quite robust with no indication of cell death. In Dr John Lopes' lab, they observed that the isolated rat cardiomyocyte cells were resistant to death even at higher concentrations of sodium dithionate (SDT) than used by us. They used 5 mM 2-deoxy-glucose (2DG) (inhibits glycolysis) and 5 mM SDT (inhibits the electron transport chain (Lumkwana, et al., 2017). Whereas, we used 0.5 mM SDT and 20 mM 2DG. Contrary to this, Dr Derick Van Vuuren (PhD thesis), implemented the exact same conditions for H9c2 cells as in this study. They measured cell death using annexin V and PI following 2 hours SI. They found that 2 hours SI induced cell death both by apoptosis and necrosis (Van Vuuren, 2014). However, we still reason that perhaps longer duration of SI could have induced cell death in both the cell lines in this study even though, Dr van Vuuren results pose a conundrum. Further investigations are required to evaluate cell death in H9c2 and MDA-MB 231 due to SI, especially the duration required to ensure cell death. However, another possibility could be accounted for the techniques used to measure cell death because it is strange how such a profound loss in ATP as observed in our study, could results in no indication of mitochondrial dysfunction or membrane change.

We would have expected that the exposure of H9c2 cells to SI would lead to a rounding of the cells with a withered appearance as seen under the microscope. However, JC-1 imaging showed that H9c2 cells exposed to 2 hours SI retained their spindle shaped morphology. 10000 cells/100 µl were exposed to Esumi buffer with metabolic inhibition in addition to incubation with a (0 % O_2/5 % CO_2/ 95 % N_2) hypoxic gas mixture. We expected this to have been a major insult to the cells, however, there was no measurable change in the cell morphology. On the other hand, JC-1 imaging of MDA-MB 231 cells showed a change in the morphology from spindle shaped to spherical. However, this observation seemed to have nothing to do with the ischemic insult since it was also observed in normoxic samples. We suspect that the cells may have changed morphology probably due to the cell detaching from the 96 well plate due to the 3X washing with PBS and or the reperfusion prior the staining, or due to the pH changes that occurs when the buffering capacity of DMEM is altered, as would be the case when cells are outside of the CO_2 incubator for a lengthy period of time. A study by Mohsin Ali Khan (2004) showed that an alkaline pH of up to 8.3 is enough to change the morphology of MDA-MB 231 from

spindle shape to spherical (Khan, et al., 2004). Moreover, we have observed this in earlier studies in our lab, when MDA-MB 231 cells were cultured in DMEM and then taken out of the incubator for more than at least 10-15 minutes for microscopic imaging. Although we had many samples to handle simultaneously in this study, since the assays were done in a 96 well plate for both normoxia and SI, we doubt that the duration outside the incubator while cells are still in the DMEM media reached 10 minutes before simulated reperfusion. Also, we did not directly measure the alkalinity of our DMEM containing samples during that time. MDA-MB 231 containing Esumi buffer also showed a transition of morphology from spindle shape to spherical, although to a lesser degree compared to the DMEM counterpart. Esumi buffer had a set pH of 6.4. However, both the DMEM and Esumi buffer containing samples were exposed to PBS and calcium reperfusion buffer, which is a more likely the cause of morphology transition. Future studies are required, looking at the effect of washing buffer and reperfusion buffer on MDA-MB 231 morphology transition, probably due to cell detachment.

Aim 2: The effect of simulated ischemia on the activity and expression of phosphatases following 2 hours SI with metabolic inhibition in H9c2 and MDA- MB 231 cell lines.

In a previous study, we investigated the effect of SI on phosphatase activity and expression in H9c2 cells. Ischemia was simulated by incubating cells for 2 hours in a modified Esumi buffer under hypoxic conditions (0 % O_2/5 % CO_2/ 95 % N_2) in 5 % CO_2 at 37°C in a humidified atmosphere. Using Western blotting, we blotted for PP1 alpha, PP2B, PP2Ac and Pan Phospho serine/threonine. There was no measurable change in phosphatase expression, as well as the phosphorylation status of serine/threonine residues between control versus SI. The quantification of protein phosphatase activity using the para-Nitrophenylphosphate (pNPP) colorimetric assay, showed that there was no change in the activity of phosphatases between control and SI. In this project we aimed to repeat the same experiments on MDA-MB 231 cells to evaluate whether the behaviour of protein phosphatases due to ischemia would give different results in a cancer cell line. Moreover, we were interested to evaluate whether 6,8-Difluoro-4-Methylumbelliferyl Phosphate (DiFMUP), a synthetic non-specific fluorescent substrate for alkaline and acidic phosphatase would report the same data as the pNPP assay (Welte, et al., 2005). The activity of the protein phosphatases was quantified and compared between control and SI. Our results suggest that there is no measurable change in phosphatase activity following 2 hours SI measured with both pNPP and DiFMUP.

The expression of phosphatases was quantified in MDA-MB 231 cell line under the same cell culturing and SI conditions. Using Western blotting, the phosphorylation status of proteins was quantified for all proteins phosphorylated at tyrosine residue using pan phospho tyrosine. The antibody didn't work well (results not included). Probing for proteins phosphorylated at all serine/threonine residues using pan phospho serine/threonine antibody, showed that there was no change in phosphorylation due to SI.

However, there was an intense phosphorylation on the proteins with the molecular weight between 72kDa and 55kDa. What was interesting was that of all the ser/thr phosphorylated proteins in the sample, only proteins within this molecular weight showed to be highly phosphorylated. This spiked an idea to investigate whether this high phosphorylation was related to gain-of-function mutations of upstream kinases or loss-of-function of the related inhibitory phosphatases. Akt/PKB is 60kDa and seemed to be more likely the protein occupying this band location. Phosphorylated Akt/PKB has two isoforms: Akt/PKB S473 and Akt/PKB S473. We were able to confirm that the phosphorylated proteins were not Akt/PKB S473. However, we were unable not confirm whether it could be Akt/PKB T308. MDA-MB 231 is an oncogenic cell line mutated on the gene *KRAS*, which encodes for small G-proteins. This type of mutation suggests that MDA-MB 231 has a gain-of-function mutation on the *KRAS* gene, rendering it constitutively activated (Kim, et al., 2015). The small G-proteins can activate the MEK/ERK pathway as well as PI3-K/Akt/PKB pathway (Li, Zhao, & Fu, 2016). The limitations observed in this experimental model is due to that the lack of negative control of MDA-MB 231 (non-cancerous breast cell line). To further investigate phosphorylation in MDA-MB 231 line, the inclusion of the negative control such as MCF 10A cell line, which is a non-tumorigenic epithelial cell line could have enabled comparison to see the difference in phosphorylation against the wild type. Another possibility is that the high phosphorylated proteins might be non-specific; likely to be any one of the other 100s of protein composition with the same/similar molecular weight.

The expression of PP2Ac in MDA-MB 231 cells showed a statistical increase following 2 hours SI. Previous work done in our laboratory evaluated the regulation of PP2A by ischemia in the same cell culture conditions, but in the H9c2 cell line. Their results suggest that SI did not influence the expression of PP2Ac while PP2A- A showed a reduction in expression. However, the results from isolated rat hearts showed that the expression of PP2Ac had a significant increase at 20 minutes regional ischemia (Van Vuuren, 2014). Hypoxia suppressed the expression of PP2A in cardiac endothelial, smooth muscle and fibroblast with kinetics that are both cell and time dependent (Elgenaidi & Spiers, 2017). If we were to increase the duration of SI, could this change in PP2Ac and Akt/PKB expression fluctuate or remain constant? Answering this question, would give insight on whether these pathways are involved in the adaptation to ischemia by MDA-MB 231 cells.

Literature has suggested that there is a correlation between phosphatases and HIF-1α (Hofstetter C. , et al., 2012). The quantification of HIF-1α expression following 2 hours SI showed that HIF-1α expression was not elevated to a statistically significant level to consider hypoxia in this model to have been a success. In fact, the normoxic samples showed an expression of HIF-1α in our blots even though HIF-1α is supposed to be degraded under normoxic conditions. However, HIF-1α has also been shown to be regulated by cytokines, hormones and genetic alterations in vitro (Stroka, et al., 2001). Nonetheless, the mechanisms for HIF-1α stabilization under normoxic conditions have not been elucidated. We were unable to clarify why HIF-1α was present in normoxic cells. PP1α and PP2B expression also did not

show statistically significant difference following 2 hours SI. The intention with this study was that cancer cells are more robust and heart cells are less so, therefore, what is the difference and can that difference be used to either save heart cells or kill cancer cells? The results we collect from these studies shows that H9c2 cells did not have any changes in the activity and expression of phosphatases under SI conditions. However, MDA-MB 231 cells showed an increase in the expression of PP2Ac and a reduction in the expression of total Akt/PKB. Unfortunately, our Western blot results did not tell us about the consequences of these changes in protein expression related to cell viability.

Aim 3: The effect oacological manipulation of PP2A in heart cells (H9c2) and cancer cell lines (MDA-MB231) exposed to 2 hours SI followed by 30 minutes reperfusion.

Table 7.1: Summary of the PI and JC-1 stain results showing both H9c2 and MDA-MB 231 cells treated with cantharidin (2 µM and 5 µM) and FTY 720 (1 µM and 5 µM) under both normoxic and SI conditions.

RESULTS SUMMARY

	H9c2 cells				MDA-MB 231 cells			
ASSAYS	PI stain		JC- Stain		PI stain		JC- Stain	
TREATMENT	Normoxia	SI	Normoxia	SI	Normoxia	SI	Normoxia	SI
2µM CANTHARIDIN	No change	No change	No change	No change	No change	No change	No change	No change
5µM CANTHARIDIN	No change	No change	No change	CELL DEATH	No change	No change	No change	CELL DEATH
1 µM FTY 720	No change	No change	No change	No change	CELL DEATH	No change	No change	No change
5 µM FTY 720	No change	No change	No change	No change	No change	No change	No change	No change

[5]Cell viability test measured by PI stain and JC-1 stain (plate reader and microscopy)

1x 10^4 H9c2 cells/100 µl were seeded, whereas 2.5 10^4 MDA-MB 231 cells/100 µl were seeded for experimentation. H9c2 and MDA-MB 231 cells were exposed to 2 hours SI followed by 30 minutes reperfusion by a calcium reperfusion buffer at pH 6.4. Although acidic reperfusion is known to have a protective effect (Inserte, et al., 2008), we doubt that it was protective in this setup due to the duration of reperfusion.

Figure 5.10 shows an upregulation in the expression of PP2Ac in MDA-MB 231 cell line due to SI. To evaluate the effect of PP2Ac, H9c2 and MDA-MB 231 cell lines were treated with cantharidin (2 µM and 5 µM) which inhibits both PP2A and PP1 at higher concentrations, and FTY 720 (1 µM and 5 µM) which activates PP2A. Cantharidin and FTY 720 were dissolved in DMSO vehicle control. DMSO showed not to have significantly affect the viability of both cell lines. dH_2O was used as a positive

5

control to induce cell death in H9c2 cell line and 0.5 % and 1% Triton X-100 in MDA-MB 231 cells. All three viability assays used was able to measure cell death induced by positive controls.

Cells in a 96 well plate were treated with the same drugs for both control and SI. This was done so there could be a direct comparison to distinguish between drug and SI effect. Cells that were not treated with any drugs served as the standard control for normoxia or SI. SI showed to have indeed caused a significant reduction in ATP levels in both cell lines. Interestingly, treatment with 5 µM cantharidin under SI might suggests an elevation in ATP levels or a reduction in ATP consumption by the cells. Yang X et al. (2011) found that the inhibition of PP2A by cantharidin was cardioprotective (Yang, et al., 2011). Moreover, observations by Christof Weinbrenner et al. (1998) reported that Fostriecin, a potent and selective inhibitor of PP2A was highly protective against infarction in the rabbit heart (Weinbrenner , et al., 1998).

MDA-MB 231 cells treated with cantharidin (2 µM and 5 µM) and FTY 720 (1 µM and 5 µM) did not influence ATP levels, either under normoxic or SI conditions. Conversely, a study by Christoph P. Hofstetter et al. (2012) on Glioblastoma-derived tumour stem cell-like cells reported that severe hypoxia (1% O_2 for 6 hours) increased PP2A activity, which in turn mediated G1/S phase growth inhibition and reduced cellular ATP consumption. Whereas, the inhibition of PP2A activity led to exhaustion of intracellular ATP, and accelerated p53-independent cell death (Hofstetter, et al., 2012).

Normoxic MDA-MB 231 cells treated with an activator of PP2A, FTY 720 (1 µM) showed that the activation of PP2A induced cell death indicated by a significant elevation in PI fluorescence. SI treated cells showed no effect (Figure 6.9B). Strangely, 5 µM FTY 720 did not have an effect. It is interesting that the increase in PP2A activity by FTY 720 induced cell death in normoxic cells whereas had no effect on SI treated cells. A pre-clinical study showed that oestrogen receptor negative (ER-) breast cancer cell lines were more sensitive to FTY 720 than cells that express the oestrogen receptor (ER+) (Baldacchino, et al., 2014). This is attributed to ER- breast cancer cell lines having suppressed levels of PP2A activity in comparison to ER+ breast cancer cell lines thus having a higher sensitivity to a PP2A activator such as FTY 720 (Kiely & Kiely, 2015). Figure 5.10 showed that 2 hours SI induced an upregulation in the expression of PP2Ac in MDA-MB 231 cells (triple negative breast cancer cell line); this abundance in PP2A protein may have reduced sensitivity of MDA-MB 231 SI treated cells to FTY 720, thus we saw no cell death due to PP2A activation under SI conditions.

The activation of PP2A by FTY 720 has shown promise as an anti-cancer therapy in many pre-clinical studies. These studies have investigated the use of FTY 720 as a potential therapy for a number of cancer cell types including but not limited to, neuroblastoma, bladder, renal, colorectal, breast, ovarian and lung cancers (Cristobal, et al., 2014; Li, Hla, & Ferrer, 2013; Saddoughi, et al., 2013). Another study reported that the administration of FTY 720 activated PP2A and in turn reduced cell growth and caused cell death in breast cancer cells (Rincón, et al., 2015) . A study on FTY 720 as an anti-tumor

treatment in prostate cancer revealed that the activation of PP2A led to a reduction in cell growth and decreased phosphorylation of pro-survival kinases Akt/PKB and ERK (Cristóbal, et al., 2015).

On the other hand, a growing body of evidence suggests an anti-apoptotic role for PP2A, challenging the predominant perception that PP2A function solely as a tumour suppressor and a regulator of pathways that promote apoptosis. This was first observed in Drosophila (Van Hoof & Goris, 2003) and in mammalian cell models where inactivation of PP2A induces apoptosis in a number of cancer cell types including cancers of the pancreas, testes, liver and in leukemic cells (Li, et al., 2010; Schweyer, et al., 2007; Duong, et al., 2014; Lu, et al., 2009; Boudreau, Conrad, & Hoskin, 2007). Cantharidin, an inhibitor of PP2A is a known anti-cancer agent (Liu & Chen, 2009). MDA-MB 231 cells treated with 5 µM cantharidin reduced the function and integrity of mitochondria under SI conditions, indicative of apoptosis. Moreover, the apoptotic effect of 5 µM cantharidin was also observed in H9c2 cells as measured by JC-1 staining. Other studies shows that the inhibition of PP2A in malignant testicular germ cell tumours using okadaic acid and cantharidin induces pro-apoptotic effect through phosphorylation and subsequent activation of both MEK and ERK which, in turn, activate one of the most prominent inducers of apoptosis, caspase-3 (Schweyer, et al., 2007). Wei Li et al. (2010) reported that treatment with 10 µM cantharidin showed a significant increase in apoptotic cells in a dose-dependent manner as measured by Annex V- EGFP/PI and flow cytometry in a model of pancreas cancer (Li, et al., 2010). Therefore, PP2A plays a dual regulatory role in apoptosis, facilitating both pro- and anti-apoptotic signalling depending on the holoenzyme assembled and pathways targeted as well as the cell line (Santoro, et al., 1998; Li, Scuderi, Letsou, & Virshup, 2002; MacKeigan, Murphy, & Blenis, 2005; Ruvolo, Deng, & May, 2001).

JC-1 stain was measured by both the plate reader and fluorescence imaging. The results generated by the two techniques did not show consistent data regarding cantharidin treatment. MDA-MB 231 cells treated with 5 µM cantharidin was observed to have induced cell death under SI conditions as measured by the plate reader, whereas, image analysis showed no change in cell viability. The similar trend was observed in H9c2 cells, whereby image analyses showed that 5 µM cantharidin induced cell death under SI conditions, whereas, the reduction in mitochondrial function and integrity measured by the plate reader was not significant. H9c2 cells treated with 5 µM cantharidin under SI conditions appear shredded or shrunken compared to the cells treated with SI alone.

It is interesting that Figure 6.1A suggests that inhibition of PP2A in H9c2 cell line using 5 µM cantharidin under SI conditions might have been protective, whereas JC-1 staining suggests that the same treatment killed the cells. A study done by Fan et al. (2010) investigated kinases and phosphatases in ischemic preconditioning in rat hearts using 5 µM cantharidin. They proposed that myocardial ischemia and reperfusion induces the activation of certain phosphatases. Pre-treatment of hearts with 5 µM cantharidin caused a significant reduction in mechanical recovery after 15- or 20-minutes global ischemia. Moreover, administration of cantharidin during an ischemic preconditioning phase abolished

the beneficial effects of the preconditioning intervention on infarct size, while its administration during reperfusion was without effect in both non-preconditioned and preconditioned hearts (Fan, et al., 2010). Other inhibitors such as calyculin A which inhibits PP1 and PP2A and fostriecin, a selective inhibitor of PP2A was found to protect isolated rabbit cardiomyocytes against ischaemic damage (Armstrong, et al., 1998). Moreover, fostriecin reduced infarct size when administered 10 min before and 15 min after onset of regional ischemia (Weinbrenner, et al., 1999). A study on isolated rat hearts showed that the protection induced by hypoxic preconditioning was abolished by the inhibitor of protein phosphatases 1 and 2A cantharidin (20 or 5 µM) and partially enhanced by the inhibitor of protein phosphatase 2A okadaic acid (5 nM). Fan and colleagues (2010) argued that the contradiction observed on the effect of inhibition of PP2A on ischemic heart might be due to the species differences: increased activation of p38MAPK during sustained ischemia has been observed in preconditioned rabbit cardiomyocytes and isolated rabbit hearts (Weinbrenner, et al., 1999), in contrast to the reduction in p38MAPK seen in perfused preconditioned rat hearts (Steenbergen, 2002; Schneider, Chen, Hon, Steenbergen, & Murphy, 2001). It is therefore difficult to say whether the inhibition of PP2A by cantharidin always leads to protection or cell death in ischemic hearts.

Like any other study, our study was faced with several limitations. Our laboratory experience with JC-1 staining was usually on isolated cardiomyocytes, therefore, H9c2 and MDA-MB 231 cells are quite small in comparison, thus deciding on the appropriate concentration of JC-1 to use was a challenge. Also, the protocol we got for PI staining was for 12 well plates assays and was predominately used for endothelial cells; we used a 96 well plate, thus we had to make estimations regarding the appropriate concentration to use for PI. Moreover, we did not have enough resources or time to test for dosages. Another challenge we faced was with the inhibitors used in conjugations with the phosphatase activity assays. The inhibitors used were not specific enough and we did not observe significant inhibition with all of them. We also faced challenges with some of the antibodies we used such as pan phospho tyrosine and PP1 alpha. The concentrations needed to inhibit and activate PP2A were quite small, which opens us to a technical error. This is also the reason we used 2 µM and 5 µM cantharidin which inhibits both PP1 and PP2A instead of 0.2 µM which inhibits PP2A alone. Another great challenge we faced in this study was with MDA-MB 231 cells' morphology that seem to have transitioned from spindle to spherical shape, also reduced in number. We suspect that either the washing with saline buffer or reperfusion buffer were causing the cells to detach from the 96 well plate. Other researchers on research gate have reported on the same issue. We also tried attachment factors and there was no difference. Therefore, to maintain a steady confluence, we increased the number of cells seeded overnight from 10 000 MDA-MB 231 cells/ 100 µl to 25 000 cells/100 µl/well.

In conclusion, 2 hours SI with metabolic inhibition significantly reduced ATP levels in both H9c2 and MDA-MB 231 cells, indicative of metabolic stress. However, cell death was not observed as measured by PI and JC-1 staining following 2 hours SI and 30 minutes reperfusion. Further investigations are

required to evaluate the duration required to ensure cell death in H9c2 and MDA-MB 231 cell lines due to SI (as simulated by the modified Esumi buffer). SI did not influence the activity of phosphatases in both H9c2 and MDA-MB 231 cells as measured by the pNPP and DiFMUP phosphatase assay. Therefore, we cannot reject our null hypothesis in terms of phosphatase activity. However, SI induced an upregulation in the expression of PP2Ac in MDA-MB 231 cells; which lead us to reject the null hypothesis with regards to the expression of phosphatases. Therefore, SI only affected the expression of protein phosphatase 2A in MDA-MB 231 cells only. This observation led to the manipulation of PP2A. The activation of PP2A by FTY 720 in normoxic MDA-MB 231 induced necrosis as measured by PI staining. Interestingly, JC-1 staining showed that the inhibition of PP2A by 5 µM cantharidin induced cell death under SI conditions in both H9c2 and MDA-MB 231 cells. Other researchers reported that the activation of PP2A lead to cell death, making PP2A a tumour suppressor. However, other studies reported that the inhibition of PP2A can also lead to cell death, making it a tumour promotor. To explain this contradiction, researchers argues that because PP2A has many holoenzymes, it matters which one is targeted to induce either a pro-apoptotic or anti-apoptotic effect. The type of the cell line can also be a determining factor. Interestingly, the inhibition of PP2A by 5 µM cantharidin in H9c2 cells under SI conditions seemed to reduce the consumption of ATP levels although not statistically significant. Therefore, it is not possible to assess whether cantharidin under SI conditions is protective or damaging to the cells based on this data, because our data suggest that the inhibition of PP2A conserves energy (ATP) whereas when measured by JC-1 staining it suggested cell death. However, literature suggests that the inhibition of PP2A is protective in the heart. Therefore, the dual role of PP2A as a pro-apoptotic or an anti-apoptotic mediator is increasingly evident. If PP2A is to be used as a target for cancer therapy, or protective agent against myocardial ischemia, more research is required to investigate the effect or the role of PP2A both in the heart and in cancer cells with the focus on which holoenzyme to target using which inhibitors or activators. Therefore, more research must be focused on devising specific inhibitors for PP2A holoenzymes.

References

Agarwal, S. et al., 2016. p53 Deletion or Hot-spot Mutations Enhance mTORC1 Activity by Altering Lysosomal Dynamics of TSC2 and Rheb. *Molecular Cancer Research,* 14(1), pp. 66-77.

Alberts, B. et al., 2002. *Molecular Biology of the Cell.* 4 ed. New York: Garland Science.

Ali, S., Hippenmeyer, S. & Ardehali, R., 2014. Existing Cardiomyocytes Generate Cardiomyocytes at a Low Rate After Birth in Mice.. *Proceedings of the National Academy of Sciences.*

Alonso, A. et al., 2004. Protein Tyrosine Phosphatases in the Human Genome. *Cell,* 117(6), pp. 699–711.

Andreassen, P., et al., 1998. Differential Subcellular Localization of Protein Phosphatase-1a, g1, and a¨ Isoforms During both Interphase and Mitosis in Mammalian Cells. *Journal of Cell Biology,* 141, pp. 1207–1215.

Armstrong, S. & Ganote, 1992. Effects of the Protein Phosphatase Inhibitors Okadaic Acid and Calyculin A on Metabolically Inhibited and Ischaemic Isolated Myocytes. *Journal of Molecular and Cellular Cardiology,* 24(8), pp. 869–884.

Armstrong, S. et al., 1998. Protein Phosphatase Inhibitors Calyculin A and Fostriecin Protect Rabbit Cardiomyocytes in Late Ischemia. *Journal of Molecular and Cellular Cardiology,* 30, pp. 61–73.

Aubert, G. et al., 2016. The Failing Heart Relies on Ketone Bodies as a Fuel. *Circulation. ,* 133(8), pp. 698-705.

Bacus, S. et al., 2002. AKT2 is Frequently Upregulated in HER2/neu-positive Breast Cancers and May Contribute to Tumor Aggressiveness by Enhancing Cell Survival. *Oncogene,* 21, pp. 3532-3540.

Baldacchino, S. et al., 2014. Deregulation of the Phosphatase, PP2A is a Common Event in Breast Cancer, Predicting Sensitivity to FTY720. *EPMA Journal,* 5, pp. 3.

Barford, D., Das, A. & Egloff, M., 1998. The Structure and Mechanism of Protein Phosphatases: Insights into Catalysis and Regulation. *Annual Review of Biophysics and Biomolecular Structure,* 27(1), pp. 133–164.

Barford, D., 1996. Molecular Mechanisms of the Protein Serine/threonine Phosphatases. *Trends in Biochemical Sciences,* 21, pp. 407–412.

Bensaad, K. & Vousden, K., 2007. p53: New Roles in Metabolism. *Trends in Cell Biology,* 17(6), pp. 286-291.

Berra, E. et al., 2000. Signalling Angiogenesis via p42/p44 MAP kinae and Hypoxia. *Biochemical Pharmacology,* 60, pp. 1171-1178.

Bhaduri, A. & Sowdhamini, R., 2003. A Genome-wide Survey of Human Tyrosine Phosphatases. *Protein Engineering Design and Selection,* 16(12), pp. 881–888.

Bio Rad, 2017. *Stain-Free Imaging Technology.* [Online] Available at: http://www.bio-rad.com/enza/ [Accessed 22 November 2017].

Blanchetot, C. et al., 2002. Intra- and Intermolecular Interactions between Intracellular Domains of Receptor Protein-Tyrosine Phosphatases. *Journal of Biological Chemistry,* 277(49), pp. 47263-47269.

Boudreau, R., Conrad, D., & Hoskin, D., 2007. Apoptosis Induced by Protein Phosphatase 2A (PP2A) Inhibition in T Leukemia Cells is Negatively Regulated by PP2A-associated p38 Mitogen-activated Protein Kinase. Cell Signaling, 19, 139–151.

Bradford, M., 1976. A Rapid and Sensitive Method for the Quantitation of Microgram Quantities of Protein Utilizing the Principle of Protein-dye Binding. *Analytical Biochemistry,* 72, pp. 248-254.

Bradshaw, R. & Dennis, E., 2010. *Handbook of Cell Signaling.* 2 ed. s.l.:Elsevier BV.

Brandon, M., Baldi, P. & Wallace, D., 2006. Mitochondrial Mutations in Cancer. *Oncogene,* 25(34), pp. 4647-4662.

Brinkmann, V. et al., 2001. FTY720: Altered Lymphocyte Traffic Results in Allograft Protection. *Transplantation,* 72, pp. 764-769.

Brooks, C. & Gu, W., 2003. Ubiquitination, Phosphorylation and Acetylation: the Molecular Basis for p53 regulation. *Current Options in Cell Biology,* 15(2), pp. 164-71.

Brown GC, 1992. Control of Respiration and ATP synthesis in Mammalian Mitochondria and Cells. *Biochemistry Journal,* 284, pp. 1-13.

Bueno, C. et al., 2002. The Excited-State Interaction of Resazurin and Resorufin with Aminesin Aqueous Solutions. Photophysics and Photochemical Reaction. *Photochemistry and Photobiology,* 76(4), pp. 385–390.

Burke, A. & Virmani, R., 2007. Pathophysiology of Acute Myocardial Infarction. *Medical Clinics of North America,* 91(4), pp. 553-572.

Bürkle, A., 2001. *Encyclopedia of Genetics.* 1 ed. s.l.:Academic Press.

Burnett, G., 1954. The Enzymatic Phosphorylation of Proteins. *Journal of Biological Chemistry,* pp. 969-980.

Burotto, M., et al., 2014. The MAPK Pathway Across Different Malignancies: A New Perspective. *Cancer,* 120(22), pp. 3446–3456.

Cailleau, R., Olive, M. & Cruciger, Q., 1978. Long-term Human Breast Carcinoma Cell Lines Of Metastatic. *In Vitro,* 14(11), pp. 911– 915.

Cai, Z. et al., 2003. Hearts from Rodents Exposed to Intermittent Hypoxia or Erythropoietin are Proteed against Ischamia-Reperfusion Injury. *Circulation,* 108(1), pp. 79-85.

Cai, Z. et al., 2008. Complete Loss of Ischemic Preconditioning-Induced Cardioprotection in Mice with Partial Deficiency of HIF-1 alpha. *Cardiovascular research,* 77, pp. 463-470.

Calin, G. et al., 2000. Low Frequency of Alterations of the Alpha (PPP2R1A) and Beta (PPP2R1B) Isoforms of the Subunit A of the Serine-threonine Phosphatase 2A in Human Neoplasms. *Oncogene,* 19(9), pp. 1191-1195.

Campbell, K. et al., 1995. Identification of Regions in Polyomavirus Middle T and Small t Antigens Important for Association with Protein Phosphatase 2A. *Journal of Virology,* 69, pp. 3721-3728.

Campbell, N., Williamson, B. & Heyden, R., 2006. *Biology: Exploring Life.* Boston: Massachusetts: Pearson Prentice Hall.

Carden, D. & Granger, D., 2000. Pathophysiology of Ischaemia-reperfusion Injury. *The Journal of Pathology,* 190(3), pp. 255–266.

Carling, D., 2004. The AMP-Activated Protein Kinase Cascade- a Unifying System for Energy Control. *Trends in Biochemical Science ,* 29(1), pp. 18-24.

Carnero, A. & Paramio, J., 2014. The PTEN/PI3K/AKT Pathway in Vivo, Cancer Mouse Models. *Frontiers in Oncology,* 4(252), pp. 1-10.

Ceulemans, H. & Bollen, M., 2004. Functional Diversity of Protein Phosphatase-1, a Cellular Economizer and Reset Button. *Physiology Reviews,* 84(1), pp. 1-39.

Chalhoub, N. & Baker, S., 2009. PTEN and the PI3-Kinase Pathway in Cancer. *The Annual Review of Pathology,* 4, pp. 127–150.

Chang, L. & Karin, M., 2001. Mammalian MAP kinase signalling cascades. *Nature,* 410, pp. 37-40.

Chen, J., Steele, T. & Stuckey, D., 2015. Modeling and Application of a Rapid Fluorescence-based Assay for Biotoxicity in Anaerobic Digestion.. *Environemntal Science and Technology,* 49(22), pp. 13463-13471.

Chen, W. et al., 2005. Cancer-associated PP2A Aalpha Subunits Induce Functional Haploinsufficiency and Tumorigenicity. *Cancer Research,* 65, pp. 8183-8192.

Chernoff, J. & LI, H., 1983. Multiple Forms of Phosphotyrosyl- and Phosphoseryl-Protein Phosphatase From Cardiac Muscle: Partial Purification and Characterization of an EDTA-Stimulated Phosphotyrosyl-Protein Phosphatase. *Archives of Biochemistry and Biophysics,* 226(2), pp. 517–530.

Cho, H. et al., 1992. Isolation and Structural Elucidation of a Novel Phosphocysteine Intermediate in the LAR Protein Tyrosine Phosphatase Enzymic Pathway. *Journal of the American Chemical Society,* 114(18), pp. 7296–7298.

Cho, U. & Xu, W., 2007. Crystal Structure of a Protein Phosphatase 2A Heterotrimeric Holoenzyme. *Nature,* 445(7123), pp. 53-57.

Ciccone, M., Calin , G. & Perrotti , D., 2015. From the Biology of PP2A to the PADs for Therapy of Hematologic Malignancies. *Frontiers in Oncology,* 5(21).

Cohen, P., 2002. Protein Phosphatase 1–Targeted in Many Directions. *Journal of Cell Science,* 115, pp. 241-256.

Comerford, K. et al., 2006. Regulation of Protein Phosphatse 1y ctivity in Hypoxia Through Increased Interaction with NIPP1: Implications for Cellular Metabolism. *Journal of Cellular Physiology,* 209, pp. 211-218.

Cossarizza, A., Baccaranicontri, M., Kalashnikova, G. & Franceschi, C., 1993. A New Method for the Cytofluorometric Analysis of Mitochondrial Membrane Potential Using the J-Aggregate Forming Lipophilic Cation 5,5′,6,6′-Tetrachloro-1,1′,3,3′-tetraethylbenzimidazolcarbocyanine Iodide (JC-1). *Biochemical and Biophysical Research Communications,* 197(1), pp. 40-45.

Cristóbal, I. et al., 2015. Activation of the Tumor Suppressor PP2A Emerges as a Potential Therapeutic Strategy for Treating Prostate Cancer. *Marine Drugs,* 13, pp. 3276-3286.

Cristofano, D. & Pandolfi, P., 2000. The Multiple Roles of PTEN in Tumor Suppression. *Cell,* 100(4), pp. 387–390.

Crouch, S. et al., 1993. The use of ATP Bioluminescence as a Measure of Cell Proliferation and Cytotoxity. *Journal of immunology,* 160, pp. 81-88.

De Bolster, M., 1997. Glossary of Terms Used in Bioinorganic Chemistry: Catabolism. International Union of Pure and Applied Chemistry.

DeGrande, S. et al., 2012. Molecular Mechanisms Underlying Cardiac Protein Phosphatase 2A Regulation in Heart. *The Journal of Biological Chemistry,* 288, pp. 1032-1046.

Denko, N., 2008. Hypoxia, HIF1 and Glucose Metabolism in the Solid Tumour. *Nature Reviews Cancer,* 8, pp. 705–713.

Denu, J. & Dixon, J., 1995. A Catalytic Mechanism for the Dual-Specific Phosphatases. *Proceedings of the National Academy of Sciences of the United States of America,* 92(13), pp. 5910–5914.

Desjardins, P., Frost, E. & Morais, R., 1985. Ethidium Bromide-Induced Loss of Mitochondrial DNA from Primary Chicken EmbryoFibroblasts. *Molecular Cell Biology,* 5, pp. 1163-1169.

Deussen, A. et al., 2012. Mechanisms of Metabolic Coronary Flow Regulation. *Journal of Molecular and Cellular Cardiology,* 52(4), pp. 794-801.

Dixon, J. & Denu, J., 1998. Protein Tyrosine Phosphatases: Mechanisms of Catalysis and Regulation. *Current Opinion in Chemical Biology,* 2(5), pp. 633–641.

D'Souza, K., Nzirorera, C. & Kienesberger, P., 2016. Lipid Metabolism and Signaling in Cardiac Lipotoxicity. *Biochimica et Biophysica Acta,* 1861, pp. 1513-1524.

Duong, F. et al., (2014). Protein Phosphatase 2A Promotes Hepatocellular Carcinogenesis in the Diethylnitrosamine Mouse Model Through Inhibition of p53. Carcinogenesis, 35, 114–122.

Duvel, K. et al., 2010. Activation of a Metabolic Gene Regulatory Network Downstream of mTOR Complex 1. *Molecular Cell,* 39(2), pp. 171-183.

Eagle, H., 1955. The Specific Amino Acid Requirements of a Human Carcinoma Cell (Stain HeLa) in Tissue Culture. *Journal of Experimental Medicine,* 102(1), pp. 37-48.

Egloff, M. et al., 1997. Structural Basis for the Recognition of Regulatory. *The EMBO Journal,* 16(8), pp. 1876–1887.

Elgenaidi, I. & Spiers, J., 2017. Effect of Hypoxia on Expression of the PP2A System in Primary Human Cardiovascular Cells: Post-translation Modification and Involvement of HIF1α. *Heart,* 103, pp. A6.

Esumi, K. et al., 1991. NADH Measurements in Adult Rat Myocytes During Simulated Ischemia. *American Journal of Physiology-Heart Circulatory Physiology,* 260(6 Pt 2), pp. H1743-H1752.

Eswaran, J. et al., 2006. The Crystal Structure of Human Receptor Protein Tyrosine Phosphatase κ Phosphatase Domain 1. *Protein Science,* 15(6), pp. 1500–1505.

Fan , W. J., van Vuuren , D., Genade, S. & Lochner, A., 2010. Kinases and Phosphatases in Ischaemic Preconditioning: a Re-evaluation. *Basic Research in Cardiology,* 105(4), pp. 495–511.

Fischer, B. & Bavister, B., 1993. Oxygen Tension in the Oviduct and Uterus of Rhesus Monkeys, Hamsters and Rabbits. *Journal of Reproduction and fertility,* 99(2), pp. 673-679.

Forrest, A. et al., 2003. Phosphoregulators: Protein Kinases and Protein Phosphatases of Mouse. *Genome Research,* 13(6b), pp. 1443–1454.

Gatenby, R. & Gawlinski, E., 2003. The Glycolytic Phenotype in Carcinogenesis and Tumor Invasion: Insights Through Mathematical Models. *Cancer Research,* 63(14), pp. 3847-3854.

Gilkes, et al., 2014. Hypoxia and the Extracellular Matrix: Drivers of Tumour Metastasis. *Nature Reviews Cancer 14.6,* pp. 430-439.

Goldberg, J. et al., 1995. Three-dimensional Structure of the Catalytic Subunit of Protein Serine/threonine Phosphatase-1. *Nature,* 376(6543), pp. 745–53.

Goldberg, M., Zhang, H. & Steinberg, S., 1997. Hypoxia Alters the Subcellular Distribution of the Protein Kinase C Isoforms in Neonatal Rat Ventricular Myocytes. *Journal of Clinical Investigation,* 99, pp. 55-61.

Graeber, T. et al., 1996. Hypoxia-mediated Selection of Cells with Diminished Apoptotic Potential in Solid Tumors. *Nature,* pp. 379:8891.

Greenberg, C., Jurczak, M., Danos, A. & Brady, M., 2006. Glycogen Branches Out: New Perspectives on the Role of Glycogen Metabolism in the Integration of Metabolic Pathways. *American Journal of Physiology-Endocrinology and Metabolism,* 291(1), pp. E1-8.

Griffiths, E. & Halestrap, A., 1991. Further Evidence that Cyclosporin A Protects Mitochondria from Calcium Overload by Inhibiting a Matrix Peptidyl-prolyl cis-trans Insomerase,Implications for the Immunosuppresive and Toxic Effect of Cyclosporin. *Biochemistry Journal,* 274(Pt 2), pp. 611-614.

Griffiths, E. & Halestrap, A., 1993. Protection by Cyclosporin A of Ischemia/reperfusion-induced Damage in Isolated Rat Hearts. *Journal of Molecular Cell Cardiology,* 25(12), pp. 1461-1469.

Grotzer, M. et al., 2000. Resistance to TRAIL-induced Apoptosis in Primitive Neuroectodermal Brain Tumor Cells Correlates with a Loss of Caspase-8 Expression. *Oncogene,* 19, pp. 4604-4610.

Guroff,, G., 1991. Methods in Enzymology. *Analytical Biochemistry,* 198(2), pp. 395.

Haase, V., 2009. The VHL Tumor Suppressor: Master Regulator of HIF. *Current Pharmaceutical Design,* 15(33), pp. 3895–3903.

Harris, A., 2002. Hypoxia-a Key Regulatory Factor in Tumour Growth. *Nature Reviews Cancer,* 2, pp. 38-47.

Hausenloy, D., Duchen, M. & Yellon , D., 2003. Inhibiting Mitochondrial Permeability Transition Pre Opening at Reperfusion Protects againts Ischamia-Reperfusion Injury. *Cardiovascular Research,* 60, pp. 617-625.

Hausenloy, D., Tsang, A. & Yellon, D., 2005. The Reperfusion Injury Salvage Kinase Pathway: a Common Target for both Ischemic Preconditioning and Postconditioning. *Trends in Cardiovascular Medicine,* 15(2), pp. 69-75.

Hausenloy, D. & Yellon, D., 2004. New Directions for Protecting the Heart Against Ischaemia-Reperfusion Injury: Targeting the Reperfusion Injury Salvage Kinase(RISK)- Pathway. *Cardiovascular Research,* 61(3), pp. 448-460.

Hausenloy, D. & Yellon, D., 2006. Survival Kinases in Ischemic Preconditioning and Postconditioning. *Cardiovascular Research ,* 70, pp. 240–253.

Hoehn, M. et al., 2015. Overexpression of Protein Phosphatase 2A in a Murine Model of Chronic Myocardial Infarction Leads to Increased Adverse Remodelling but Restores The Regulation of B-catenin by Glycogen Synthase Kinase 3B. *International Journal of Cardiology.*

Hofstetter , C. et al., 2012. Protein Phosphatase 2A Mediates Dormancy of Glioblastoma Multiforme-Derived Tumor Stem-Like Cells during Hypoxia. *PLOS ONE,* 7(1), pp. e30059.

Hogan, P., Chen, L., Nardone, J. & Rao, A., 2003. Transcriptional Regulation by Calcium, Calcineurin, and NFAT. *Genes & Development,* 17(18), pp. 2205-2232.

Hojo, M., Morimoto, T. & Maluccio, M., 1999. Cyclosporine Induces Cancer Progression by a Cell-autonomous Mechanism. *Nature,* 397(6719), pp. 530–534.

Holmgren, I., O'Reilly, M. & Folkman, J., 1995. Dormancy of Micrometastases: Balanced Proliferation and Apoptosis in the Presence of Angiogenesis Suppression. *Nature Medicine,* 1, pp. 149-153.

Honkanen, R., 1993. Cantharidin, another Natural Toxin that Inhibits the Activity of Serine/threonine Protein Phosphatases Type 1 and 2A. *FEBS Letters,* 330(3), pp. 283-286.

Inserte, J. et al., 2008. Effect of Acidic Reperfusion on Prolongation of Intracellular Acidosis and Myocardial Salvage. *Cardiovascular Research,* 77(4), pp. 782–790.

Ishihara, H. et al., 1989. Calyculin A and Okadaic Acid: Inhibitors of Protein Phosphatase Activity. *Biochemical and Biophysical Research Communications,* 159(3), pp. 871-877.

Jacob, S. & Cory , F., 2008. *Common Surgical Diseases.* New York: Springer.

Janssens, V. et al., 2016. PP2A Binds to the LIM Domains of Lipoma-preferred Partner Through its PR130/B" Subunit to Regulate Cell Adhesion and Migration. *Journal of Cell Science,* 129, pp. 1605–1618.

Janssens, V., Goris, J. & Van Hoof, C., 2005. PP2A: The Expected Tumor Suppressor. *Current Opinio In Genetics & Development,* 15(1), pp. 31-41.

Jennings, R., 2013. Historical Perspective on the Pathology of Myocardial Ischemia/Reperfusion Injury. *Circulation Research,* 113, pp. 428-438.

Jennings, R., Murry, C. & Reimer, K., 1991. Preconditioning Myocardium with Ischemia. Cardiovascular Drugs and Therapy, 5(5), pp. 933–938.

Jennings, R., et al., 1964. Electrolyte Alterations in Acute Myocardial. *Circulation Research,* 14, pp. 260-269.

Juhaszova, M. et al., 2004. Glycogen Synthase Kinase-3β Mediates Convergence of Protection Signaling to Inhibit the Mitochondrial Permeability Transition Pore. *The Journal of Clinical Investigation,* 113, pp. 1535–1549.

Kalogeris, T., et al., 2012. Cell Biology of Ischemia/Reperfusion Injury. *International Review of Cell and Molecular Biology ,* 298, pp. 229–317.

Karin, M., Liu, Z. & Zandi, E., 1997. AP-1 Function and Regulation Curr Opin. *Cell Biology,* 9, pp. 240-246.

Kemp, D. & Daly, P., 2016. The Ketogenic Kitchen. In: s.l.:Gill & Macmillan Ltd, pp. 226.

Kerr, J., Wyllie, A. & Currie, A., 1972. Apoptosis: a Basic Biological Phenomenon with Wide-ranging Implications in Tissue Kinetics, Br. J. *Cancer,* 26, pp. 239-257.

Khan, M., Misra, A., Trivedi, A. & Srivastava, A., 2004. Effect of Alkalinity on Cancerous Cells at different pH and Morphological Variations In-vitro. *International Journal of Bioassays,* pp. 3297-3302.

Khew-Goodall, Y. & Hemmings, B., 1988. Tissue-specific Expression of mRNAs Encoding Alpha- and Beta-catalytic Subunits of Protein Phosphatase 2A. *FEBS Letters,* 238, pp. 265–268.

Kiely, M. & Kiely, P., 2015. PP2A: The Wolf in Sheep's Clothing?. *Cancers,* 7, pp. 648-669.

Kimes, B. & Brandt, B., 1976. Kimes BW and Brandt BLProperties of a Clonal Muscle Cell Line from Rat Heart. Exp Cell Res 98: 367-381. *Experimental Cell Research,* 98(2), pp. 367- 381.

Kim, R. et al., 2015. Activation of KRAS Promotes the Mesenchymal Features of Basal-type Breast Cancer. *Experimental & Molecular Medicine,* 47(1), pp. e137.

Klabunde, R., 2017. Cardiac Electrophysiology: Normal and Ischemic Ionic Currents and the ECG. *Advances in Physiology Education,* 41, pp. 29 –37.

Klee, C. & Yang, S., 2010. Calcineurin. In: R. Bradshaw & E. Dennis, eds. *The Handbook of Cell Signalling.* s.l.:Academic Press, pp. 705-710.

Kodama, I., Kondo, N. & Shibata, S., 1986. Electromechanical Effects of Okadaic Acid Isolated from Black Sponge in Guinea-pig Ventricular Muscles. *Journal of Physiology ,* 378, pp. 359-373.

Kresge, N., Simoni , R. & Hill, R., 2005. Reversible Phosphorylation and Kinase Cascades: the Work of Edwin G. Krebs. *The Journal of Biological Chemistry,* 280(43), pp. e40.

Kruger , N. & von Schaewen, A., 2003. The Oxidative Pentose Phosphate Pathway: Structure and Organisation. *Current Opinion in Plant Biology,* 6(3), pp. 236–246.

Kung, A. et al., 2000. Suppression of Tumor Growth through Disruption of Hypoxia-inducible Transcription. *Nature Medicine,* 6, pp. 1335-1340.

Kunz, M. et al., 2002. Hypoxia/reoxygenation Induction of Monocyte Chemoattractant Protein-1 in Melanoma Cells: Involvement of Nuclear Factor-kappaB, Stimulatory Protein-1 in Melanoma Cell. *Biochemistry Journal,* 366, pp. 299-306.

Laderoute, K. et al., 1999. Mitogen-activated Protein Kinase Phosphatase-1 (MKP-1) Expression is Induced by Low Oxygen Conditions Found in Solid Tumor Microenvironment. *Journal of Biological Chemistry,*274, pp. 12890-12897.

Lee, S. et al., 2007. Protein Phosphatase 1 Nuclear Targeting Subunit is a Hypoxia Inducible gene:its role in Post-translational Modification of p53 and MDM2. *Cell Death and Differentiation,* 14, pp. 1106-1116.

Li, D. et al., 2006. Protein Serine/threonine Phosphatase-1 Dephosphorylaytes p53 at Ser-15 and Ser-37 to Modulate its Transcriptional and Apoptotic Activities. *Oncogene,* 25(21), pp. 3006-3022.

Li, L., Zhao, G. & Fu, Z., 2016. The Ras/Raf/MEK/ERK Signaling Pathway and Its Role in the Occurence and Development of HCC. *Oncology Letters,* 12(5), pp. 3045-3050.

Li, M., Hla, T., & Ferrer, F., 2013. FTY720 Inhibits Tumor Growth and Enhances the Tumor-suppressive Effect of Topotecan in Neuroblastoma by Interfering with the Sphingolipid Signaling Pathway. Pediatric Blood & Cancer, 60, pp. 1418–1423.

Li, X. et al., 2002. B56-associated Protein Phosphatase 2A is Required for Survival and Protects from Apoptosis in Drosophila Melanogaster. Molecular and Cellular Biology, 22, pp. 3674–3684.

Liu, D. & Chen, Z., 2009. The Effects of Cantharidin and Cantharidin Derivates on Tumour cells. *Anti-Cancer Agents in Medicinal Chemistry,* 9(4), pp. 392-396.

Liu, L. et al., 2005. Characterization of a Human Regulatory Subunit of Protein Phosphatase 3 Gene (PPP3RL) Expressed Specifically in Testis. *Molecular Biology Reports,* 32(1), pp. 41-45.

Liu, Y. et al., 2007. Calcineurin Promotes Hypoxia-inducible Factor 1a Expression by Dephosphorylating RACK1 and Blocking RACK1 Dimerization. *The Journal of Biological Chemistry,* 282(51), pp. 37064-37073.

Li, W. et al., 2010. Cantharidin, a Potent and Selective PP2A Inhibitor, Induces an Oxidative Stress-independent Growth Inhibition of Pancreatic Cancer Cells Through G2/M Cell-cycle Arrest and Apoptosis. *Cancer Science,* 101(5), pp. 1226-1233.

Li, X. et al., 2017. Paeonol Protects H9C2 Cardiomyocytes from Ischemia/reperfusion Injury by Activating Notch1 Signaling Pathway In Vitro. *International Journal of Clinical and Experimental Medicine,* 10(2), pp. 2866-2873.

Lu, J. et al., 2009. Inhibition of Serine/threonine Phosphatase PP2A Enhances Cancer Chemotherapy by Blocking DNA Damage Induced Defense Mechanisms. Proceedings of the National Academy of Sciences of the United States of America, 106, pp. 11697–11702.

Lumkwana, D. et al., 2017. Laminin, Laminin-entactin and Extracellular Matrix are Equally Appropriate Adhesive Substrates for Isolated Adult Rat Cardiomyocyte Culture and Experimentation. *Cell Adhesion & Migration,* 0(0), pp. 1–9.

Lunt, S. & Vander Heiden, M., 2011. Aerobic Glycolysis: Meeting the Metabolic Requirements of Cell Proliferation. *Annual Review of Cell and Developmental Biology,* 27(1), pp. 441–464.

MacDougall, L., Jones, L. & Cohen, P., 1991. Identification of the Major Protein Phosphatases in Mammalian Cardiac Muscle which Dephosphorylate Phospholamban. *European Journal of Biochemistry,* 196(3), pp. 725-734.

MacKeigan, J., Murphy, L., & Blenis, J., 2005. Sensitized RNAi Screen of Human Kinases and Phosphatases Identifies New Regulators of Apoptosis and Chemoresistance. Nature Cell Biology, 22, pp. 591–600.

Malhotra, R., et al., 2001. Hypoxia Induces Apoptosis via two Independent Pathways in Jurkat cells: Differential Regulation by Glucose. *American Journal of Physiololy - Cell Physiology,* Volume 281, pp. C1596-C1603.

Marbaniang, C. & Kma, L., 2018. Dysregulation of Glucose Metabolism by Oncogenes and Tumor Suppressors in Cancer Cells. *Asian Pacific Journal of Cancer Prevention,* 19(9), pp. 2377–2390.

Matoba, S. et al., 2006. P53 Regulates Mitochondrial Respiration. *Science,* 312, pp. 1650–1653.

Ma, W. et al., 2009. [18F]Fluorodeoxyglucose Positron Emission Tomography Correlates with Akt Pathway Activity but is not Predictive of Clinical Outcome During mTOR Inhibitor Therapy. *Journal Of Clinical Oncology,* 27(16), pp. 2697–2704.

Mayr, B. & Montminy, M., 2001. Transcriptional Regulation by the Phosphoryltion-Dependent Factor CREB. *Nature Reviews in Molecular Cell Biology ,* 2(8), pp. 599-609.

Miranda-Gonçalves, V., et al., 2018. Metabolism and Epigenetic Interplay in Cancer: Regulation and Putative Therapeutic Targets. *Frontier in Genetics,* 9, pp. 427.

Moorman, A. et al., 2003. Development of the Heart: (1) Formation of the Cardiac Chambers and Arterial Trunks. *Heart,* 89(7), pp. 806–814.

Morgan, M., Perry, S. & Ottaway, J., 1976. A New Protein Phosphatase From Skeletal Muscle: Myosin Light-chain Phosphatase. *Biochemical Society Transactions,* 4(2), pp. 351–352.

Morita, S., 2011. Remote Ischemic Preconditioning: is it Time to Introduce it in Clinical Practice. *Circulation Journal,* 75.

Mumby, M., 2007. PP2A: Unveiling a Reluctant Tumor Suppressor. *Cell,* 130(1), pp. 21–24.

Murry, C., Jennings, R. & Reimer, K., 1986. Preconditioning with Ischemia: a Delay of Lethal Cell Injury in Ischemic Myocardium. *Circulation,* 74(5), pp. 1124-1136.

Nagao, M. et al., 1995. Protein Serine/threonine Phosphatases as Binding Proteins for Okadaic Acid. *Mutation Research,* 333(1-2), pp. 173-179.

Neel, B. & Tonks, N., 1997. Protein Tyrosine Phosphatases in Signal Transduction. *Current Opinion in Cell Biology,* 9(2), pp. 193-204.

Olsen, J. et al., 2006. Global, in vivo, and site-specific Phosphorylation Dynamics in Signaling Networks. *Cell,* 127(3), pp. 635–648.

Paradis, A., Gay, M. & Zhang, L., 2014. Binucleation of Cardiomyocytes: the Transition from a Proliferative to a Terminally Differentiated State. Drug Discovery, 19(5), pp. 602-609.

Patterson, K. et al., 2009. Dual-Specificity Phosphatases: Critical Regulators with Diverse Cellular Targets. *Biochemical Journal,* 418(3), pp. 475–489.

Paul, S. & Lombroso, P., 2003. Receptor and Nonreceptor Protein Tyrosine Phosphatases in the Nervous System. *Cellular and Molecular Life Sciences,* 60(11), pp. 2465–2482.

Pauwels, E. et al., 1998. FDG Accumulation and Tumor Biology. *Nuclear Medicine and Biology ,* 25, pp. 317–322.

Peuker, K., Muff, S. & Wang, J., 2016. Epithelial Calcineurin Controls Microbiota-dependent Intestinal Tumor Development. *Nature Medicine,* 22, pp. 506-515.

Posch, A. et al., 2013. V3 Stain-free Workflow for a Practical, Convenient, and Reliable Total Protein Loading Control in Western Blotting.. *The Journal of Visualized Experiments,* Volume 82.

Puzio-Kuter, A. et al., 2009. Inactivation of p53 and Pten Promotes Invasive Bladder Cancer. *Genes & Development,* 23(6), pp. 675-680.

Ravi, R. et al., 2000. Regulation of Tumor Angiogenesis by p53-induced Degradation of Hypoxia-inducible Factor 1alpha. *Genes Development,* 14, pp. 34-44.

Rincón, R. et al., 2015. PP2A Inhibition Determines Poor Outcome and Doxorubicin Resistance in Early Breast Cancer and its Activation Shows Promising Therapeutic Effects. *Oncotarget,* 6(6), pp. 4299-4314.

Riss, T. et al., 2003. Choosing The Right Cell-Based Assay For Your Research. *Cell Notes,* Issue 6.

Ritchie, R. & Delbridge, L., 2006. Cardiac Hypertrophy, Substrate Utilization and Metabolic Remodelling Effet. *Clinical and Experimental Pharmacology and Physiology,* 33(1-2), pp. 159-166.

Romero-Garcia, S. et al., 2011. Tumor Cell Metabolism. *Cancer Biology & Therapy,* 12(11), pp. 939-948.

Rupec, R. & Baeuerle, P., 1995. The Genomic Response of Tumor Cells to Hypoxia and Reoxygenation. Differential Activation of Transcription Factors AP-1 and NF-κB. *European Journal of Biochemistry,* 234, pp. 632-640.

Rusnak, F. & Mertz, P., 2000. Calcineurin: Form and Function. *Physiological Reviews,* 80(4), pp. 1483-1521.

Ruvolo, P. et al., 2011. Low Expression of PP2A Regulatory Subunit B55alpha is Associated with T308 Phosphorylation of AKT and Shorter Complete Remission Duration in Acute Myeloid Leukemia Patients. *Leukemia,* 25, pp. 1711–1717.

Ruvolo, P., Deng, X., & May, W., 2001. Phosphorylation of Bcl2 and Regulation of Apoptosis. Leukemia, 15, pp. 515–522.

Saddoughi, S. et al., 2013. Sphingosine Analogue Drug FTY720 Targets I2PP2A/SET and Mediates Lung Tumour Suppression via Activation of PP2A-RIPK1-dependent Necroptosis. EMBO Molecular Medicine, 5, 105–121.

Saikumar, P. et al., 1998. Role of Hypoxia-induced Bax Translocation and Cytochrome c Release in Reoxygenation Injury. *Oncogene,* 17, pp. 3401-3415.

Santoro, M. et al., 1998. Regulation of Protein Phosphatase 2A Activity by Caspase-3 During Apoptosis. The Journal of Biological Chemistry, 273, pp. 13119–13128.

Schneider, S. et al., 2001. Inhibition of p38MAPK α/β Reduces Ischemic Injury and does not Block Protective Effects of Preconditioning. American Journal of Physiology, 280, H499–H508.

Schönthal, A., 2001. Role of Serine/threonine Protein Phosphatase 2A in Cancer. *Cancer Letters,* 170(1), pp. 1–13.

Schweyer, S. et al., 2007. Expression and Function of Protein Phosphatase PP2A in Malignant Testicular Germ Cell Tumours. *The Journal of Pathology,* 213(1), pp. 72-81.

Semenza, G., 2001. Hypoxia-inducible Factor 1: Oxygen Homeostasis and Disease. *Trends in Molecular Medicine,* 7(8), pp. 345-350.

Semenza, G., Roth, P., Fang, H. & Wang, G., 1994. Transcriptional Regulation of Genes Encoding Glycolytic Enzymes by Hypoxia-inducible Factor 1. *The Journal of Biological Chemistry,* 269, pp. 23757-23763.

Seshacharyulu, P., Pandey, P., Datta, K. & Batra, S., 2013. Phosphatase: PP2A Structural Importance, Regulation and its Aberrant Expression in Cancer. *Cancer Letters,* 335 (1), pp. 9-18.

Shi, Y., 2009. Serine/Threonine Phosphatases: Mechanism Through Structure. *Cell,* 139(3), pp. 468–484.

Shouse, G., Nobumori, Y. & Liu, X., 2010. A B56gamma Mutation in Lung Cancer Disrupt the p53-dependent Tumour-suppresor Function of Protein Phosphatase 2A. *Oncogene,* 29, pp. 3933-3941.

Smith, R., Soeters, M., Wüst, R. & Houtkooper, R., 2018. Metabolic Flexibility as an Adaptation to Energy Resources and Requirements in Health and Disease. *Endocrine Reviews,* 39(4), pp. 489–517.

Smoly, I. et al., 2017. An Asymmetrically Balanced Organization of Kinases versus Phosphatases across Eukaryotes Determines Their Distinct Impacts. *PLoS Computational Biology.,* 13(1), pp. e1005221.

Srinivasan, B., 2012. Mitochondrial Permeability Transition Pore: an Enigmatic Gatekeeper. *New Horizons in Science & Technology,* 1(3), pp. 47–51.

St John, J. et al., 2005. The Expression of Mitochondrial DNA Transcription Factors During Early Cardiomyocyte In Vitro Differentiation From Human Embryonic Stem Cells. *Cloning Stem Cells,* 7(3), pp. 141-153.

Steenaart, N. et al., 1992. The Phospholamban Phosphatase Associated with Cardiac Sarcoplasmic Reticulum is a Type 1 Enzyme. *Archives of Biochemistry and Biophysics,* 293(1), pp. 17-24.

Steenbergen, C., 2002. The Role of p38 Mitogen-activated Protein Kinase in Myocardial Ischaemia/reperfusion Injury: Relationship to Ischemic Preconditioning. Basic Research in Cardiology, 97, pp. 276–285.

Stemke-Hale, K., Gonzalez-Angulo, A. & Lluch, A., 2008. An Integrative Genomic and Proteomic Analysis of PIK3CA, PTEN, and AKT Mutations in Breast Cancer. *Cancer Research,* 68(15), pp. 6084–6091.

Stroka, D. et al., 2001. HIF-1 is Expressed in Normoxic Tissue and Displays an Organ-specific Regulation Under Systemic Hypoxia. *The Federation of American Societies for Experimental Biology Journal,* 15(13), pp. 245-24453.

Suganuma, M., Fujiki, H. & Suguri, H., 1988. Okadaic Acid: an Additional Non-phorbol-12-tetradecanoate-13-acetate-type Tumor Promoter. *Proceedings of the National Academy of Sciences of the United States of America,* 85(6), pp. 1768–1771.

Sun, J., Zhang, Z. & Wang, W., 2003. An Overview of the Protein Tyrosine Phosphatase Superfamily. *Current Topics in Medicinal Chemistry,* 3(7), pp. 739–748.

Suzuki, H., Tomida, A. & Tsuruo, T., 2001. Dephosphorylated Hypoxia-inducible Factor 1alpha as a Mediator of p53-dependent Apoptosis During Hypoxia. *Oncogene,* 20, pp. 5779-5788.

Swarup, G., Cohen, S. & Garbers, D., 1982. Inhibition of Membrane Phosphotyrosyl-Protein Phosphatase Activity by Vanadate. *Biochemical and Biophysical Research Communications,* 107(3), pp. 1104–1109.

Świderska, E. et al., 2018. *Role of PI3K/AKT Pathway in Insulin-Mediated Glucose Uptake.* [Online] Available at: https://www.intechopen.com/online-first/role-of-pi3k-akt-pathway-in-insulin-mediated-glucose-uptake [Accessed 5 November 2018].

Takada, Y. et al., 2004. Cytoprotective Effect of Sodium Orthovanadate on Ischemia/Reperfusion-Induced Injury in the Rat Heart Involves Akt Activation and Inhibition of Fodrin Breakdown and Apoptosis. *Journal of Pharmacology and Experimental Therapeutics,* 311(3), pp. 1249-1255.

Tamareille, S. et al., 2011. RISK and SAFE Signaling Pathway Interactions in Remote Limb Ischemic Perconditioning in Combination with Local Ischemic Postconditioning. *Basic Research in Cardiology,* 106(6), pp. 1329-1239.

Thundathil, J., Fillion, F. & Smith, L., 2005. Molecular Control of Mitochondrial Function in Preimplantation Mouse Embryos. *Molecular Reproduction and Development,* 71, pp. 405-413.

Tobiume, K. et al., 2001. ASK1 is Required for Sustained Activations of JNK/p38 MAP Kinases and Apoptosis. *EMBO Reports,* 2, pp. 222-228.

Tonks, N., 2006. Protein Tyrosine Phosphatases: from Genes, to Function, to Disease. *Nature Reviews Molecular Cell Biology,* 7(11), pp. 833–846.

Tournebize, R. et al., 1997. Distinct Roles of PP1 and PP2A-like Phosphatases in Control of Dynamic During Mitosis. *The EMBO Journal,* 16(18), pp. 5537–5549.

Uygur, A. & Lee, R., 2016. Mechanisms of Cardiac Regeneration. *Development Cell,* 36(4), pp. 362-374.

Van Hoof, C. & Goris, J., 2003. Phosphatases in Apoptosis: To be or not to be, PP2A is in the Heart of the Question. *Biochimica et Biophysica Acta,* 1640, pp. 97–104.

Van Vuuren, D., 2014. The Role of Protein Phosphatase 2A (PP2A) in Myocardial Ischaemia/reperfusion injury*Stellenbosch University.* [Online] Available at: http://scholar.sun.ac.za

Vander H, M., Cantley, L. & Thompson, C., 2009. Understanding the Warburg Effect: The Metabolic Requirements of Cell Proliferation. *Science,* 324(5930), pp. 1029–1033.

Vander Heiden, M. et al., 2001. Growth Factors can Influence Cell Growth and Survival through Effects on Glucose Metabolism. *Molecular and Cell Biology,* 21(17), pp. 5899–5912.

Vlastaridis, P. et al., 2017. The Pivotal Role of Protein Phosphorylation in the Control of Yeast Central Metabolism. *G3 (Bethesda),* 7(4), pp. 1239-1249.

Voet, P., Voet, J. & Charlotte, W., 2006. *Fundamentals of Biochemistry : Life at the Molecular Level.* 2 ed. Wiley: Hoboken, NJ.

Wang S.S, et al., 1998. Alterations of the PPP2R1B Gene in Human Lung and Colon Cancer. *Science,* Volume 282, pp. 284-287.

Wang, X. et al., 2017. MicroRNA-145 Aggravates Hypoxia-Induced Injury by Targeting Rac1 in H9c2 Cells. Cellular Physiology and Biochemistry, 43, pp. 1974–1986.

Warburg, O., 1931. The Oxygen-Transfering Ferment of Respiration. *Nobel Lectures.*

Weinbrenner, C., 1998. Cyclosporine A Limits Myocardiallinfarct size even when Administered after onset of Ischemia. *Cardiovascular Research,* 38(3), pp. 676–684.

Weinbrenner, C. et al., 1999. Fostriecin, an Inhibitor of Protein Phosphatase 2A, Limits Myocardial Infarct Size even when Administered after Onset of Ischemia.. *Circulation,* 98, pp. 899–905.

Welte, S. et al., 2005. 6,8-Difluoro-4-methylumbiliferyl Phosphate: a Fluorogenic Substrate for Protein Tyrosine Phosphatases. *Analytical Biochemistry,* 1;338(1), pp. 32-38.

Woo, M. et al., 1997. Toxicities of Tacrolimus and Cyclosporin A after Allogeneic Blood Stem Cell Transplantation. *Bone Marrow Transplant,* 20(12), pp. 1095-1098.

Xie, J. et al., 2016. Hypoxia Regulates Stemness of Breast Cancer MDA-MB-231 Cells. *Medical oncology,* 33, pp. 42.

Yamashita, M. et al., 2000. T cell Receptor-Induced Calcineurin Activation Regulates T Helper Type 2 Cell Development by Modifying the Interleukin 4 Receptor Signaling Complex. *Journal of Experimental Medicine,* 191(11), pp. 1869–1879.

Yang, X. et al., 2011. Cardioprotection by Mild Hypothermia During Ischemia Involves Preservation of ERK Activity. *Basic Research in Cardiology,* 106(3), pp. 421-430.

Yun, J. et al., 2009. Glucose Deprivation Contributes to the Development of KRAS Pathway Mutations in Tumor Cells. *Science,* 325(5947), pp. 1555-1559.

Zhao, Z. et al., 2003. Inhibition of Myocardial Injury by Ischemic Postconditioning During Reperfusion: Comparison with Ischemic Preconditioning. *American Journal of Physiology. Heart and circulatory Physiology,* 285(2), pp. H579-588.